

SOLID STATE NMR CHEMICAL SHIFTS
AS AN ALTERNATIVE TO DIFFRACTION DATA
IN THE DETERMINATION OF
SIC POLYTYPIC STRUCTURES

BY DEQI GUO (B. Sc. Hons., China)

A thesis
submitted to the Department of Chemistry
in partial fulfilment of the requirements
for the degree of
Master of Science.

Brock University
St. Catharines, Ontario
Canada

August, 1988.

© D. Guo, 1988

ACKNOWLEDGEMENT

I would like to express my heartfelt thanks to Professor Mary Frances Richardson for her supervision, teaching, and assistance.

In addition, I would like to thank Dr.J. S. Hartman for his valuable discussion on the subject of nmr, and Dr. S. M. Rothstein for his help and encouragement.

Thanks are also offered to Tim, Donna, and Beatrice for their friendly help with acquisition of nmr spectra, and to the departmental faculties and graduate students for their valuable advice.

Finally, I am grateful to NSERC for the financial support to this program.

ABSTRACT

Silicon carbide, which has many polytypic modifications of a very simple and very symmetric structure, is an excellent model system for exploring, the relationship between chemical shift, long-range dipolar shielding, and crystal structure in network solids. A simple McConnell equation treatment of bond anisotropy effects in a polytype predicts chemical shifts for silicon and carbon sites which agree well with the experiment, provided that contributions from bonds up to 100 Å are included in the calculation. The calculated chemical shifts depend on three factors: the layer stacking sequence, electrical centre of gravity, and the spacings between silicon and carbon layers. The assignment of peaks to lattice sites is proved possible for three polytypes (6H, 15R, and 3C).

The fact that the calculated chemical shifts are very sensitive to layer spacings provides us a potential way to determine and refine a crystal structure. In this work, the layer spacings of 6H SiC have been calculated and are within X-ray standard deviations. Under this premise, the layer spacings of 15R have been determined.

^{29}Si and ^{13}C single crystal nmr studies of 6H SiC polytype indicate that all silicons and carbons are magnetically anisotropic. The relationship between a magnetic shielding tensor component and layer spacings has been derived. The comparisons between experimental and semi-empirical chemical shielding tensor components indicate that the paramagnetic shielding of silicon should be included in the single crystal chemical shift calculation.

TABLE OF CONTENTS

Acknowledgements	i
Abstract	ii
Table of contents	iii
List of tables	vii
List of figures	ix
CHEPTER I : INTRODUCTION	1
I.A Polytypism and the description of polytypic structures	1
I.A.1 Close packing	1
I.A. 2 Notations to describe polytypic structures	2
I.A.2.a Ramsdell's notation	2
I.A.2.b The classical ABC notations	3
I.A.2.c The h-c notation	3
I.A.2.d Ramsdell's zig-zag sequence	3
I.B Silicon carbide	4
I.B.1 Preparation and crystallographical properties	4
I.B.2 Determination of SiC polytypes by precession method	7
I.C Recent progress in silicon carbide research	9
I.C.1 Nmr studies	9
I.C.1.a ^{29}Si and ^{13}C MAS nmr	10
I.C.1.b ^{29}Si and ^{13}C nmr spectra of a SiC 6H single crystal	10
I.C.2 Theoretical studies on SiC polytypic structures	12
I.C.2.a Designation of crystallographical types	12
I.C.2.b Semi-empirical and ab initio MO calculations	15
I.D.1 Chemical shift and nuclear shieldings	18
I.D.1.a Theory of Chemical shift	18

I.D.1.b	General aspects of nuclear shieldings	19
I.D.2.a	Theory of long-range dipolar shielding	20
I.D.2.b	Application of long-range dipolar shielding	21
I.E	Thesis scope	23
CHAPTER II	THEORETICAL CALCULATIONS OF CHEMICAL SHIFTS FOR SiC POWDER SAMPLES	24
II.A	Introduction	24
II.B	Computer program set-up	25
II.B.1	Procedure	25
II.B.1.a	Coordinate input	26
II.B.1.b	Calculations of R and $\cos\theta$	26
II.B.1.c	Method of summation	27
II.C	Selections of unit cell dimensions and layer spacings	29
II.C.1	SiC 6H	29
II.C.2	SiC 15R	29
II.C.3	SiC 3C and 2H	31
II.D	Preliminary studies on chemical shift calculations	32
II.D.1	Convergences of geometric factors	32
II.D.2	Contribution from individual layers	32
II.E	Peak assignments and chemical shift calculations	33
II.E.1	Calculations of geometric factors	33
II.E.2	Peak assignments and chemical shift calculations in SiC 6H	34
II.E.3	Peak assignments and chemical shift calculations in SiC 15R	38
II.F	Relationships between the observed shifts and the calculated geometric factors	38

II.G	Determination of electrical centre of gravity	38
II.H	Discussions	45
CHAPTER III	REFINEMENT OF SIC POLYYPIC STRUCTURES	48
III.A	Introduction	48
III.B	Preliminary studies on layer spacing shifts	48
III.B.1	Relationship between chemical shift change and layer spacing shift	49
III.B.2	Additivity of geometric factor changes	49
III.C	Crystal structure refinements	51
III.C.1	Equation set-up and layer spacing changes-a combined refinement of 6H and 15R all at once	51
III.C.2	Refinement of 6H and 15R by using a common Δx and distinct intrinsic chemical shift σ_i	53
III.D	Discussions	57
CHAPTER IV	PRELIMINARY STUDIES ON CALCULATION OF MAGNETIC SHIELDING TENSOR COMPONENTS OF 6H SIC VIA SINGLE CRYSTAL METHOD	64
IV.A	Introduction	64
IV.A.1	Theory and determination of nuclear magnetic shielding tensor	64
IV.A.2	Advances in ^{13}C and ^{29}Si single crystal nmr	67
IV.B.	Experimental	69
IV.B.1	Samples	69
IV.B.2	Identification of polytypes by precession method	69
IV.B.3	^{29}Si and ^{13}C single crystal nmr	69
IV.C.1	Results and rotation plots	70
IV.C.2	Extraction of magnetic shielding tensor components	

	via least squares fits	76
IV.D	Theoretical approach	77
IV.D.1	Tensor rotations	78
IV.D.2	Theoretical calculation of tensor components and determination of layer spacings	81
IV.E	Results and discussions	82
CHAPTER V	CONCLUSIONS	87
	REFERENCES	89
	APPENDICES	
1	Derivation of the shielding constant σ_N^G from the shielding tensor σ_N^G	95
2	Program for the calculation of geometric factors of silicon (SiC 6H powdered sample)	97
3	Program for the calculation of geometric factors of silicon (SiC 15R powdered sample)	105
4	Program for least squares fits and layer spacing shifts in MAS nmr chemical shift calculation	114
5	Program for the determination of layer spacing shifts of 15R and 6H by using common intrinsic shifts and bond magnetic anisotropy	120
6	Program for the calculation of geometric factors of silicon (SiC 6H single crystal)	124
7	Program for the calculation of magnetic shielding tensor components by least squares fits	133
8	Program for least squares fits and layer spacing shifts in single crystal nmr chemical shift calculation	135

LIST OF TABLES

Number	Title	Page
1	The structures of some polytypes of SiC as described in the various notations	6
2	Type designations in silicon carbide polytypes	15
3	Categorized types of Si sites in some SiC polytypes	17
4	Bond lengths in SiC 6H	24
5	Lattice constants of some SiC polytypes	31
6	Geometric factors of silicons for individual layers (SiC 6H, R=150 Å)	34
7	Summary of calculated geometric factors of four polytypes	35
8	Assignments of nmr chemical shifts to the calculated geometric factors (SiC 6H)	36
9	Calculated bond magnetic anisotropy (Δx) and intrinsic chemical shifts of Si and C for two assignments	36
10	Observed chemical shifts versus calculated (ppm) before shifting layer spacings (SiC 6H)	37
11	Peak assignments in SiC 15R	39
12	Calculated chemical shifts in SiC 15R	40
13	Summary of calculated intrinsic chemical shifts, bond magnetic anisotropies for various assignments in SiC 15R	42
14	Calculated chemical shifts for different electrical centre of gravities (SiC 6H)	43
15	Calculated intrinsic chemical shifts, bond magnetic anisotropies for different electrical centre of gravities (6H)	44
16	Example of additivity of geometric factor changes	51

17	Example of geometric factors when one of the atoms is moved up or down by 0.001 Å (ECG=0.498)	52
18	Spacing shifts in SiC polytypes (6H & 15R, ECG=0.490)	54
19	Layer spacing shifts in various ways of peak assignment (ECG=0.490)	56
20	Comparisons between the observed chemical shifts and the calculated after shifting layers for SiC 6H polytype	57
21	Summary of single crystal nmr chemical shifts	74
22	²⁹ Si single crystal and MAS nmr result	77
23	¹³ C single crystal and MAS nmr result	77
24	The observed chemical shielding tensor components versus calculated for various ways of assignments in single crystal chemical shift calculation	83
25	Summary of the bond magnetic anisotropies, intrinsic shielding tensor components for each of the six assignments	84
26	The layer spacing shifts of silicons and carbons for each of the six assignments	84
27	Comparisons between the assignments from MAS and single crystal nmr spectra	85

LIST OF FIGURES

Fig. No.	Title	Page
1	The close packing of spheres	1
2	Zigzag sequences of Si and C atoms in the (1120) plane of the type 6H (a) and type (15R)	5
3	The model of the structure of ∂ SiC type 6H. Black balls represent C atoms and white balls Si atoms	8
4	^{29}Si and ^{13}C MAS nmr spectra of silicon carbide polytypes. Spectra were obtained at a magnetic field of 9.4 T with relaxation delays between pulses of 15 min.	11
5	Plots of ^{29}Si chemical shifts versus crystal orientation angles, \emptyset	13
6	Plots of ^{13}C chemical shifts versus crystal orientation angles, \emptyset	13
7	First and second neighbours for the possible types of silicon (or carbon) surroundings in silicon carbide polytypes	14
8	Zigzag sequences for the four types of silicon surroundings	16
9	Structures of amides with magnetically non-equivalent sites marked A and B	22
10	Relationship among bond vector, radius vector(R), and angle(\emptyset) in the geometric factor calculation	25
11	Diagram of calculation network projected on (001) plane	28
12	Bond distances and layer spacings in SiC 6H(\AA)	30
13	Geometric factors versus radii of interaction spheres	33
14	Silicon-29 chemical shifts v.s. geometric factors for SiC polytypes before layer spacing changes	41
15	Carbon-13 chemical shifts v.s. geometric factors for SiC polytypes before layer spacing changes	41
16	Change in the calculated chemical shifts of three silicons of the 6H	

	polytype when the Si(3) layer is moved up or down along the c-axis	50
17	Change in the calculated chemical shifts of three silicons of the 6H polytype when the C(1) layer is moved up or down along the c-axis	50
18	Si-C bond distances and Si-Si layer spacings of 6H after shifting, calculated by using common bond magnetic anisotropy and distinct intrinsic shifts of 6H and 15R , compared with those from X-ray refinement	58
19	C-C layer spacings of 6H after shifting, calculated by using common bond magnetic anisotropy and distinct intrinsic shifts of 6H and 15R , compared with those from X-ray refinement	59
20	Si-C bond distances and Si-Si layer spacings of 15R after shifting, calculated by using common bond magnetic anisotropy and distinct intrinsic shifts of 6H and 15R , compared with those from X-ray refinement	60
21	C-C layer spacings of 15R after shifting, calculated by using common bond magnetic anisotropy and distinct intrinsic shifts of 6H and 15R , compared with those from X-ray refinement	61
22	Orientation of the rotation axis and the plane of measurement with respect to the crystal axes X, Y, Z	66
23	Diagram of an apparatus used in the single crystal nmr experiement to set the orientation angle, \emptyset	71
24	^{29}Si single crystal nmr spectra of 6H SiC, orientated at series angles to the applied magnetic field H_0 ; relaxation delay was thirty seconds	72
25	^{13}C single crystal nmr spectra of 6H SiC, orientated at series	

	angles to the applied magnetic field H_0 ; relaxation delay was twenty seconds	73
26	Plots of ^{29}Si chemical shift versus orientation angle (θ) for single crystal nmr experiment; slashed lines are symmetry based extrapolations	75
27	Plots of ^{13}C chemical shift versus orientation angle (θ) for single crystal nmr experiment; slashed lines are symmetry based extrapolations	75
28	Schematic representation of bond magnetic susceptibility tensor of silicon carbide polytype	79

CHAPTER I INTRODUCTION

I.A Polytypism and the description of polytypic structures

I.A.1 Close packing

A large number of crystal structures can be described geometrically in the form of a close-packing of rigid spheres, held together by the interatomic forces. A close packing of equal spheres in a plane has only one pattern, which is called a hexagonal close-packed layer with 6mm symmetry, as shown in Figure 1.

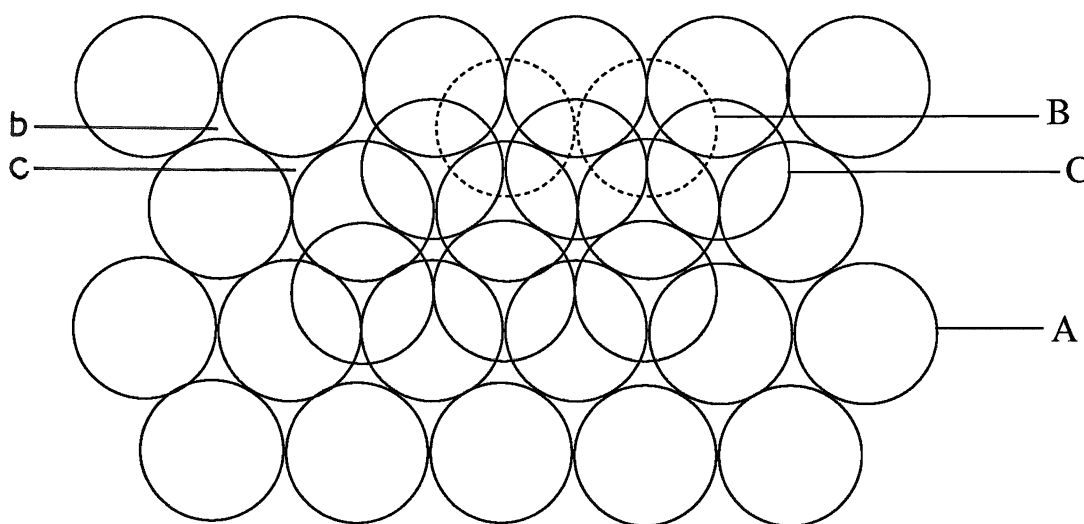


Figure 1. The Close Packing of Spheres

Let's label the positions of spheres in this layer as A's. Such a layer contains two types of triangular voids; the one pointed upwards is labeled b, and the other is labeled c. A 60° rotation about an A exchanges b's and c's.

In three dimensional close-packing, the next layer of spheres can occupy either b or c position, and they are named B or C accordingly. No two successive layers can be alike. It is said that three dimensional packing in this way provides maximum density, in the case of infinite lattice arrangement.¹

Polytypic modifications of one compound have the same dimensions along the a and b axes, but different along the c axis.^{2,3} Most polytypes are formed under the same temperature, pressure, and other conditions. Polytypism is different from polymorphism, in which different polymorphs form under different temperature and pressure and undergo transformation as these conditions are changed.⁴

The number of different close packed structures for a polytype in three dimensions is infinite. Each has its own c-dimension of the unit cell, depending on the number of layers after which the stacking sequence repeats itself.⁵

I.A.2 Notations to describe polytypic structures

Many different notations have been used to describe polytypic structures. A detailed description of them is summarized by Verma and Krishna.⁵ Only those commonly encountered will be mentioned here.

I.A.2.a Ramsdell's notation⁶

A polytype can be designated by the number of layers in the unit cell followed by H or R or C to specify the lattice type. For example, 6H represents the structure with a six layer period along the c axis and the unit cell is primitive hexagonal, and 15R denotes the structure whose primitive cell is rhombohedral and that contains fifteen layers in its unit cell. The cubic structure is described as 3C. This type of notation is too simple to tell anything about the arrangement along the c

axis, and creates confusion when the number of layers along the c axis is the same but the packing sequence is different. An improvement of it is to use subscripts such as a , b , c or 1 , 2 , 3 to distinguish them. For example, two known polytypes of SiC with identical lattice dimensions but different structures are designated by $51R_a$ and $51R_b$.

I.A.2.b The classical ABC notation

As pointed out in I.A.1, the letters A , B , C are used to describe stacking sequence along the c axis for close-packed structures. Thus SiC 6H can be designated as ABCACB. This notation actually means $AaBbCcAaCcBb$, where capital letters represent silicon atoms and the small letters represent carbon atoms which are displaced by about 1.89 \AA from silicon atoms. The small letters may be omitted if the position of one kind of atoms is fixed relative to the positions of the other kind.

I.A.2.c The h-c notation

Each layer can be specified in terms of the orientation of layers above and below it. The letter h is used to designate the layer whose immediate upper and lower layers are in the same orientation, that is, hexagonal layer; and the letter c in different orientation, that is, cubic layer. Thus for a stacking sequence ABCBA CABAC BCACB, the h-c notation will be $hchcc hchcc hchcc$. This notation is useful in the chemical shift calculation and peak assignment, as will be discussed in the next chapter.

I.A.2.d Ramsdell's zig-zag sequence

Ramsdell schematically represented silicon carbide polytypes in terms of the zig-zag sequence of silicon and carbon atoms in the (1120) planes of the structures.⁶ Since all three symmetry axes lie on this plane, the planes contain all atoms of the structures. An illustration of the meaning of zig-zag sequence is given in Figure 2, showing the atomic arrangements of 6H and 15R in (1120) planes. If a silicon or a carbon atom lies on A in one layer, the next must be either to the right on B, or to the left on C. If to the left, the third layer may have its atom continue to the left, or change to the right. Such repeated changes of the sequences produce zig-zag patterns. The unit cell is completed after arriving at an identical atom that has the same environment as the starting one. For example, the unit cell of 6H is completed at atom 2 (see Figure 2(a)).

Other notations are also available in the literature, these are: Ott's interval sequence,⁷ Hagg's notation,⁸ and Zhdanov symbol.⁹ Description to these notations will not be given here, for they not encountered in this thesis. A summary of notations of interest is given in Table 1.

I.B Silicon carbide

I.B.1 Preparation and crystallographical properties of silicon carbide

Most commercial preparations of silicon carbide are obtained by passing electric current through a mixture of carbon and silica, with a few percent of sawdust and salt in an electric furnace, a method discovered by Acheson.¹⁰ The crystals are grown at a temperature over 2000 degree Celsius for more than thirty hours.

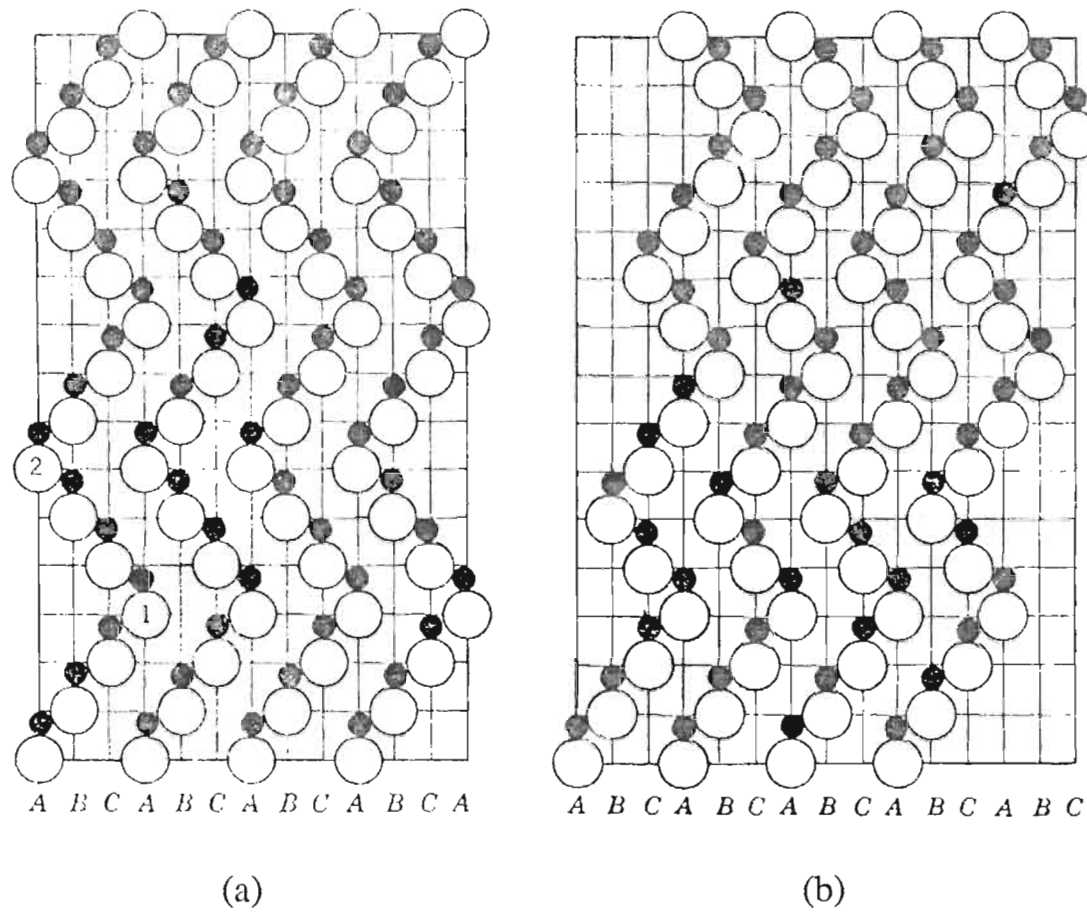


Figure 2 Zigzag sequences of Si and C atoms in the $(11\bar{2}0)$ plane of type 6H (a) and type 15R (b).

Table 1 The Structures of Some Polytypes of SiC as
Described in the Various Notations

Old Notation	Ramsdell Notation	ABC Sequence	h-c Notation
SiC I	15R	ABCBACABACBCACB	(hchcc) ₃
SiC II	6H	ABCACB	(hcc) ₂
SiC III	4H	ABCB	(hc) ₂
SiC IV	21R	ABCACBACABCBACBCABACB	(hcchccc) ₃
SiC V	51R	ABCACBABCACBABCAC BCABACBCABACBCABA CABCBACABCBACABCB	[(hcc) ₅ hc] ₃
SiC VI	33R	ABCACBABCACBCABAC BCABACABCBACABCB	[(hcc) ₃ hc] ₃
—	2H	AB	h ₂

It is evident that silicon carbide can crystallize in many polytypes. More than 200 of them have been discovered so far, among which 6H SiC is the most common and 15R is second most common polytypes. The structures of silicon carbide polytypes are similar to the familiar structure of diamond, except half of the carbon atoms in diamond are replaced by silicon atoms. Each silicon atom is bonded to four carbon atoms and vice versa. The bonding between Si and C is predominantly covalent (about 12% ionic, calculated on Pauling's electronegativity scale¹¹). A typical SiC polytype (6H) is shown in Figure 3. Although one may write many polytypes for silicon carbide, there are only four possible space groups—P3m1, R3m1, P63mc and $F\bar{4}3m$, for the tetrahedral arrangement of Si and C excludes the existence of either a centre of symmetry or a mirror plane perpendicular to [001]⁵. Typical examples of polytypes with space groups of R3m1 and P63mc are 15R and 6H SiC, respectively.

I.B.2 Determination of SiC polytypes by precession method

The precession camera, designed by Buerger in the early 1940s, provides an undistorted record of reciprocal lattices from which the angles and distance of the lattice may be determined directly.¹² The method has two advantages: first, the experimental period is relatively short; second, the photograph is easy to index, measure, and search for symmetry. Therefore, it will be used in this work to search for polytypes. SiC 6H and 15R are distinguishable by this method. Although both polytypes have the same $hk0$ precession pictures (e.g. both have six-fold symmetry axes), $h0l$ reflections are different. In 6H, the spots are symmetric about the c axis (or c^* axis), for example, there are spots at 101 and $\bar{1}01$. However, the

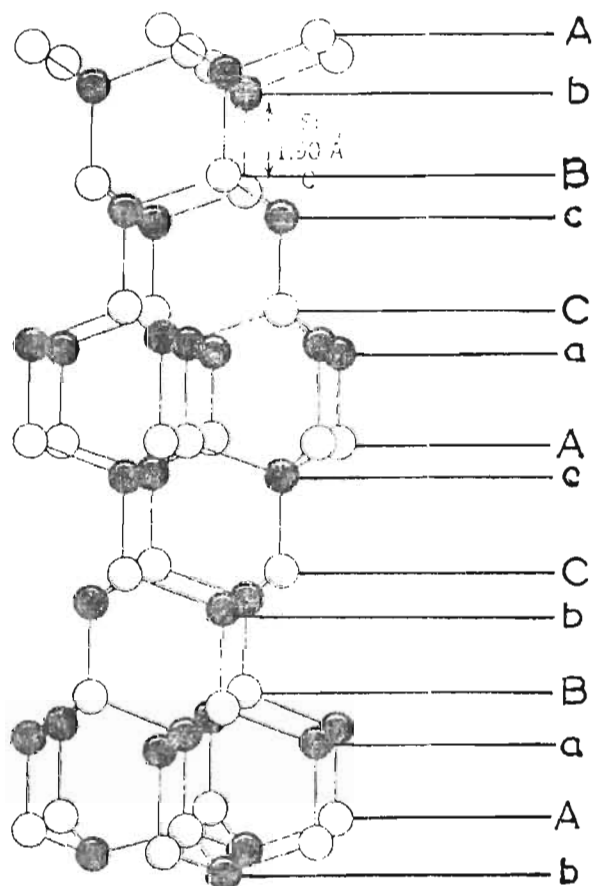


Figure 3 The model of the structure of α SiC type 6H. Black balls represent C atoms and white balls Si atoms.

arrangement of diffraction spots in 15R hol photograph is not symmetric about that axis. On one side, the 10l reflections are present only when $l=3n+1$ (n is an integer), so the present reflections on this side are 101, 104, 107, etc. On the other side of the C axis, the present reflections are 10l with $l=3n-1$, that is, $\bar{1}0\bar{1}$, $\bar{1}02$, $\bar{1}05$, etc. Similar considerations are applicable to other columns. As a conclusion, the 6H and 15R polytypes can be distinguished by the investigation of hol precession photographs.

I.C Recent progress in silicon carbide research

I.C.1 NMR studies

Since its first application to study the correlation of chemical shift to the polymerization in silicate crystals by Lippmaa et al.,¹³ ^{29}Si MAS-NMR has been used more and more extensively to study the structures of silicon containing compounds and materials, such as zeolites,¹⁴ silicates,¹⁵ silicate glasses,¹⁶ ceramic materials,¹⁷ silicon containing amorphous solids,¹⁸ and polymeric materials.¹⁹ A few years ago, another research field—the use of ^{29}Si MAS NMR to detect polytypic structures appeared. Finlay et al.,²⁰ Guth et al.²¹ have reported ^{29}Si MAS NMR spectra of the 3C, 6H, and 15R polytypic structures. Both ^{29}Si and ^{13}C spectra have been reported by Hartman et al.²² In her M. Sc. thesis, Winsborrow also obtained spectra of a single crystal of 6H SiC at different orientation of the c-axis with respect to the external magnetic field, besides MAS NMR studies.²³ From these papers, it appears that NMR would become a highly efficient technique for polytypic structure determination. A summary of results from these papers will be given.

I.C.1.a ^{29}Si and ^{13}C magic angle spinning (MAS) nmr

When a powdered sample is spun at the "magic angle (54.7°)" to the applied magnetic field, the chemical shift anisotropy is averaged to isotropy as in liquids, and the dipole-dipole interaction reduces to zero, since the term $(1-3\cos^2\theta)$ disappears. As a result, the line width decreases considerably and the line position can be determined as accurately as that in liquids. Details of MAS nmr are discussed in the literature.^{22(a)}

Silicon carbide 6H, 3C, and 15R spectra have been acquired by long pulse delay MAS nmr.²² The ^{29}Si spectrum of 6H SiC shows three well-separated peaks (1:1:1 ratio) whose chemical shifts are -13.9, -20.2, -24.5 ppm. Similarly, three peaks (1:1:1) are observed in the ^{13}C spectrum, and the chemical shifts for these peaks are 15.2, 20.2, 23.2 ppm, respectively. The numbers of peaks in ^{29}Si and ^{13}C spectra are equal to the numbers of crystallographically distinguishable sites.

Only one peak (-18.3 ppm) is observed in the ^{29}Si MAS nmr spectrum of 3C SiC. No peak has been observed in ^{13}C MAS nmr spectra of 3C SiC. The reason for this is clear when one compares the structure of diamond with that of 3C SiC in which all Si-C bond lengths are equal. The relaxation time T_1 is very long for diamond (65 hours),²⁴ therefore, one would expect a quite long T_1 for 3C SiC and no observable peak.

^{29}Si MAS nmr spectra of 15R polytype have three peaks (1:2:2 ratio) : -14.9, -20.8, -24.4 ppm, while four peaks (1:1:1:2) appear in ^{13}C spectrum and the chemical shifts are 13.3, 16.0, 20.7, 22.7 ppm. No satisfactory interpretation has been given.²² A collection of spectra is shown in Figure 4.

I.C.1.b ^{29}Si and ^{13}C nmr spectra of a SiC 6H single crystal

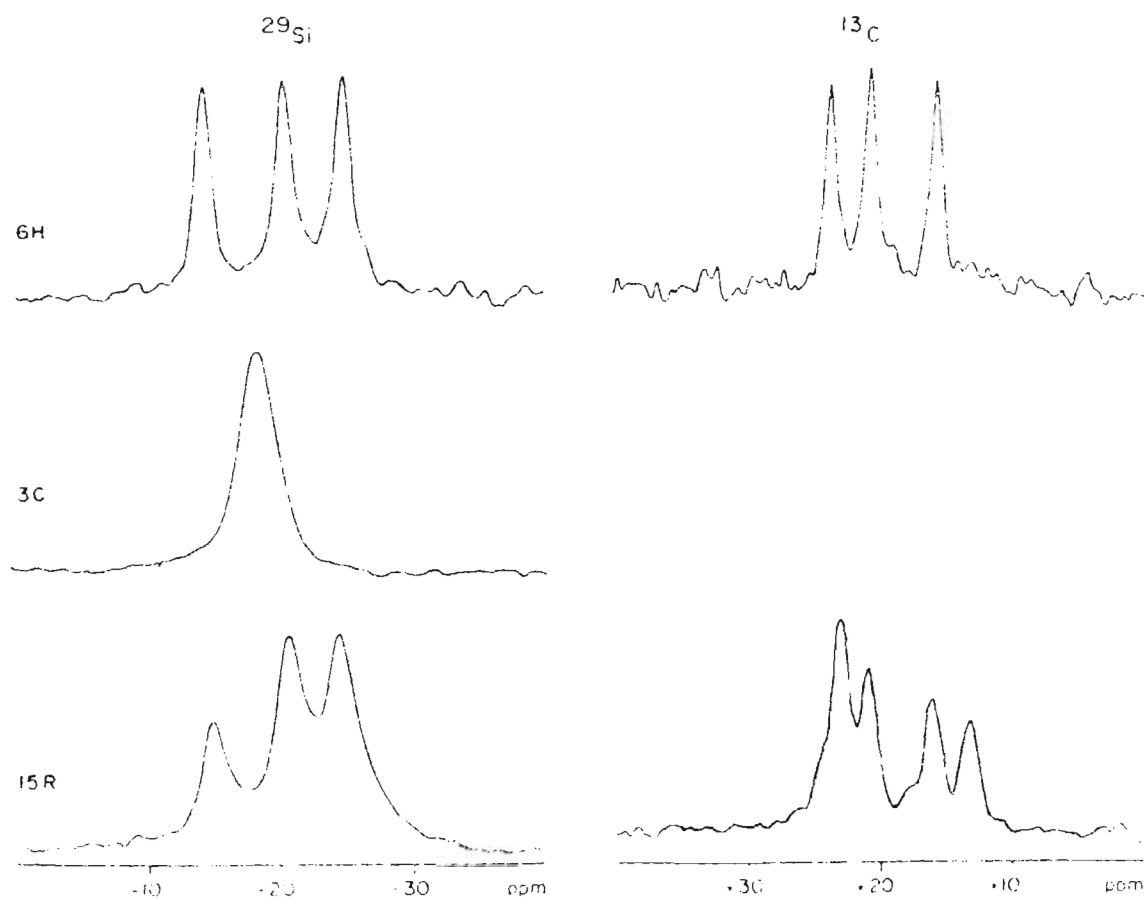


Figure 4 ^{29}Si and ^{13}C MAS nmr spectra of silicon carbide polytypes. Spectra were obtained at a magnetic field of 9.4 T with relaxation delays between pulses of 15 min.

^{29}Si and ^{13}C nmr studies were performed on a SiC 6H single crystal²³. The crystal was about $5 \times 5 \times 2 \text{ mm}^3$ in size. The plots of chemical shift versus orientation angle (defined as the angle between the applied magnetic field and the crystal c-axis) are demonstrated in figure 5 and figure 6. From the diagrams, we see two of the three silicons exhibit little difference between chemical shifts parallel and perpendicular to the c-axis, that is, the chemical shift changes slightly as the crystal is rotated so that the angle between the external magnetic field and the crystal c-axis varies. However, the other silicon and all of the carbons show differences of several ppm. An obvious conclusion is : chemically equivalent but crystallographically independent silicons or carbons in SiC polytypes have different magnetic anisotropies.

I.C.2 Theoretical studies of SiC polytypic structures

I.C.2.a Designation of crystallographical types

Since the first discovery of α -SiC structure by Ott^{7,25} and β -SiC structure by Hull,^{26,27} many SiC crystallographical data have been published.⁵ The only detailed and accurate X-ray structure refinement of a SiC polytype was performed on type 6H by Gomes de Mesquita.²⁸

By using the SiC approximate unit cell dimensions ($a=b=3.08\text{\AA}$) and layer spacings (2.52\AA), the number and distances of the second nearest neighbours have been calculated out to 5.00\AA from central atoms, and the crystallographical types have been created.²² As shown in Table 2, there are eight different sites; however, only four of them are distinct (see Figure 7), for the primed and non-primed types are the same except a difference of 60° rotation about the c-axis. All sites in a layer

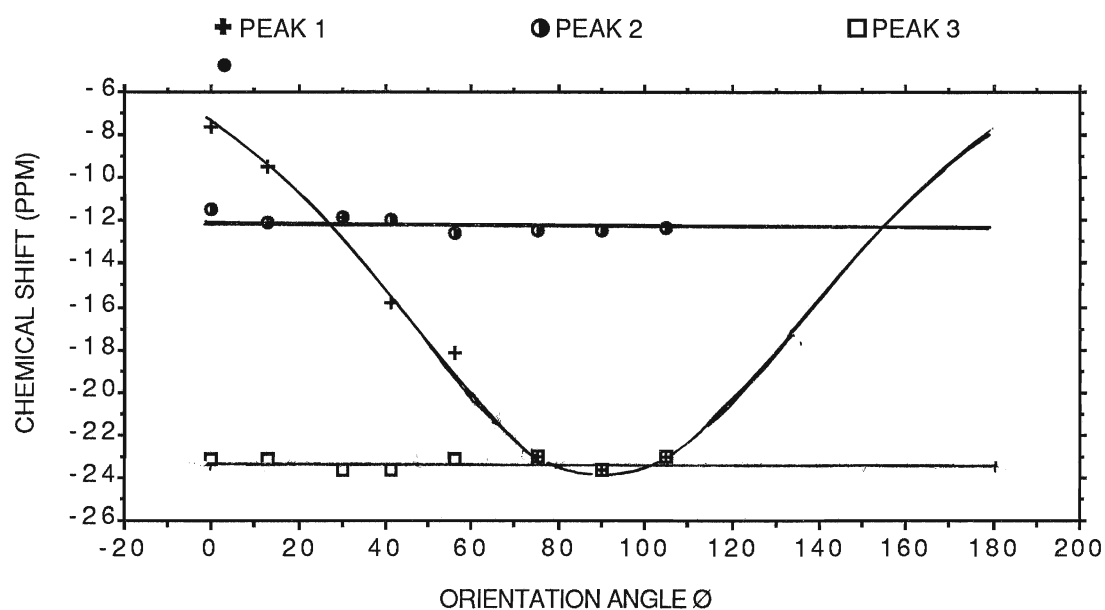


Figure 5 Plots of ^{29}Si -silicon chemical shifts versus orientation angles, \emptyset

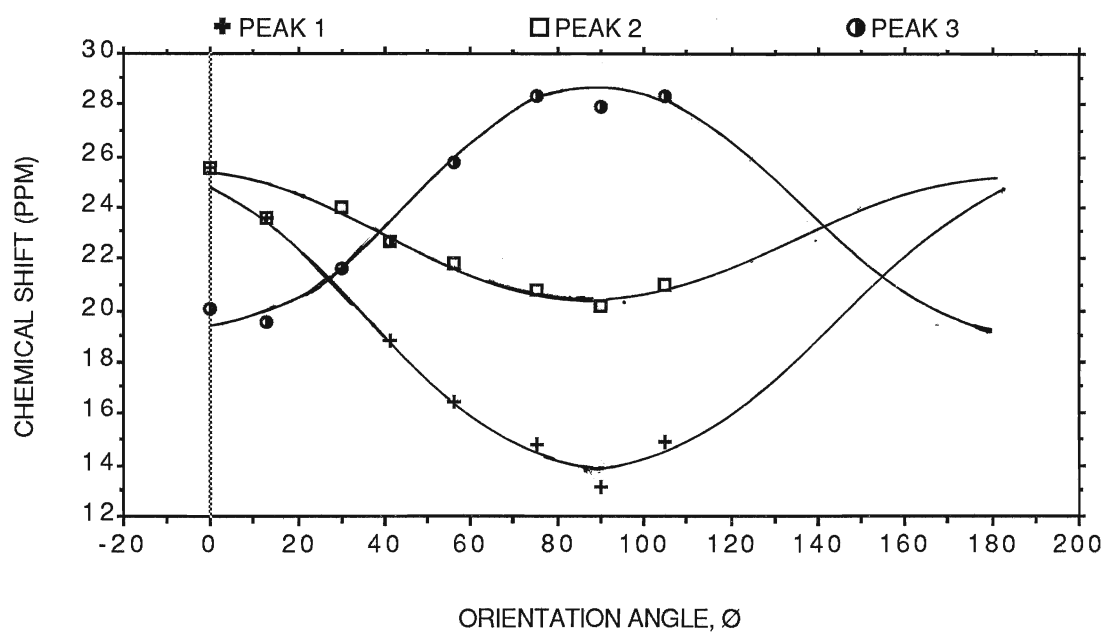
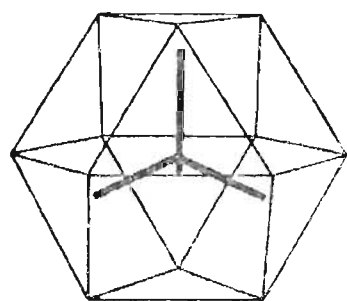
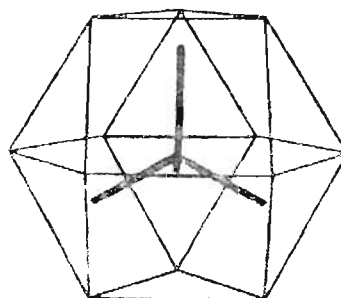


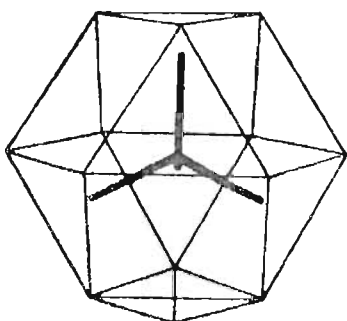
Figure 6 Plots of ^{13}C -carbon chemical shifts versus orientation angles, \emptyset



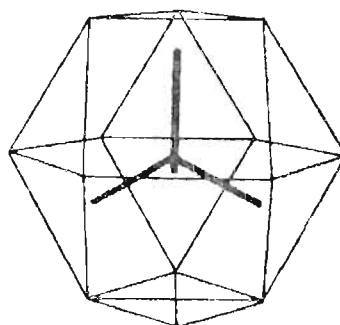
TYPE A



TYPE B



TYPE C



TYPE D

Figure 7 First and second neighbours for the possible types of silicon (or carbon) surroundings in silicon carbide polytypes.

Table 2 Type Designations in Silicon Carbide Polytypes

Type	Stacking Sequence	Type	Stacking Sequence
A	BCA*B	A'	CBA*C
B	CBA*B	B'	BCA*C
C	ACA*B	C'	ABA*C
D	ABA*B	D'	ACA*C

A*—the central atom.

are the same. Figure 8 shows the zig-zag sequences of the four types. The same relationship is applicable to A and C layer by using circular permutation of ABC, for instance, BCAC=ABCB=CABA. The number of crystallographically different sites in various polytypes and thus the possible number of nmr peaks and the relative intensity (based on relative abundance) have been deduced according to the type designation above.²² For example, ^{29}Si and ^{13}C nmr spectra of SiC 3C should have only one peak, and so should those of SiC 2H. Similarly, both ^{29}Si and ^{13}C spectra for SiC 6H and 15R should have three peaks, but the intensity ratios are 1:1:1 for 6H and 1:2:2 for 15R (see table 3). The only inconsistency between the theoretical predictions and the experimental results is the ^{13}C nmr spectrum of 15R where four peaks are actually observed (The expected number of peaks is three, see Figure 4).

I.C.2.b Semi-empirical and ab initio MO calculations

While nmr experimental determination of polytypic structures proved promising, theoretical consideration of structural aspects of bonding in silicon

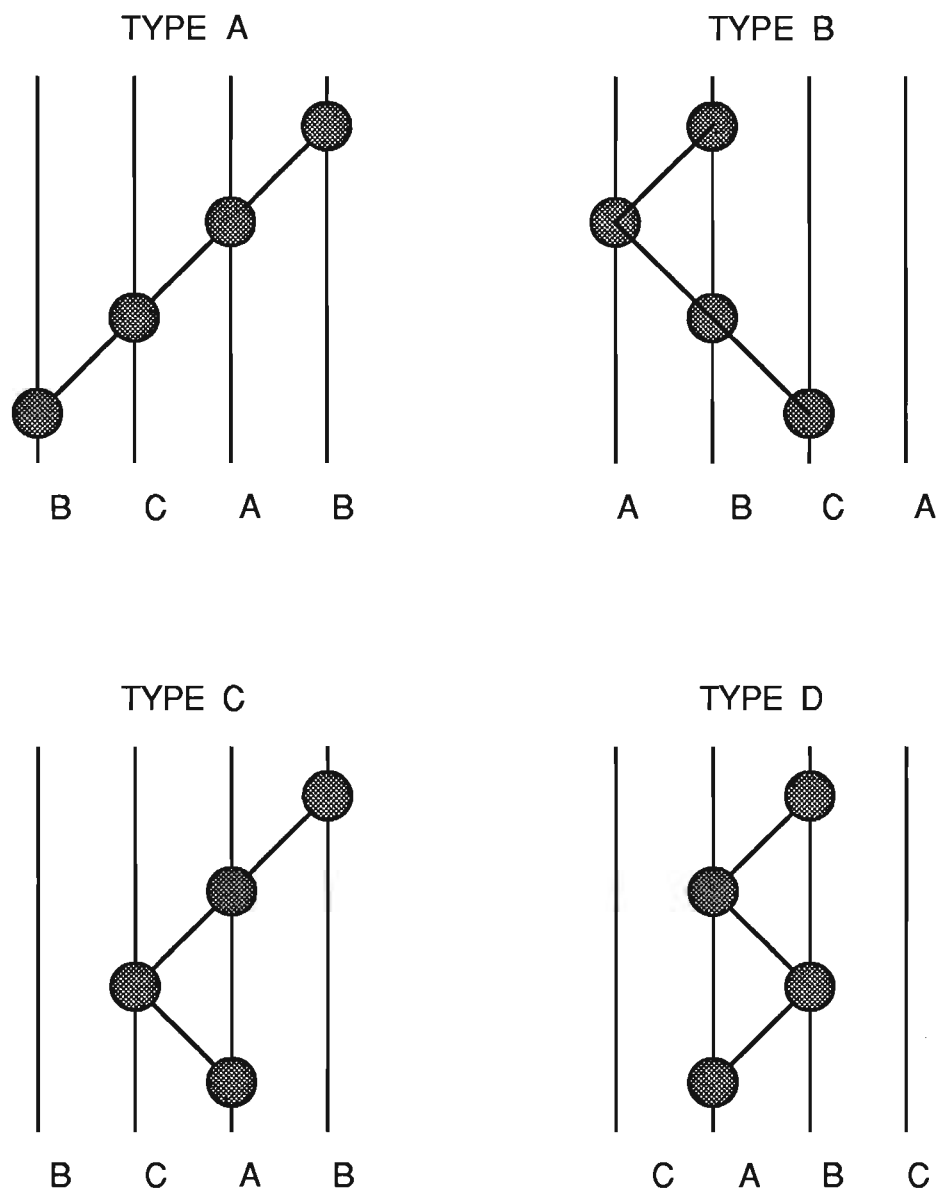


Figure 8. ZigZag sequences for the four types of silicon surroundings. Carbon atoms have been omitted for simplicity. The sequences shown are BCA*B (TYPE A), CBA*B (TYPE B), ACA*B (TYPE C), and ABA*B (TYPE D). The atom asterisked is the central silicon.

Table 3 Categorized Types of Si Sites in Some SiC Polytypes (reference 22)

Polytype	Sequence	Si Type	Cryst. Indep.	Equiv.nmr
			Si #	types #
2H	/AB/..	DD'	1	1
3C	/ABC/..	AAA	1	1
4H	/ABAC/..	CB'C'B	2	2 (1:1)
6H	/ABCACB/..	BCAB'C'A'	3	3 (1:1:1)
9R	/ABCBC-	DCB'DC		
	ACAB/..	B'DCB'	3	3 (1:1:1)
15R	/ABCBACAB-	BCB'C'A'BCB'		
	ACBCACB/..	C'A'BCB'C'A'	3	3 (1:2:2)

carbide also caught attention. In a recent paper by Guth et al.,²⁹ the Si-C bond lengths and angles were calculated using ab initio molecular orbital method, where SiC polytypes were modeled as $\text{Si}(\text{CH}_3)_4$ and $\text{C}(\text{SiH}_3)_4$, and the dimension of the molecules were constrained to the lattice dimensions of polytypes. Plots of calculated bond lengths and angles as a function of % hexagonality (defined as the number of hexagonal sites divided by the sum of the numbers of hexagonal and cubic sites in one unit cell) were given. From this, the following conclusions were drawn : 1) as the percent of hexagonality increases, vertical bonds lengthen and lateral bonds shorten with respect to the regular tetrahedral structures; 2) the difference between a vertical and a lateral bond length in cubic sites is smaller than that in hexagonal sites. Linear regressions of data of average spacings (c/a) and a-dimension from various sources ³⁰⁻³⁴ as a function of the % hexagonality were demonstrated and compared with those from calculations, such comparisons are

used to support the conclusions. Unfortunately, the linear regressions were based on the the average values of layer spacings (c/a) for each polytype of a corresponding percent hexagonality. Furthermore, the series of polytypic structures of SiC were simplified to the models of $\text{Si}(\text{CH}_3)_4$ and $\text{C}(\text{SiH}_3)_4$ in the MO calculation.

Another theoretical study related to SiC is concerned with Si-Si interactions in silicates.^{35(a)} It was expected that Si-Si interactions in SiC polytypes were responsible for the stretching of layer spacings along c -direction in a polytype of more percentage of hexagonal sites.²⁹

I.D.1 Chemical shift and nuclear shielding

I.D.1.a Theory of chemical shift

Chemical shift originates from the magnetic screening produced by electrons. It is a measurement of the extent that a nucleus is shielded with respect to the bare nucleus and to the other nuclei. In the external magnetic field, a nucleus experiences not the field applied, but rather the one that has been changed by the shielding of electrons surrounding the nucleus. Since electrons are magnetic particles, their motion in the applied field would induce a magnetic field that is opposite to the applied one. Thus, at a nucleus, the magnetic field is

$$H_{\text{local}} = H_0(1 - \sigma) \quad (1.1)$$

where σ is shielding factor.

The Larmor frequency, the frequency at which a nuclear magnetic resonance occurs, is directly proportional to the gyromagnetic ratio (γ) of the nucleus and the local magnetic field,

$$\nu = \gamma H_{\text{local}} / (2\pi) \quad (2.2)$$

The gyromagnetic ratio is a constant for a particular nucleus. The frequency at which the resonance occurs is called chemical shift. Thus chemical shift can be used to distinguish different nuclei and the same nucleus in different environments. A detailed discussion of the theory and application of nmr is given by Becker,^{35(b)} and will not be reproduced here.

I.D.1.b General aspects of nuclear shielding

The total electrons in a molecule can be divided to two parts : the local part with respect to the nuclei of interest (that is, the electrons constrained in the atomic orbital on the nucleus concerned and in the bond that is directly connected to the nucleus) and the non-local part which makes up the remainder electrons of the molecule. Nuclear magnetic shieldings are generally considered to be composed of three contributions : 1) local diamagnetic shielding ($\sigma^{\text{d}}_{\text{loc.}}$) arising from the magnetic field induced by local diamagnetic currents; 2) local paramagnetic shielding ($\sigma^{\text{p}}_{\text{loc.}}$) due to the magnetic field created by local paramagnetic currents; 3) non-local diamagnetic shielding ($\sigma^{\text{d}}_{\text{nl.}}$) due to dipolar interaction from distant anisotropic bonds $\sigma^{\text{d}}_{\text{loc.}}$ and $\sigma^{\text{p}}_{\text{loc.}}$ may be affected by various processes, such as induction,³⁶ resonance,³⁷ intramolecular electric fields,³⁸ steric effects,³⁹ and van der Waals interactions.⁴⁰ Besides long-range dipolar effects, $\sigma^{\text{d}}_{\text{nl}}$ may also be affected by ring currents elsewhere in the molecule.⁴¹

The mathematical expression for $\sigma_{P_{loc}}$ includes in the denominator energies of excitation, that is the differences in energy between ground and excited electronic state. For our purpose, only the theory and application of long-range shielding effects will be discussed in detail in the following subsection.

I.D.2.a Theory of long-range dipolar shielding

Theoretical investigation of magnetic shielding of a nucleus in a molecule due to distant electron clouds dates back to three decades ago.⁴²⁻⁴⁹ It was defined that long-range shielding was created by fields which did not arise from electrons constrained in atomic orbitals on the nucleus concerned, or in the chemical bonds directly connected to the nucleus. A general equation for tensorial shielding of nucleus N was derived by Ramsey by means of second order perturbation theory.⁵⁰ By considering the shielding of the nucleus N due to the circulation of specific group G electrons along an anisotropic bond A-B and assuming that the electron cloud in group G does not interact appreciably with nuclei, McConnell⁴⁸ introduced Ramsey's equation⁵⁰ and approximated it to a simple formula by the definition of "long-range shielding":

$$\sigma_N^G = 1/L_0 [X_G/R^3 - 3X_G \cdot \mathbf{RR}/R^5] \quad (1.3)$$

where L_0 —Avogadro's number

X_G —the molar magnetic susceptibility tensor

\mathbf{R} —the radius vector pointed from the nucleus to the origin of group G

\mathbf{RR} —a dyad

Actually, the magnetic field \mathbf{H}_N that a nucleus actually sees can be related to the externally applied uniform magnetic field \mathbf{H}_0 by the shielding tensor σ_N as

$$\mathbf{H}_N = \mathbf{H}_0 - \sigma_N \mathbf{H}_0 \quad (1.4)$$

In liquids, the only observable shielding of nucleus N due to group G is the average of the tensor over molecular tumbling and internal motions of the molecule. Assuming that the group G is axially symmetric, that is $\chi_{xx} = \chi_{yy}$, the shielding σ_N^G is given by (see appendix 1)

$$\sigma_N^G = \Delta\chi_G / (3L_0 R^3) (1 - 3\cos^2\phi)_{\text{ave}} \quad (1.5)$$

where $\Delta\chi = \chi_{\parallel} - \chi_{\perp}$ is the bond anisotropy in molar susceptibility of group G

ϕ —the angle between vector **R** and the symmetry axis of group G

χ_{\parallel} , χ_{\perp} —the magnetic susceptibilities parallel and perpendicular to the symmetry axis of group G

I.D.2.b Application of long-range dipolar shielding

The theory of long-range dipolar shielding was first applied to proton shielding in formamide and dimethylformamide.⁵¹ The proton and nitrogen-14 nmr spectra of formamide were obtained by Piette et al.⁵² and those of dimethylformamide were acquired by Phillips⁵³ and Gutowsky.^{54(a)} The results indicated that the rotation about the C-N bond was restricted and that the two sites marked A and B were chemically equivalent but magnetically non-equivalent (figure 9), since the spectra showed two distinct resonance lines corresponding to two types of protons. If one made a reasonable assumption that the effect of distant groups (e.g. C=O) on local diamagnetic shielding (σ_{loc}^d) on proton A and B are approximately equal, then the difference between nuclear shieldings of proton A and B is the result of the difference between $\sigma_{\text{nl}}^d(\text{A})$ and $\sigma_{\text{nl}}^d(\text{B})$, for σ_{loc}^p can be neglected for proton. The magnetic anisotropy of the C=O bond was calculated and the sites of proton A and B were identified.⁵¹ For dimethylformamide, the rotation

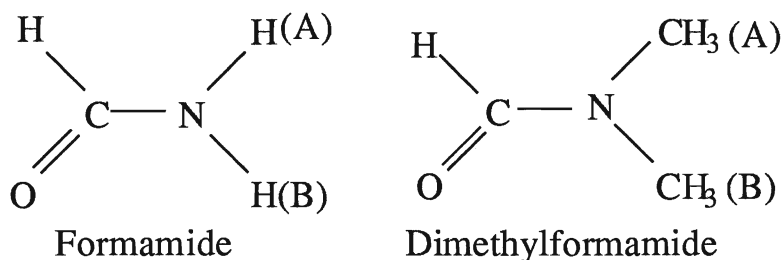


Figure 9 Structures of amides with magnetically non-equivalent sites marked A and B.

of the methyl groups around C-N bonds causes the distances and angles between the C-H bond and the C=O bond to vary, and appropriate averages of distances and angles have to be used to calculate magnetic anisotropies in this molecule.⁵¹

A review of the contribution to the shielding of a nucleus arising from the magnetic fields of distant bonds or groups within the molecule was given in the literature,^{54(b)} in which point dipole approximation of equation 1.5 was extended to include higher magnetic multipoles such as quadrupole and octupole.

More recently, the long-range shielding was employed to evaluate the diamagnetic anisotropies of organometallic moieties—carbonyl ligands in $M(\text{CO})_3$ fragments ($M=\text{Cr}, \text{Mo}, \text{W}$).⁵⁵ The χ values of the carbonyl ligands yielded by using McConnell relationship reveal that the organometallic fragments have large bond magnetic anisotropies than the commonly encountered organic moities and thus have profound effects on the shifts of neighbour nuclei.

I.E Thesis scope

Each crystallographically independent silicon atom (or carbon atom) is bonded to its first nearest carbon atoms (or silicon atoms) in the same way as the others. The fact that different chemical shifts are observed for them inspires us to consider long-range dipolar shielding. With this focus in mind, we carried out the following theoretical and experimental studies: (1) calculations of the long-range shieldings according to McConnell's equation,⁴⁸ (2) assignments of the observed shifts to the crystal lattice sites, (3) determination of the factors that affects the magnitude of the long-range shielding (the stacking sequence, the layer spacings, and the electrical centre of gravity), (4) the development of equations relating the chemical shift to layer spacings, (5) the refinements of the 6H and 15R polytypic structures by using MAS nmr chemical shifts, and (6) the use of single-crystal chemical shift tensors for refining 6H SiC polytypic structure.

CHAPTER II

THEORETICAL CALCULATIONS OF CHEMICAL SHIFTS OF SILICON CARBIDE POWDER SAMPLES

II.A Introduction

Early calculation of bond distances was done by Gomes de Mesquita for SiC 6H polytype.²⁸ He showed that there were one long bond and three short bonds for each crystallographically independent silicon or carbon (table 4). Further calculations of distances from the central atom to the second nearest neighbour

Table 4 Bond Lengths in 6H Silicon Carbide

TYPE	1 LONG BOND (Å)	3 SHORT BONDS (Å)
Si(1)	1.894	1.886
Si(2)	1.891	1.885
Si(3)	1.894	1.885

atoms were reported by Hartman, et al.²² The calculations and considerations of surroundings at the second-neighbour level have produced type designations which accounts for the number and relative intensity of nmr peaks. However, the prediction gives three peaks but actually four peaks were observed in ¹³C nmr spectrum of 15R; it is also desirable to become more quantitative and to increase the predictive capacity of this approach, therefore, computer programs calculating the chemical shift increment $\Delta \sigma$ due to long-range effects are considered.

II.B Computer program set-up

II.B.1 Procedure

Using the relationship between chemical shift increment $\Delta\sigma$ and the molar diamagnetic anisotropy ($\Delta\chi$) of a distant bond (axially symmetrical), the chemical shift of a given silicon or carbon is given by

$$\sigma_{x(j)} = \sigma_i^x + \Delta\chi g(j) \quad (2.1)$$

$$g(j) = \sum_n [(1 - 3\cos^2\phi_n)/(3R_n^3)] \quad (2.2)$$

where $\Delta\chi$ is the difference between the susceptibility parallel to, and perpendicular to, the bond direction in the unit of cubic Angstroms per bond; R is the distance between the atom concerned and the electrical centre of gravity of the bonds in unit of Angstroms; ϕ is the angle between the vector R and the bond vector

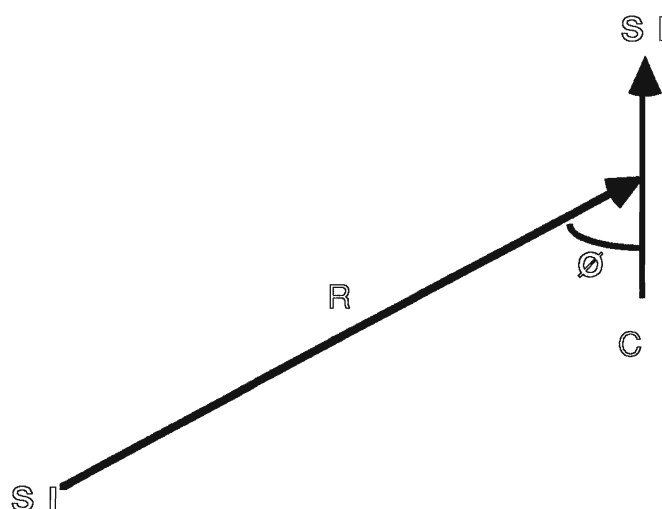


Figure10 Relationship among bond vector, radius vector(R), and angle(ϕ) in the geometric factor calculation.

in degrees (see figure 10); $\sigma_{x(j)}$ is the chemical shift (ppm) of atom $x(j)$ in the structure; σ_i^x is the intrinsic chemical shift (ppm), i.e. the shift that atom x would have if it were bonded only to its four nearest neighbours; $g(j)$ is the geometric factor of atom j ; $(\Delta\chi)(g)$ means the chemical shift due to long-range shielding from the diamagnetic susceptibility of bonds. The sum is over all bonds n out to a certain limit.

II.B.1.a Coordinates input

All of our programs are written in Fortran language. For each silicon and carbon in the unit cell, the fractional coordinates are supplied to it with respect to the crystallographical frame. By giving a silicon (or a carbon) a two dimensional array where the first subscripted variable represents crystallographically independent silicon (or carbon) and the second the crystal axes (e.g. x,y,or z), each silicon or carbon can be specified. For example, a value given to Si(2,3) means the fractional coordinate along z-axis of Si number two.

II.B.1.b Calculation of R and $\cos\phi$

The programmable calculations of various distances from some atoms to distant bonds, and angles between radius and bond vectors are possible with vector and tensor algebra. The basic equations used in the calculation of R and $\cos\phi$ are given by,⁵⁶

$$R = \sqrt{\mathbf{U} \cdot \mathbf{V}} = \sqrt{\bar{\mathbf{U}} \mathbf{g} \mathbf{V}} = \sqrt{\bar{\mathbf{V}} \mathbf{g} \mathbf{U}} \quad (2.3)$$

$$\cos\phi = \mathbf{U} \cdot \mathbf{V} / (UV) \quad (2.4)$$

where R, ϕ, U, V are scalars

\mathbf{U}, \mathbf{V} are vectors, described in terms of contravariant quantities, for instance,

$$U = \begin{bmatrix} u^1 \\ u^2 \\ u^3 \end{bmatrix}$$

U, V are the magnitudes of vector U and V

\bar{U}, \bar{V} are transposes of vectors U and V, e.g. $U = [u^1, u^2, u^3]$

$$g = \begin{bmatrix} g_{11} & g_{12} & g_{13} \\ g_{21} & g_{22} & g_{23} \\ g_{31} & g_{32} & g_{33} \end{bmatrix} = \begin{bmatrix} a_1 a_1 & a_1 a_2 \cos \phi_3 & a_1 a_3 \cos \phi_2 \\ a_1 a_2 \cos \phi_3 & a_2 a_2 & a_2 a_3 \cos \phi_1 \\ a_1 a_3 \cos \phi_2 & a_2 a_3 \cos \phi_1 & a_3 a_3 \end{bmatrix} \text{ is a}$$

symmetric second-rank tensor, in which a_1, a_2, a_3 are the unit cell dimensions along crystal a, b, c axes, and ϕ_1, ϕ_2, ϕ_3 are angles between crystal b and c, a and c, a and b axes respectively.

The calculations involving components of the second-rank tensor g are processed in a subroutine subprogram. The latest edition of programs are capable of geometric factor calculations for different selection of electrical centre of gravity.

II.B.1.c Method of summation

The summation of calculated geometric factors is accomplished in a three-dimensional network style with each of the units being a crystal unit cell and the atom concerned lying at the centre of the interaction sphere. It starts at the first layer of the most bottom-left-back unit cell, goes through the first column, second column • • •, then does the same thing for second, third layer • • •, until the unit cell is complete (e.g. six layers for 6H), moves one unit cell up, two unit cells up, • • •. A schematic representation of the calculation net work projecting on the (001) plane is shown in figure 11.

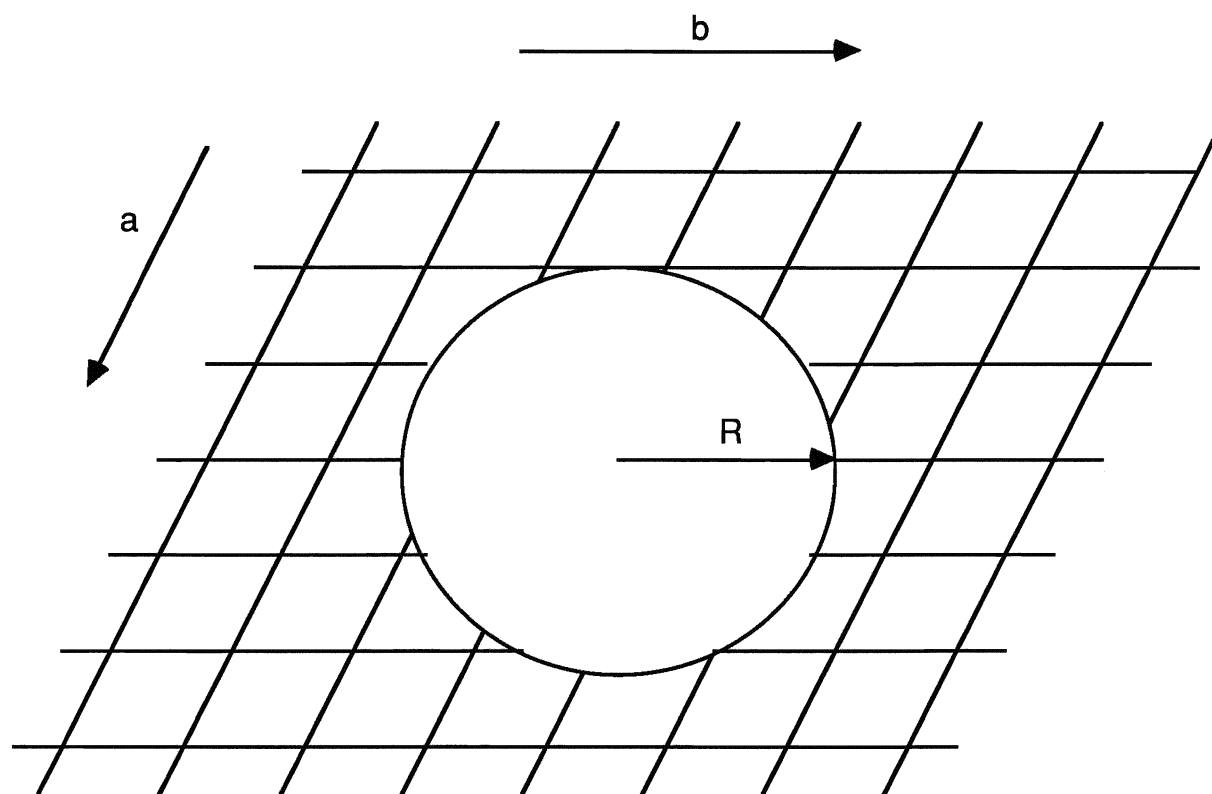


Figure 11 Diagram of calculation network projected on the (001) plane

The programs are designed to calculate long-range effects. According to McConnell's long-range shielding theory, "a shielding field at a given proton will be considered to be 'long-range' if the field does not arise from electrons contained in the atomic orbitals centered on the proton, or in the chemical bond which holds the proton to its host molecule."⁴³ Similarly, in the case of long-range shielding effect in SiC polytypes, the first nearest neighbours have to be eliminated in the calculations. The implied assumption is that the first neighbour bonds contribute the same to chemical shieldings regardless of the types of silicons or carbons, in spite of the lengths of immediate bonds around one type of silicon (or carbon) are as large as .003 Å different from those of other type. Two pieces of evidence underlie the assumption: 1) as shown in table 4, Si(1) and Si(3) have the same vertical or lateral

bond lengths,²⁸ but their chemical shifts are different;²² 2) the diamagnetic susceptibility of cubic SiC, calculated to the first neighbour level by using Hartree-Fock orbitals, is independent of the choice of origin and free from any scaling parameters.⁵⁷ From these facts follows the conclusion: it may not be the bond length differences (≤ 0.003 Å), but it is the second and higher neighbours that critically cause such big differences among chemical shifts of silicons or carbons.

II.C Selections of unit cell dimensions and layer spacings

II.C.1 SiC 6H

The unit cell dimensions are chosen from Adamsky and Mertz,⁵⁸ and shown in table 5. The layer spacings and bond distances are selected from Gomes de Mesquita.²⁸ From Mesquita's data, the only layer spacing determined explicitly is Si(2)-Si(3). The remaining $c/2$ distance was divided equally to two parts for h-c and c-h layer spacings (assuming Si(1') lying at $c/2$). All carbon atoms lie at 1.894 Å above the corresponding silicon atoms except C(2) and C(2') which are 1.891 Å above silicons (figure 12). A noticeable point from Mesquita's X-ray structure refinement of 6H is that the c-c and h-c distances are significantly different.

II.C.2 SiC 15R

The c - dimension used in the calculation of geometric factors is predicted from Mesquita's layer spacings. The stacking sequence of 15R polytype is hchcc hchcc hchcc and is different from that of 6H (hcc hcc). By assuming the spacing of h-c or c-c in 15R is the same as in 6H, the c -dimension of the unit cell in 15R is determined by summing-up all layer spacings along c -axis in one unit cell (37.8033

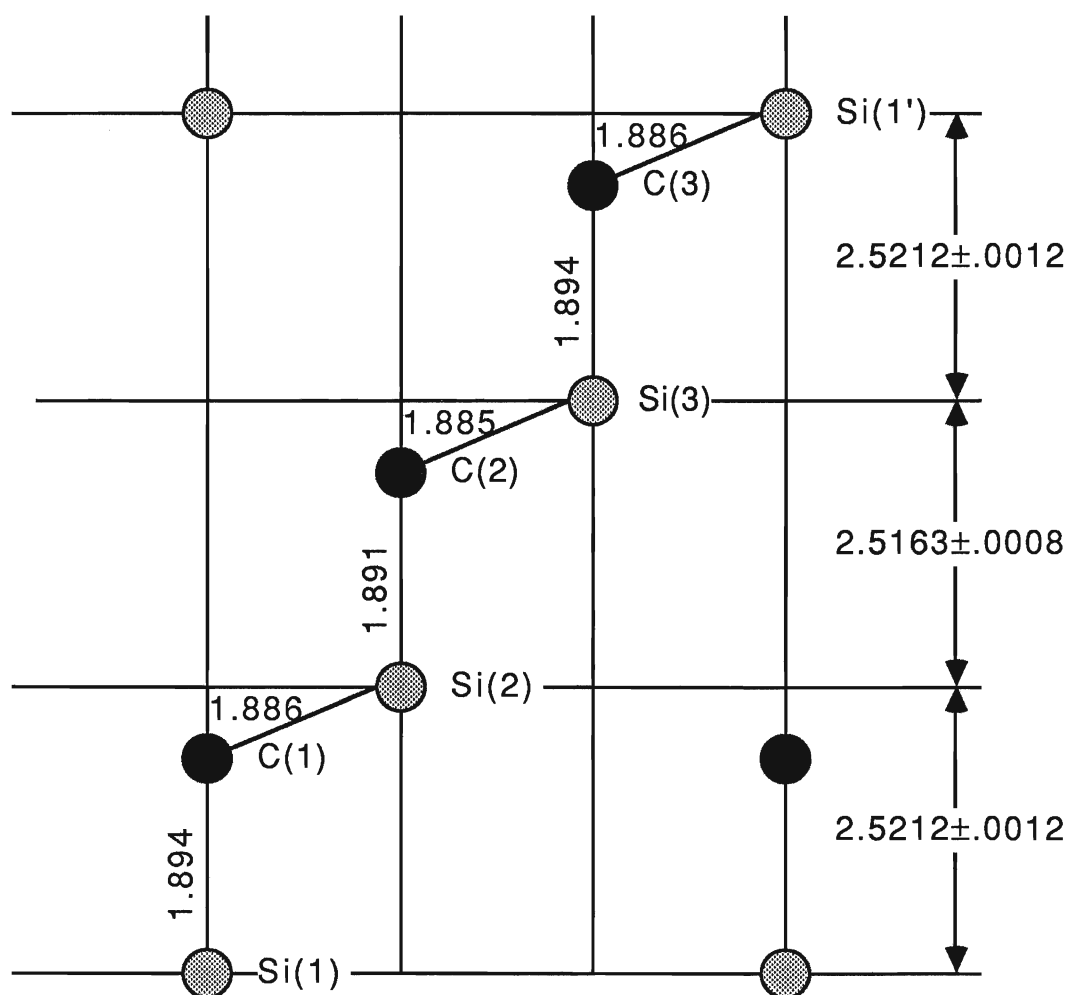


Figure 12 Bond Distances and Layer Spacings in SiC 6H (Å) (Reference 28)

Å), and thus the c fractional coordinates of all atoms can be defined. The a-dimension is derived from the c/a ratio of 15R form from Gmelin Handbook of Inorganic Chemistry⁵⁹ (3.08058Å). Compared with the a and c dimension reported by Tairov⁶⁰, the values predicted are within .002 Å error for c-dimension and .00015 Å for a-dimension. The program calculating geometric factors of 15R SiC is given in appendix 3.

Table 5 Lattice Constants of Some SiC Polytypes
(p is the number of Si-C double Layers in Hexagonal Unit)

TYPE	C(Å)	C/p(Å)	a(Å)	C/pa
3C*	7.55124	2.51708	3.08269	0.8165
6H*	15.1173 ⁸	2.5196	3.0806 ⁵	0.8179
2H [†]	5.048 ⁰	2.524	3.076 ³	0.8205
15R*	37.8014	2.52009	3.08043	0.8181

†—Reference 58

*—Reference 60

II.C.3 SiC 3C and SiC 2H

Among all SiC polytypes, 3C is the only one which has the cubic space group (F43m). This indicates that all Si-C bond lengths are equal (1.88778 Å, calculated from the unit cell dimensions reported by Tairov et al.⁶⁰). Opposite to the bond length difference in SiC 3C which has 0% hexagonal sites, the difference between vertical bond length (1.8934 Å) and lateral bond length (1.8874 Å) is the largest in SiC 2H (100% H).²⁹ The unit cell dimensions by Adamsly and Mertz⁵⁸ (a=3.076³

Å, $c=5.0480$ Å) are used to calculate the approximate geometric factors. The results of these calculations will be shown in this chapter.

II.D Preliminary studies on chemical shift calculations

II.D.1 Convergence of geometric factors.

During the preliminary period of studies, several modifications of programs were tried to determine a few unknown parameters. One of these was to calculate the total geometric factors within certain limits as a function of the distances from central atoms to the outmost bonds. As the distance increases, the number of interaction bonds increase as R^3 , e.g. from 100,000 bonds within 50 Å to 800,000 bonds within 100 Å. From figure 13, we can see that the convergences of geometric factors calculated are quite slow. The nearby bonds have the largest effect (g is proportional to $1/R^3$), but satisfactory convergences are not reached until 100 Å. Therefore, we conclude that a distance of 100 Å was required to avoid any error introduced in the calculation of long-range shielding effect.

II.D.2 Contribution from individual layers

Another interesting topic at the earlier stage was to find out which layers contributed most to the total geometric factors. For this purpose, the program for 6H SiC was modified to split the total geometric factors down to individual layer. The results from these calculations, recorded in table 6, give us a clear picture about layer contributions and distinctions among silicons. It is obvious that the main contributions come from the layers where the silicons being calculated are located and the one immediately below. However, the contributions from these two layers

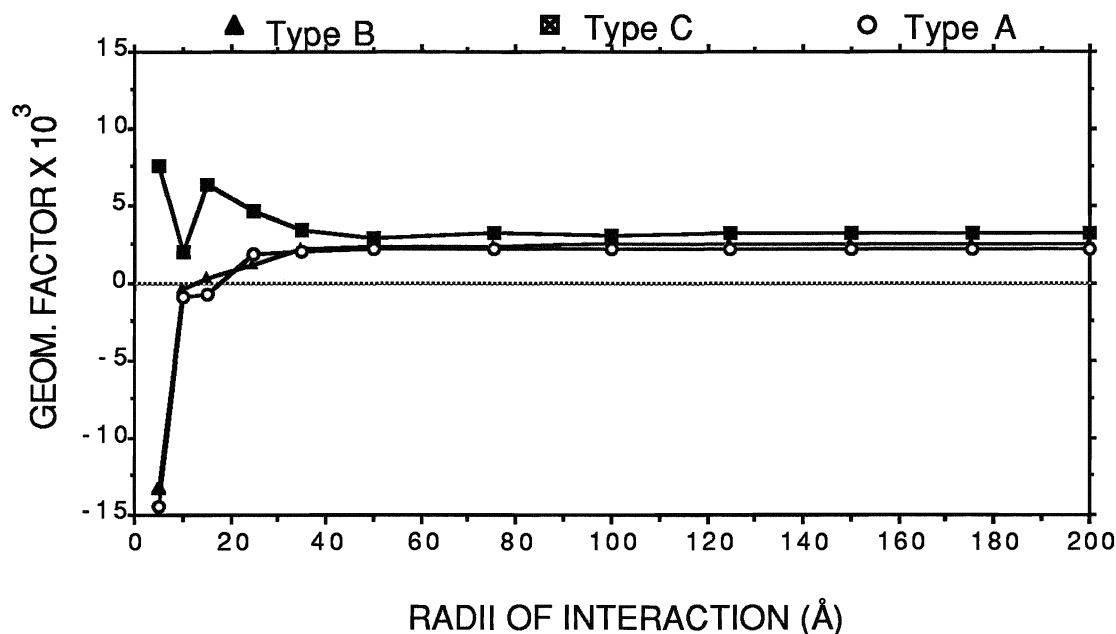


Figure13 Geometric Factors Versus Radii of Interaction Spheres (SiC 6H).

tend to cancel each other considerably. It is the one two layers' down that creates distinctions among silicons. Excitingly, these conclusions seem consistent with the earlier type assignments (table 2), in which the types were designated by considering the neighbours to one layer up and two layers down..

II.E Peak assignments and chemical shift calculations

II.E.1 Calculations of geometric factors

Assuming that the electrical centre of gravity of Si-C bond lies at the bond midpoint, we have calculated the geometric factor for each crystallographically independent atom in the unit cell by running the computer programs described in

Table 6 Geometric Factors of Silicon For Individual Layers (SiC 6H, R=150 Å)

Layer Number	Geometric Factor		
	Si(1)	Si(2)	Si(3)
+3	0.0000030	.0000069	0.00000026
+2	0.0000045	0.0000053	.0000062
+1	0.000548	0.000547	0.0005537
Central	0.0699975	0.069875	0.069997
-1	-0.070936	-0.0709073	-0.071271
-2	0.0025901	0.0033668	0.0026072
-3	0.000016	-0.0000042	0.0000133

appendix 2 (6H) and in appendix 3 (15R). The computational jobs were run on Burrough-7900 computers available at Brock University. The geometric factors of silicons and carbons are calculated in separate programs. For 2H and 3C , geometric factors were also obtained for comparison. A summary of calculated geometric factors for four polytypes is given in table 7.

II.E.2 Peak assignments and chemical shift calculations in SiC 6H

Shown in table 7, six geometric factors—three for silicons and three for carbons—are obtained for 6H-SiC. The number of distinct values corresponds exactly with the number of peaks in the ^{29}Si and ^{13}C spectra. Two ways to assign

Table 7 Summary of Calculated Geometric Factors
of four polytypes ($\times 10^3$)

Atom being Calculated	Polytypes			
	6H	15R	3C	2H
Si(1)	2.517	2.443	2.424	3.303
Si(2)	3.188	3.304		3.303
Si(3)	2.235	2.458		
Si(4)		3.142		
Si(5)		2.181		
C(1)	2.654	2.456	2.424	3.303
C(2)	2.019	3.304		3.303
C(3)	3.269	2.554		
C(4)		1.962		
C(5)		3.256		

the observed chemical shifts to calculated geometric factors are possible (see table 8). Consequently, both ways have to be adopted in the present calculation. A least squares fitting program is designed to calculate bond magnetic anisotropy, intrinsic

chemical shifts, and theoretical chemical shifts (appendix 4). These calculated values are summarized in table 9.

Table 8 Assignments of Nmr Chemical Shifts
to the Calculated Geometric Factors (SiC 6H)

Type	Si(1)	Si(2)	Si(3)	C(1)	C(2)	C(3)
$g \times 10^3$	2.517	3.188	2.235	2.654	2.019	3.26
Assig.1	-20.4	-24.7	-14.5	20.4	23.4	15.1
Assig.2	-20.4	-14.5	-24.7	20.4	15.1	23.4

Figure 9 Calculated Bond Magnetic Anisotropy ($\Delta\chi$) and
Intrinsic Chemical Shifts of Si and C For Two Assignments

Assignment Number	Intrin. Shift of Silicon	Intrin. Shift of Carbon	Magn. Suscept. ($10^{-33}\text{m}^3/\text{bond}$)
1	0.79	40.13	-97.8
2	-40.96	-1.63	100.5

Assignment 1 gives a negative $\Delta\chi$. Its sign is contradictory to that of magnetic anisotropies of single bonds; for example, $\Delta\chi$ of C-C bond ($140 \times 10^{-36} \text{ m}^3/\text{molecule}$) is positive.⁶¹ When the applied magnetic field \mathbf{H}_0 is parallel to the

C-C bond, there is hindrance to rotation of the electron cloud for such molecule as C_2H_6 . On the other hand, assignment 2 gives the more likely sign and will be adopted in the following calculations.

A short comment on the units of $\Delta\chi$ needs to be mentioned here. According to McConnell's equation,⁴³ $\Delta\chi$ is given in units of cubic centimetre per mole when σ is expressed in parts per million and R in centimetre. Multiplication by $(4\pi/N)\times 10^{-6}$, where factor 4π is required for the conversion from electromagnetic unit to SI unit, $\Delta\chi$ is converted to a value in SI unit.⁵⁵ In our case, R is given in units of Angstrom, so $\Delta\chi$ has to be expressed in $\text{ppm} \cdot \text{\AA}^3/\text{bond}$ in order to achieve a final unit of ppm for $\Delta\chi \cdot g$ term. However, the $\Delta\chi$ calculated and expressed in this way is about three orders larger than the values from the literature (e.g. $\Delta\chi = 140 \times 10^{-36} \text{m}^3/\text{molecule}$ for C-C bond).

For assignment 2, the chemical shifts of all types of silicons and carbons have been calculated and given in table 10. Compared with the observed values, some of the calculated chemical shifts show large inconsistencies (up to 1.6 ppm). As one will see later, it is these differences that lead us to consider nmr as a possible tool for crystal structure determination and refinement.

Table 10 Observed Chemical Shifts Versus Calculated (ppm)
Before shifting Layer Spacings (SiC 6H)

	Si(1)	Si(2)	Si(3)	C(1)	C(2)	C(3)
Obsd	-20.4	-14.5	-25.1	20.4	15.1	23.4
Calcd	-20.8	-15.5	-23.1	19.6	14.5	24.5

II.E.3 Peak assignments and chemical shift calculations in 15R-SiC

Unlike 6H-SiC which has only two possible ways of assignments, 15R-SiC has many ways of assigning the observed chemical shifts to geometric factors. Although the specification of the sign of $\Delta\chi$ reduces the possibilities by half, at least four assignments have to be considered (see Table 11). Table 12 shows the chemical shifts calculated via least-squares fits for each assignment. The corresponding intrinsic shifts and bond magnetic anisotropies are summarized in table 13. So far, a most probable way of peak assignment can not be decided.

II.F Relationships between the observed shifts and the calculated geometric factors

Since we have calculated the geometric factors and known the assignments of peaks to lattice sites, we can plot out the chemical shifts as a function of geometric factors for silicons and carbons. As shown in figures 14 and 15 (where the electrical centre of gravity lies at 0.498 of the Si-C bond length from carbon atom), the observed relationship is roughly as expected but not linear, as some points are far off the straight lines. In order to correlate these off points with the straight lines, we need to change the geometric factors, that is , to shift the layer spacings. This will be covered in the next chapter.

II.G Determination of electrical centre of gravity

The calculations having been done so far are based on the assumption that electrical centre of gravity (ECG) lies at the bond midpoint. We can not specify Si-C bond midpoint as the actual ECG unless we have further evidence. One way to determine the ECG is to know the place where the best least squares fits occur when

Table 11 Peak Assignments in SiC 15R

Type	Si(1)	Si(2)	Si(3)	Si(4)	Si(5)	C(1)	C(2)	C(3)	C(4)	C(5)
g x10 ³	2.443	3.304	2.458	3.142	2.181	2.456	3.304	2.554	1.962	3.256
Assign.1	-24.4	-14.9	-20.8	-20.8	-24.4	16	22.7	20.7	13.3	22.7
Assign.2	-24.4	-14.9	-20.8	-20.8	-24.4	20.7	22.7	16.0	13.3	22.7
Assign.3	-20.8	-14.9	-24.4	-20.8	-24.4	16.0	22.7	20.7	13.3	22.7
Assign.4	-20.8	-20.8	-24.4	-14.9	-24.4	16.0	22.7	20.7	13.3	22.7

Table 12 Calculated Chemical Shifts in SiC 15R

Type	Si(1)	Si(2)	Si(3)	Si(4)	Si(5)	C(1)	C(2)	C(3)	C(4)	C(5)
Assign.1	-22.9	-17.0	-22.7	-18.1	-24.6	17.4	23.1	18.0	14.0	22.8
Assign.2	-22.8	-17.1	-22.7	-18.2	-24.5	17.4	23.0	18.1	14.2	22.7
Assign.3	-22.8	-17.0	-22.7	-18.1	-24.6	17.4	23.1	18.0	14.0	22.8
Assign.4	-22.7	-17.3	-22.6	-18.3	-24.4	17.4	22.9	18.1	14.3	22.6

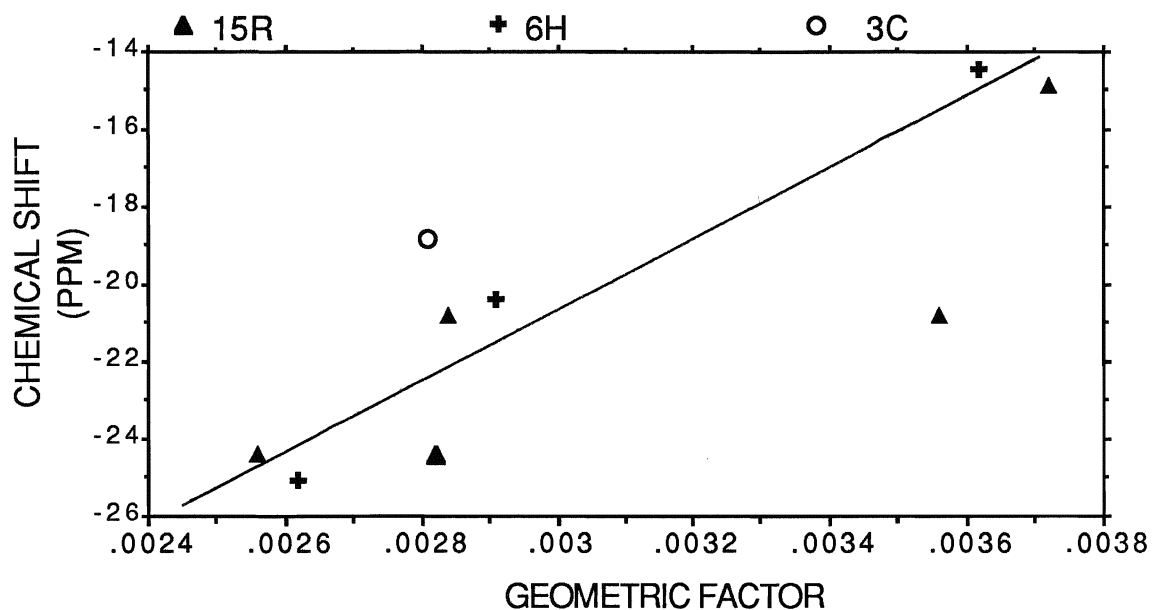


Figure 14 SILICON-29 CHEMICAL SHIFTS V.S. GEOMETRIC FACTORS FOR SiC POLYTYPES.

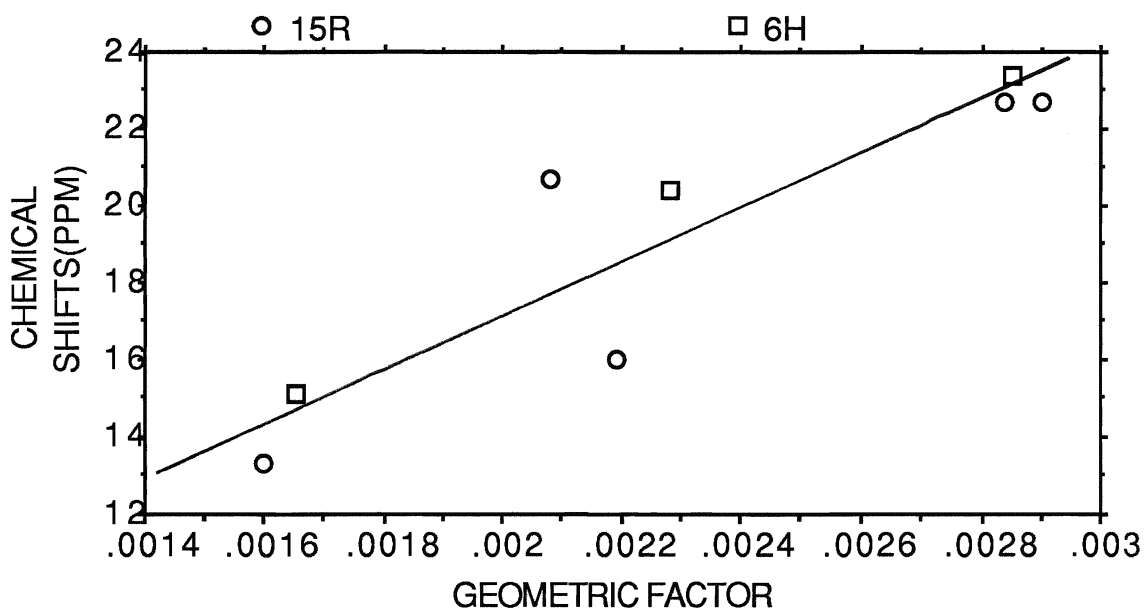


Figure 15 CARBON-13 CHEMICAL SHIFTS V.S. GEOMETRIC FACTORS FOR SiC POLYTYPES.

Table 13 Summary of Calculated Intrinsic
Chemical shifts, Bond Magnetic Anisotropies
For Various Assignments in SiC 15R

Number	$\sigma_{\text{Si}}^i(\text{ppm})$	$\sigma_{\text{C}}^i(\text{ppm})$	Δx ($10^{-33}\text{m}^3/\text{bond}$)
Assign.1	-39.49	0.64	85.59
Assign.2	-38.94	1.20	83.03
Assign.3	-39.42	0.71	85.29
Assign.4	-38.27	1.87	79.92

moving it along Si-C bond in a certain increment, while the best least squares fits could be found by examining the residual R (defined in equation 2.5).

$$R = \frac{\sum |\sigma_{\text{Obsd.}} - \sigma_{\text{Calcd.}}|}{\sum |\sigma_{\text{Obsd.}}|} \quad (2.5)$$

For example, given the ECG lies at a point which is $(\text{ECG} \cdot D)$ Å from carbon atoms and $[(1-\text{ECG}) \cdot D]$ Å from silicon atoms (where D is the Si-C bond distance), we can change ECG from 0.485 to 0.501 by a increment of 0.02, calculate intrinsic chemical shifts, magnetic anisotropies, and theoretical chemical shifts, then compare them with the observed chemical shifts in turn. The best ECG would lie approximately at the point where the minimum residual is reached. Table 14 summarizes the calculated chemical shifts and table 15 shows the corresponding intrinsic chemical shifts, bond magnetic anisotropies, and the residual values (R) for 6H SiC. From these R values, it can be concluded that the best fit occurs approximately at an ECG value of 0.489.

Table 14 Calculated Chemical Shifts for Different
Electrical Centre of Gravity (SiC 6H)

E.C.G. TYPE	.485	0.487	.489	.491	.493	.495	.497	.499	.501	Obsd.
Si(1)	-21.91	-21.87	-21.73	-21.63	-21.53	-21.37	-21.24	-21.13	-20.97	-20.4
Si(2)	-13.88	-14.03	-14.27	-14.43	-14.64	-14.86	-15.17	-15.42	-15.74	-14.5
Si(3)	-24.21	-24.10	-24.00	-23.94	-23.83	-23.77	-23.59	-23.45	-23.29	-25.1
C(1)	20.47	20.36	20.34	20.27	20.15	20.02	19.89	19.76	19.64	20.4
C(2)	15.47	15.30	15.03	14.91	14.78	14.68	14.57	14.50	14.44	15.1
C(3)	22.96	23.25	23.53	23.73	23.97	24.19	24.44	24.63	24.81	23.4

Table 15 Calculated Intrinsic Chemical Shifts, Bond magnetic
Anisotropy for Different Electrical Centre of Gravity (6H)

ECG	.485	.487	.489	.491	.493	.495	.497	.499	.501
σ_i^{Si}	-67.42	-64.35	-60.85	-57.57	-54.11	-50.61	-46.83	-43.54	-39.91
σ_i^{C}	20.72	17.84	14.83	11.74	8.62	5.53	2.55	-0.07	-3.516
$\Delta x(10^{-33}\text{m}^3$ /bond)	102.2	103.6	103.8	104.6	104.9	104.9	103.6	103.9	102.1
R	.0328	.0280	.0246	.0262	.0264	.0357	.0429	.0485	.0542

The intention to determine the ECG in 15R is less reliable, since the crystal dimensions and layer spacings are predicted from 6H, but not determined directly from experiment. Therefore, the ECG value ranging from 0.488 to 0.490 will be used in the following calculation of geometric factors.

II. H Discussions

In silicon carbide polytypes, each crystallographically independent silicon (or carbon) is bonded to its four first neighbour carbons (or silicon) in a similar way as the others. However, three peaks are observed in ^{29}Si and ^{13}C nmr spectra of 6H SiC. To account for this fact, we must consider the effect from surroundings at the second and higher neighbour level. In the present work, we are only concerned with the so-called "long-range" effect. Moreover, we have made a reasonable assumption that $\sigma_{\text{p}_{\text{loc.}}}$ and $\sigma_{\text{d}_{\text{loc.}}}$ are the same for all silicon (or carbon) types in a polytype (e.g. they are not detectably influenced by the arrangement of the neighbour atoms); therefore, they can be incorporated into intrinsic chemical shift terms. In this manner we can simplify an otherwise almost intractable problem.

The McConnell's equation treatment of the long-range diamagnetic shielding, solved by computer program, results in the calculation of geometric factors, thus, the chemical shifts by equations 2.1 and 2.2. From these the assignments of the nmr peaks to lattice sites become possible. For SiC 6H, silicon types are BCAB'C'A' in one unit cell (see table 3). Since assignment 2 (see table 8) is correct, as indicated by the Δx 's sign, the chemical shifts of type B, C, and A are -20.4, -14.5, and -24.7 ppm. For 15R, assignment 2 is most probable according to layer spacing shift arguments (This will be explained in the next chapter). From this assignment, type A has a chemical shift of -24.4 ppm which is comparable to

-24.7 ppm of type A in 6H, while both type B and C have two different chemical shifts (-24.4 and -20.8 for type B, -14.9 and -20.8 for type C). The large discrepancies between chemical shifts of the same type suggest that consideration out to the second neighbour level were not far enough and that the layer spacings for the same type of atom in 15R might not be equal.

The correlation between chemical shifts and the silicon types A, B, and C are discussed above. On the other hand, the type designations for carbons are according to a different scheme, since the carbon sequence should be counted backwards. For example, in 6H, which has a sequence of *abcacb...* according to the classical ABC notation, the C(2)'s sequence is *ACB*A* (or *BCA*B*) and thus C(2) belongs to type A. In addition, the types of C(1) and C(3) would be B and C respectively. Therefore, the type sequence in 6H would be BAC. Similarly, the type sequence in 15R is not the same for silicons and carbons, that is, the type sequence is BCBCA for silicons but BCBAC for carbons. Now the chemical shifts can be correlated with the types for carbons. For 6H, types B, A, and C have chemical shifts of 20.4, 15.1, and 23.4 ppm. For 15R, type A has a chemical shift of 13.3 ppm that is comparable to the chemical shift of type A in 6H (15.1 ppm), while type B has two chemical shifts (16.0 and 20.7 ppm) and type C has only one (22.7). As a conclusion, the assignments of chemical shifts to carbon types in 6H are consistent with those in 15R.

In the determination of electrical centre of gravity (ECG), it was found that the calculated chemical shifts of silicons tend to split further apart as the ECG is shifted away from the silicon atoms. This is not what one would intuitively expect. The problem arises from the means of calculation in which the first neighbour contribution has to be eliminated according to the definition of McConnell's long-range shielding theory. In order to determine the actual ECG value, the diamagnetic shielding from the electrons of the immediate neighbour bonds must be

included and calculated via Hartree-Fock orbitals⁵⁷ or ab initio calculations.⁶² The reason that we are calculating ECG's is to find the theoretical chemical shifts that will best fit the experimental data. For 6H SiC, the optimum ECG value is about .489, as indicated by the minimum residual value (0.0246).

As to the bond diamagnetic susceptibility ($\Delta\chi$), the magnitude obtained is three orders larger than the values from the literature (e.g. $\Delta\chi = 140 \times 10^{-36} \text{ m}^3/\text{molecule}$ for C-C bond). This large inconsistency is also the result of the elimination of the first neighbour bond contributions. The addition of a constant (the geometric factors contributed by the first neighbour bonds are about -3.17) to the geometric factors of various type of atoms increase the total geometric factors by two orders, thus decrease the order of $\Delta\chi$ by the same number, since the $(\Delta\chi) \cdot (g)$ terms have to remain constant.

CHAPTER III

REFINEMENT OF SILICON CARBIDE POLYTYPIC STRUCTURES

III.A Introduction

From the last chapter, we know that the geometric factor for a given atom in SiC polytype depends on two factors : the stacking sequence of other layers about the atom concerned and the electrical centre of gravity. Another thing similar to the latter factor but more significant is the layer spacings with respect to each other. Our earlier calculations indicated that very small changes in the spacings of layers (e.g. moving a silicon or a carbon up or down by 0.001 Å, a magnitude within the estimated standard deviation of the silicon and carbon positions in 6H-SiC) change geometric factors, thus chemical shifts, significantly. This may suggest that crystal structures can be determined more accurately by nmr information than by X-diffraction technique. It is an evident that refinement of a highly correlated structure is impossible due to the failure of least squares fits in this situation.⁶³ On the other hand, the refinement of crystal structure by MAS NMR techniques doesn't exhibit correlation problems and may overcome X-ray defects.

In order to justify the probability of this method, we need to construct an equation that would relate the intrinsic chemical shifts, spacing shifts, theoretical chemical shifts, and bond magnetic anisotropy in a reasonable way. How to design such an equation will be one of the main purposes in this chapter.

III.B Preliminary studies on layer spacing shifts

III.B.1 Relationship between chemical shift change and layer spacing shift

Attention has been paid to understanding the relationship between chemical shift change and the atomic position shift. If the geometric factor change should be linearly dependent on the atomic position shifts, such a relationship would become much more simple. For this purpose, we moved one atom up or down by a small distance (e.g. 0.001 Å), obtained the geometric factor changes of the other atoms due to this atomic position shift, and plotted the geometric factor change versus layer spacing shift. Such diagrams have been drawn for Si(3) and C(1) atomic position shifts (see Figure 16 and Figure 17). From these representative drawings follows a conclusion : chemical shift changes are linearly related to the layer spacing shifts.

III.B.2 Additivity of geometric factor changes

A crucial point to the potential of crystal structure refinement by NMR chemical shift information is the additivity of geometric factor changes for any atom. Additivity is defined in more detail as follows : the total geometric factor change for a given atom due to moving several atoms together all at once is equal to the sum of geometric factor changes caused by shifting each of these atoms separately by the same amount. An investigation of the results shown in table 16 suggests that additivity holds true, that is, the geometric factor change (0.000324) of Si(1) due to moving C(1) up 0.002 Å, Si(2) down 0.001 Å, and C(2) up 0.001 Å is approximately the same amount as the sum of geometric factor changes (0.000323) caused by moving C(1), Si(2), C(2) separately by the corresponding amount.

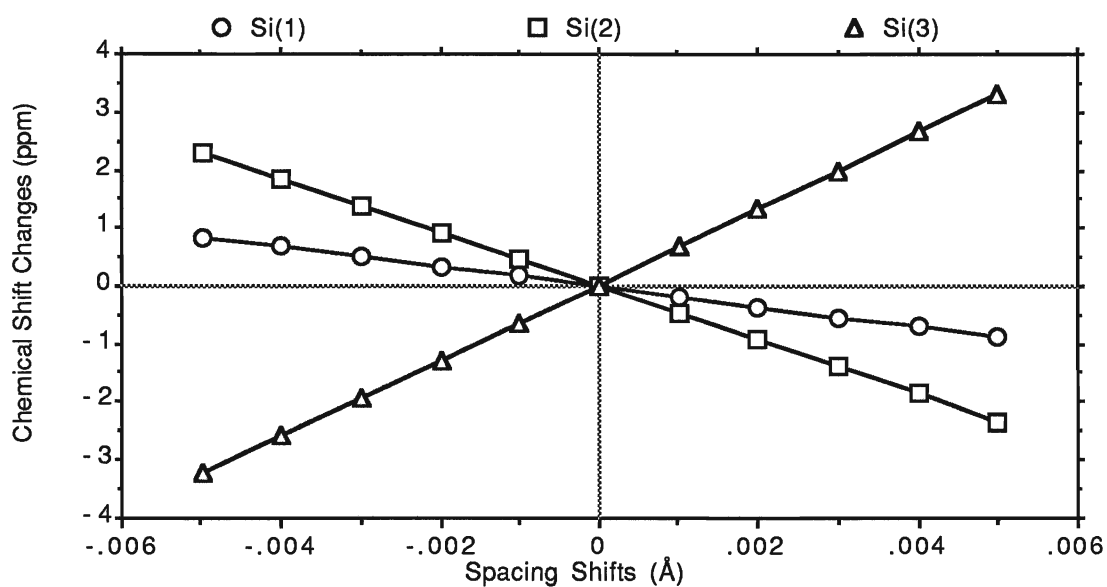


Figure 16 Change in the calculated chemical shifts of three silicons of the 6H polytype when the Si(3) layer is moved up or down along the c-axis

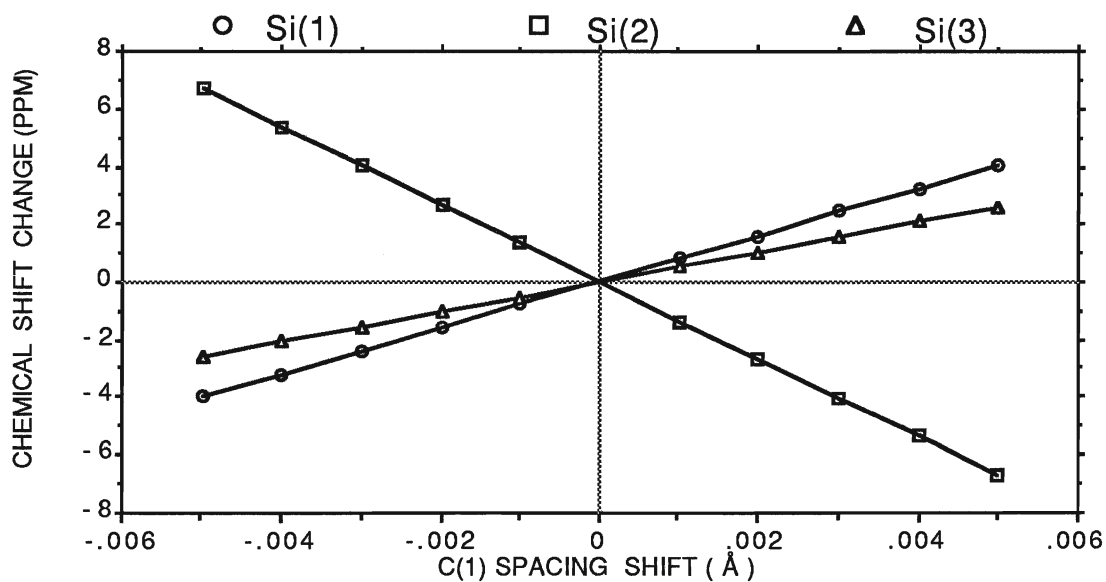


Figure 17 Change in the calculated chemical shifts of three silicons of the 6H polytype when the C(1) layer is moved up or down along the c-axis

Table 16 Example of Additivity of Geometric Factor Changes

Layer Spacing Shifts (Å)	Geometric Factor Change		
	Si(1)	Si(2)	Si(3)
C(1)+.002	0.000201	-0.000334	0.000130
Si(2)-.001	0.000057	-0.000079	0.000022
C(2)+.001	0.000065	0.000101	-0.000167
Sum	0.000323	-0.000312	-0.000015
C(1)+.002 Si(2)-.001 C(2)+.001	0.000324	-0.000312	-0.000015

III.C Crystal structure refinement

III.C.1 Equation set-up and layer spacing shifts—a combined refinement of 6H and 15R and 3C

So far, we have shown that geometric factor changes and thus chemical shift changes are both linear with positional shift and nearly additive. An equation relating the chemical shift to the z-coordinates of the layers can be written :

$$\sigma_{x(j)} = \sigma_x^i + g_{x(j)}\Delta x + \sum_k a_k \Delta x [g_{x(j)}^k] \quad (3.1)$$

where $\sigma_{x(j)}$, σ_x^i , g , and Δx have the same meanings as in equation 2.1 and 2.2; $g_{x(j)}^k$ is the change in $g_{x(j)}$ induced by moving the k th layer of atoms by a fixed

amount Δd , and a_k 's are coefficients whose values are to be determined by solving a collection of equations. The quantity $(a_k)(\Delta d)$ becomes the change in atomic position for atom k .

Selection of Δd can be arbitrary within the linear range (e.g. from -0.005 \AA to 0.005 \AA , as indicated in figure 14 and figure 15). Compared to the X-ray standard deviations of silicon and carbon, a value of -0.001 \AA is chosen for Δd 's of silicons, and of 0.001 \AA for Δd 's of carbons. In the calculations, we use Si(1) as a reference(non-shifted), move C(1) up 0.001 \AA , get the geometric factors for silicons and carbons, move Si(2) down 0.001 \AA , get the geometric factors again, then do the same things for the remainder atoms in the unit cell. A representative set of data for 6H is recorded in table 17.

Table 17 Example of Geometric Factors When One of the Atoms is moved up or down by $.001 \text{ \AA}$ (ECG=.498)

Spacing Shift (\AA)	Geometric Factor		
	Si(1)	Si(2)	Si(3)
No Shift	0.00290574	0.00361979	0.00262347
C(1)+.001	0.00300468	0.00345061	0.00268847
Si(2)-.001	0.00296557	0.00353929	0.00264549
C(2)+.001	0.00297250	0.00372106	0.00245660
Si(3)-.001	0.00292795	0.00367804	0.00254159
C(3)+.001	0.00273835	0.00368194	0.00272324

By the crystal symmetry of 6H, Si(4) lies at $c/2$; similarly, Si(6) and Si(11) lie at $c/3$ and $2c/3$ in 15R. The implication is: layers 4 to 6 are exactly the same as layers 1 to 3 in 6H, layers 6 to 10 and 11 to 15 are exactly the same as layers 1 to 5 in 15R. Although these symmetry arguments reduce the number of unknowns to be determined considerably, we have seventeen unknowns: two intrinsic chemical shifts (σ_{Si}^i and σ_C^i), five layer spacing shift coefficients from 6H, nine layer spacing shift coefficients from 15R, a bond magnetic anisotropy. It happens that the number of unknowns is equal to the total number of known data (six chemical shifts from 6H, ten from 15R, and one from 3C). The problem now becomes the solving of seventeen linear equations for seventeen unknowns. The program in appendix 6 is designed for this purpose. In the calculation, several values of ECGs have been tested, and the result from the ECG of 0.488 are demonstrated in table 18. Since the symmetry of 3C requires that the all bond distances must be equal, the spacings are definitely determined, as long as the crystal dimensions are known.

As shown in table 18, most of the spacing shifts required are outside the range of expected error (e.g. the X-ray standard deviations are $\pm 0.002 \text{ \AA}$ for carbon and $\pm 0.0008 \text{ \AA}$ for silicon in 6H SiC). This may be due to the assumption that intrinsic chemical shifts are the same for 6H and 15R and 3C. Therefore, it may be necessary to split the data and to do structure refinement for 6H and 15R separately.

III.C.2 Refinement of 6H and 15R crystal structures by using a common Δx and distinct intrinsic chemical shifts σ_i

The chemical shift related to the geometric factor was given by equation 2.1 in chapter 2. If we temporarily omit considering layer spacing shifts, it is possible to calculate the theoretical chemical shifts by the least squares fits program

Table 18 Spacing Shifts in SiC Polytypes (6H & 15R, ECG=0.490)

TYPE	SPACING SHIFT (6H) [†] (Å)	SPACING SHIFT (15R) [†] (Å)
C(1)	+0.0037	+0.0054
Si(2)	+0.0041	+0.0059
C(2)	+0.0146	+0.0134
Si(3)	+0.0138	+0.0173
C(3)	+0.0006	-0.0033
Si(4)		-0.0082
C(4)		+0.0037
Si(5)		-0.0004
C(5)		-0.0036

[†]—"+" means moving up; "-" means moving down.

in appendix 4. From table 10 in chapter II, we see that the calculated chemical shifts are not consistent with the observed values. Let these differences be $\Delta \sigma$, then

$$\Delta \sigma = \sigma_{\text{Obsd.}} - \sigma_{\text{Calcd.}} \quad (3.2)$$

One way to correct the calculated values is to change the geometric factors, that is, to change the layer spacings. The amount of layer spacing shift required for a specific atom can be related to the chemical shift discrepancy by,

$$\Delta \sigma = \Delta x \sum_k a_k [g_{x(j)}^k] \quad (3.3)$$

where a_k and $g_{x(j)}^k$ have the same meanings as in equation 3.1; Δx is the common bond magnetic anisotropy determined by using the observed chemical shift data from both 6H and 15R. The reason we are using the same Δx is that a bond magnetic anisotropy remains almost as a constant in different compounds, especially in such similar molecules as polytypes, regardless of chemical bond environments.

The program in appendix 4 is designed to solve equation 2.1, 3.2, and 3.3 sequentially. The procedure of calculation is described as follows : First, assign nmr peaks to geometric factors; second, select a suitable ECG value; third, determine a common Δx by least-square-fitting ; fourth, do least squares fits for 6H and 15R separately to get intrinsic chemical shifts σ_x^i 's for both; fifth, use the common Δx and distinct σ_x^i 's to calculate theoretical chemical shifts and layer spacing changes; sixth, repeat the procedures three to five while omitting the layer spacing change part (this can be easily done in a computer program).

A comment is given on the peak assignment problem in 15R. As given in table 11, four ways of assigning the observed chemical shifts to the calculated geometric factors are possible. The layer spacing shifts required for all atoms from the four assignments are shown in table 19. From this it is obvious that assignment 2 is most probable, since the other three assignments result in shifts much larger than the standard deviations estimated by Gomes de Mesquita.²⁸

Selection of a ECG value for 6H and 15R is a time consuming work, since the whole set of input data has to be changed for 6H and 15R. For this reason, we have tested only five values—0.500, 0.498, 0.492, 0.490, 0.488, and the best result is given by 0.490.

Using assignment 2 and an ECG value of .490, we have done calculation according to the procedure three through six. The common Δx finally calculated is $88.81 \times 10^{-33} \text{m}^3/\text{bond}$, the intrinsic chemical shifts of silicon and carbon are -53.51 ppm

Table 19 Layer spacing shifts in various ways
of peak assignment (ECG =0.490)

Layer number	Assign. 1	Assign. 2	Assign. 3	Assign. 4
Si(1)	0	0	0	0
C(1)	0	0	0	0
Si(2)	-.0032	+.0014	0	+.0016
C(2)	+.0012	-.0017	+.0047	-.0031
Si(3)	-.0006	-.0006	+.0048	+.0009
C(3)	+.0078	+.0002	+.0078	-.0060
Si(4)	+.0042	-.0021	+.0076	+.0001
C(4)	+.0033	-.0027	+.0013	-.0066
Si(5)	+.0003	-.0027	+.0017	-.0023
C(5)	+.003	0	-.0016	-.0057

and 14.21 ppm in 6H, and -54.77 ppm and 13.43 ppm for 15R. The advantage of this method can be seen from the excellent agreement between the observed and the calculated chemical shifts of 6H (table 20), especially from the Si-Si and C-C layer spacings of 6H after shifting (see figure 18 and figure 19). Finally, we may deduce the layer spacings of 15R (see figure 20 and figure 21).

Table 20 Comparisons Between the Observed Chemical Shifts and the Calculated After shifting Layers for SiC 6H Polytype (ppm)

	Si(1)	Si(2)	Si(3)	C(1)	C(2)	C(3)
Obsd	-20.6	-14.5	-25.1	20.4	15.1	23.4
Calcd	-20.60	-14.52	-25.08	20.38	15.12	23.40

III.D Discussion

The layer spacing shifts calculated in section III.C.1 indicate that the refinements of SiC polytypic structures by using the same intrinsic shifts and bond magnetic anisotropy are unsuccessful, although the advantage of having enough data for the solution of unknowns does exist. The method is improved by the assumption of different intrinsic shifts for 6H and 15R, as shown in section III.C.2 in which it was found that the intrinsic shifts for 6H and 15R exhibit approximately 1 ppm differences.

One reason that the intrinsic shifts are different for 6H and 15R is the systematic errors in the chemical shift measurement (e.g. if there were a 1 ppm difference for all of the 15R peaks). If these errors were not accounted for by

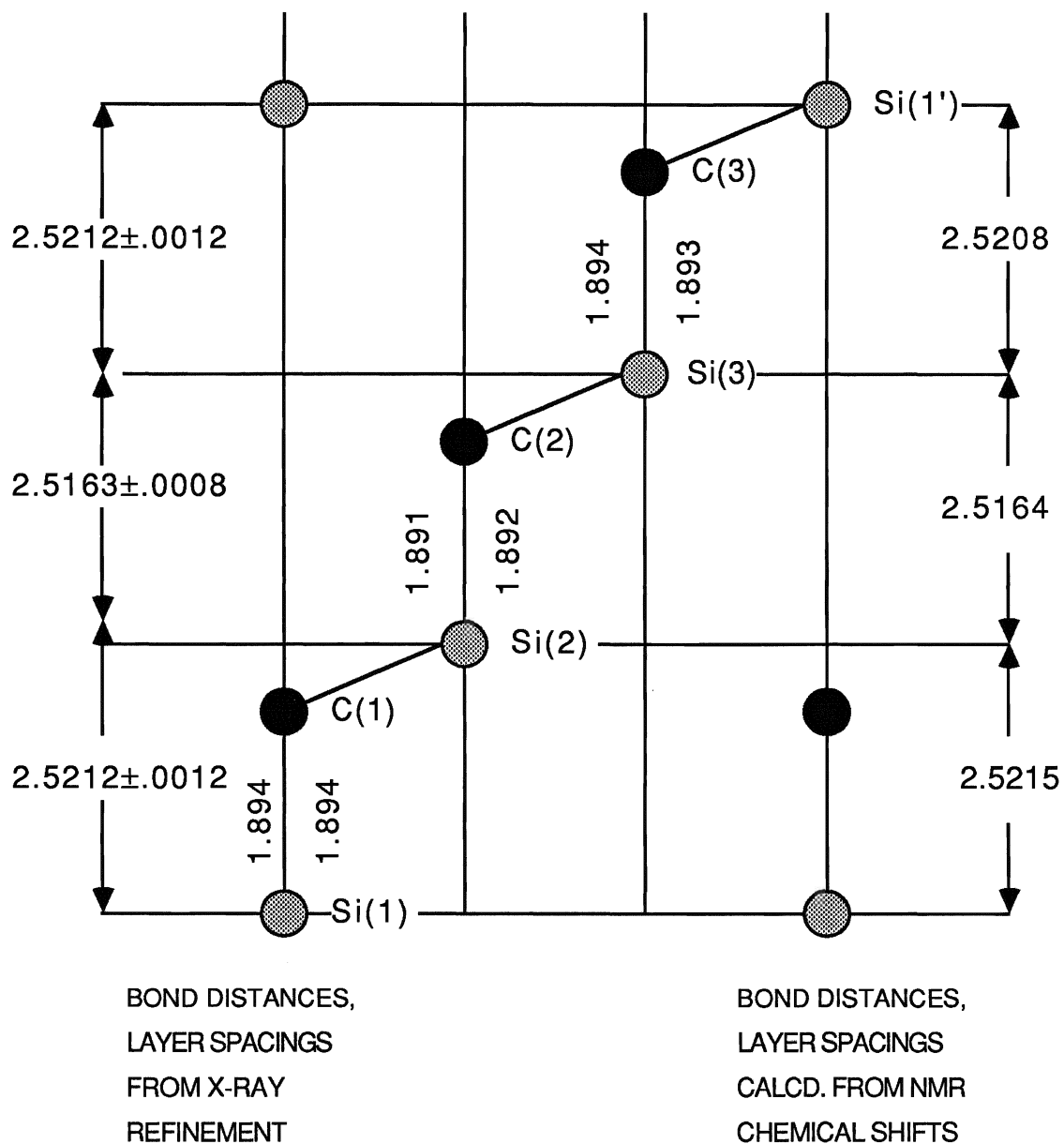


Figure 18 Si-C bond distances and Si-Si layer spacings of 6H after shifting, calculated by using common bond magnetic anisotropy and distinct intrinsic shifts of 6H and 15R, compared with those from X-ray refinement.

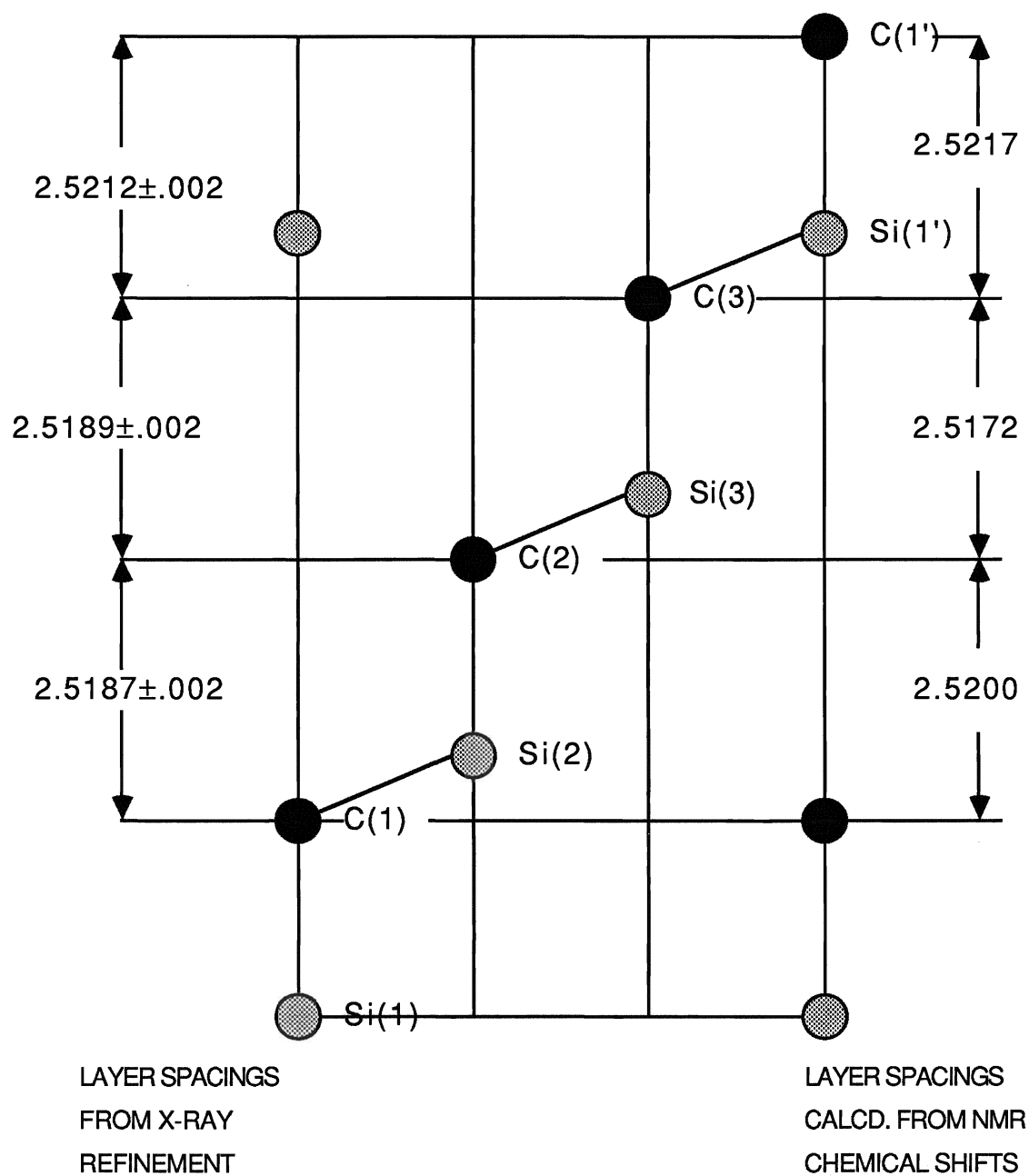


Figure 19 C-C layer spacings of 6H after shifting, calculated by using common bond magnetic anisotropy and distinct intrinsic shifts of 6H and 15R, compared with those from X-ray refinement.

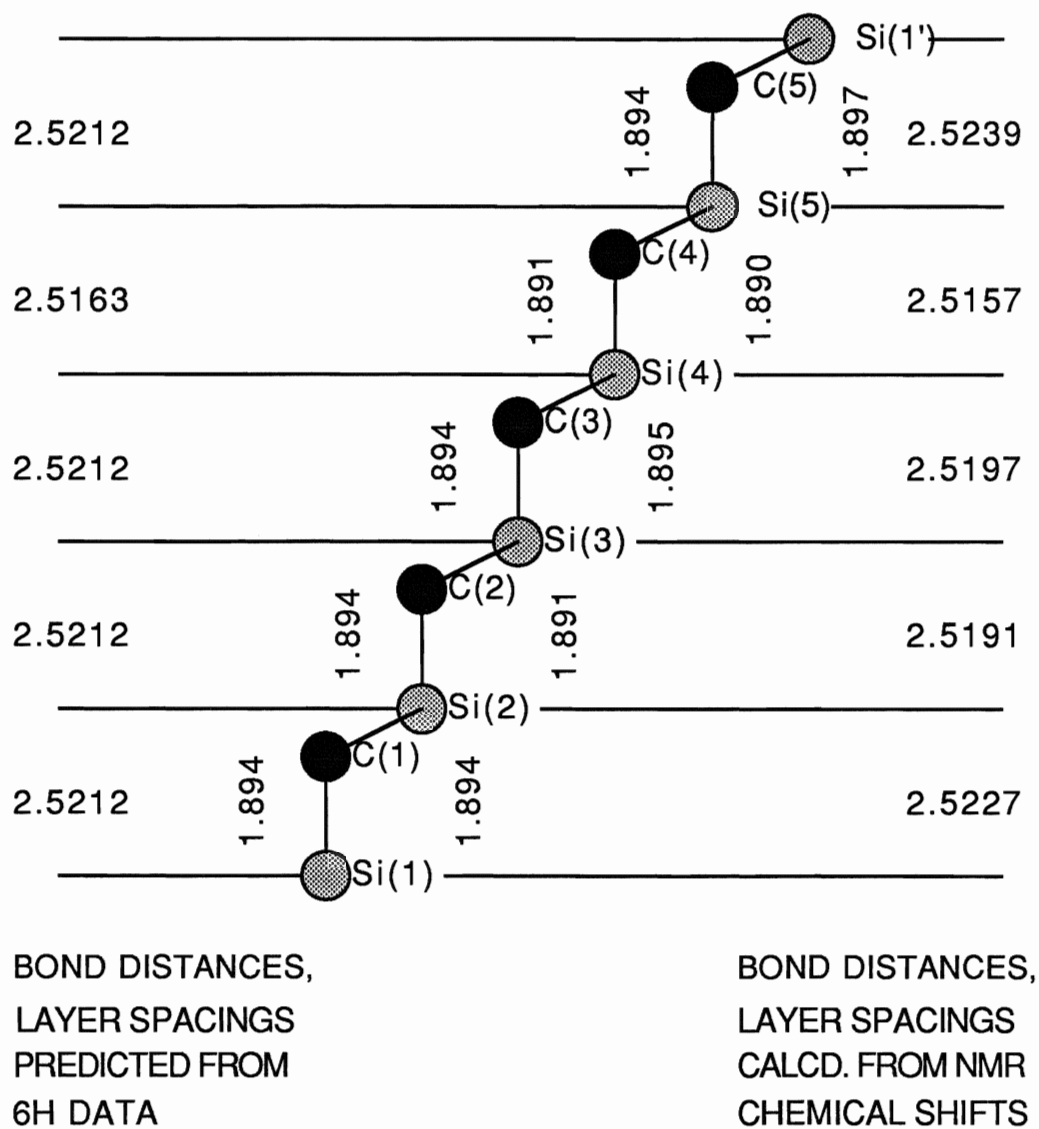


Figure 20 Si-C bond distances and Si-Si layer spacings of 15R after shifting, calculated by using common bond magnetic anisotropy and distinct intrinsic shifts, compared with those predicted from Gomes de Mesquita's 6H data.

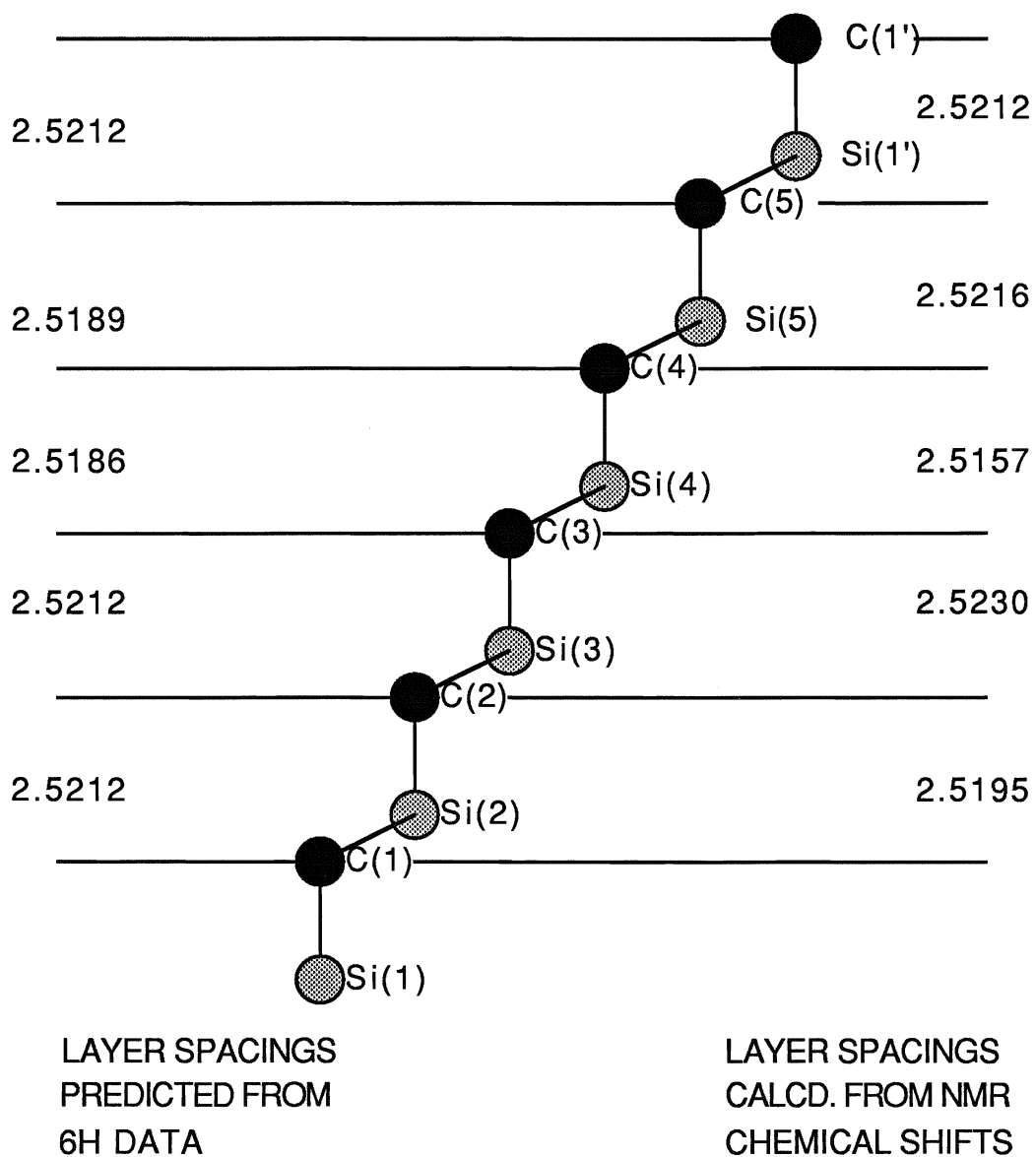


Figure 21 C-C layer spacings of 15R after shifting, calculated by using common bond magnetic anisotropy and distinct intrinsic shifts compared with those predicted from Gomes de mesquita's 6H data.

correction to the reference standard, they would appear to be a difference in the intrinsic shift. Systematic differences in chemical shifts might be due to bulk susceptibility differences for 6H and 15R which show up when an external standard is used as a reference. It may also arise from different amount of impurities in different samples.

By using the method described in section III.C.2, we have calculated the layer spacings for 6H and 15R. The calculated Si-Si layer spacings of h-c (2.5215 Å) and c-h (2.5208 Å) of 6H SiC are within X-ray standard deviations (The Si-Si layer spacings for h-c and c-h from Gomes de Mesquita are 2.5212 ± 0.0012 Å).²⁸ Moreover, the calculated Si-Si layer spacing of c-c (2.5164 Å) is considerably shorter than those of h-c and c-h, and this is very consistent with the data from Gomes de Mesquita (2.5163 ± 0.0008 Å). For 15R SiC, again the calculated c-c spacing of silicon layer is shorter than those of h-c and c-h, however, this is not true for c-c spacing of carbon layer (figure 21). One reason may be that the C-C layer spacings of 6H determined by X-ray structure refinement are less accurate (e.g. the standard deviation for C-C layers are ± 0.002 Å), and so are the C-C layer spacings of 15R predicted from 6H, consequently, the calculated C-C layer spacings in 15R are less reliable.

An advantage of nmr crystal structure refinement over X-ray diffraction technique may be the determination of some dimensional parameters in highly correlated structures such as SiC polytypes. The layer spacings of 15R still remain inaccessible due to the failure of least squares refinement of such kind of structure. From this work, the determination of layer spacings in 15R seems promising and reliable, since they are similar to the layer spacings in 6H SiC determined by this technique.

The shortcoming of this technique is the fact that the number of unknowns exceeds the number of known data. For this reason, we have to use the known

structures (e.g. 6H) as additional conditions and minimize the errors between the observed and the calculated data of known structures in order to refine other similar structures.

CHAPTER IV

PRELIMINARY STUDIES ON CALCULATION OF MAGNETIC SHIELDING TENSOR COMPONENTS OF 6H SIC VIA SINGLE CRYSTAL METHOD

IV.A Introduction

IV.A.1 Theory and determination of nuclear magnetic shielding tensor

The chemical shielding of a magnetic nucleus depends on the electronic cloud surrounding the nucleus. Unlike a free atom, the electronic cloud of a bonded atom is not spherical due to the formation of chemical bonds, that is, different electronic shielding of the nucleus would be expected for different orientations of the molecule containing this nucleus with respect to the external magnetic field. Such a property creates chemical shift anisotropy which can be described mathematically in some axis system (e.g. x, y, z axes) by a symmetric second-rank tensor⁶⁴:

$$\sigma = \begin{bmatrix} \sigma_{xx} & \sigma_{xy} & \sigma_{xz} \\ \sigma_{yx} & \sigma_{yy} & \sigma_{yz} \\ \sigma_{zx} & \sigma_{zy} & \sigma_{zz} \end{bmatrix} \quad (4.1)$$

The interaction of magnetic field \mathbf{H} with the nuclear magnetic moment \mathbf{M} is given by the following Hamiltonian⁶⁵:

$$\hat{H} = \mathbf{H} \cdot (\mathbf{1} - \sigma) \cdot \mathbf{M} \quad (4.2)$$

where $\mathbf{1}$ is a unit tensor. At the present stage of experimental accuracy, only the symmetric parts of a chemical shielding tensor can be determined. The antisymmetric parts that contribute to the second-order in the magnetic field are negligible in the normal nmr spectra.⁶⁶⁻⁶⁸ No experimental observation of

antisymmetric parts has been reported so far. The symmetric properties of the chemical shielding tensor have been investigated in detail in the literature.⁶⁹⁻⁷¹

In a single crystal nmr spectrum, each magnetically non-equivalent nucleus in a unit cell gives a line whose resonance frequency depends on the orientation with respect to the external magnetic field. A general equation of the chemical shift dependence on the crystal orientation is given by ⁷²

$$\begin{aligned}\delta_L = \mathbf{n} \cdot \boldsymbol{\sigma} \cdot \mathbf{n} = & \sigma_{xx} \sin^2 \phi \cos^2 \Omega + \sigma_{yy} \sin^2 \phi \sin^2 \Omega + \sigma_{zz} \cos^2 \phi + \\ & \sigma_{yx} \sin^2 \phi \sin(2\Omega) + \sigma_{zx} \sin(2\phi) \cos \Omega + \sigma_{zy} \sin(2\phi) \sin \Omega\end{aligned}\quad (4.3)$$

where \mathbf{n} is the unit vector defined by polar angles ϕ and Ω in the axis system x, y, z . A schematic representation of the angular relationship is illustrated in figure 22.

It is clear that measuring the chemical shift along six independent directions is sufficient to specify the six components of the shielding tensor. However, unambiguous assignments of various lines to nuclei are impossible when more than one line appears in the spectra. For this reason, the chemical shift anisotropy is explored by rotating the crystal about three orthogonal axes and by measuring the chemical shift as a function of rotation angle Ω . By inserting $\phi=90^\circ$ into equation 4.3, we can relate the position of a line $\delta_{xy}(\Omega_z)$ to the rotation angle Ω about the z axis that is perpendicular to applied magnetic field as:⁷³

$$\delta_{xy}(\Omega_z) = 1/2(\sigma_{xx} + \sigma_{yy}) + \sigma_{xy} \sin(2\Omega_z) + 1/2(\sigma_{xx} - \sigma_{yy}) \cos(2\Omega_z) \quad (4.4)$$

Similarly, for rotations about x axis and y axis, the line positions are given by

$$\delta_{yz}(\Omega_x) = 1/2(\sigma_{yy} + \sigma_{zz}) + \sigma_{yz} \sin(2\Omega_x) + 1/2(\sigma_{yy} - \sigma_{zz}) \cos(2\Omega_x) \quad (4.5)$$

and $\delta_{zx}(\Omega_y) = 1/2(\sigma_{zz} + \sigma_{xx}) + \sigma_{zx} \sin(2\Omega_y) + 1/2(\sigma_{zz} - \sigma_{xx}) \cos(2\Omega_y) \quad (4.6)$

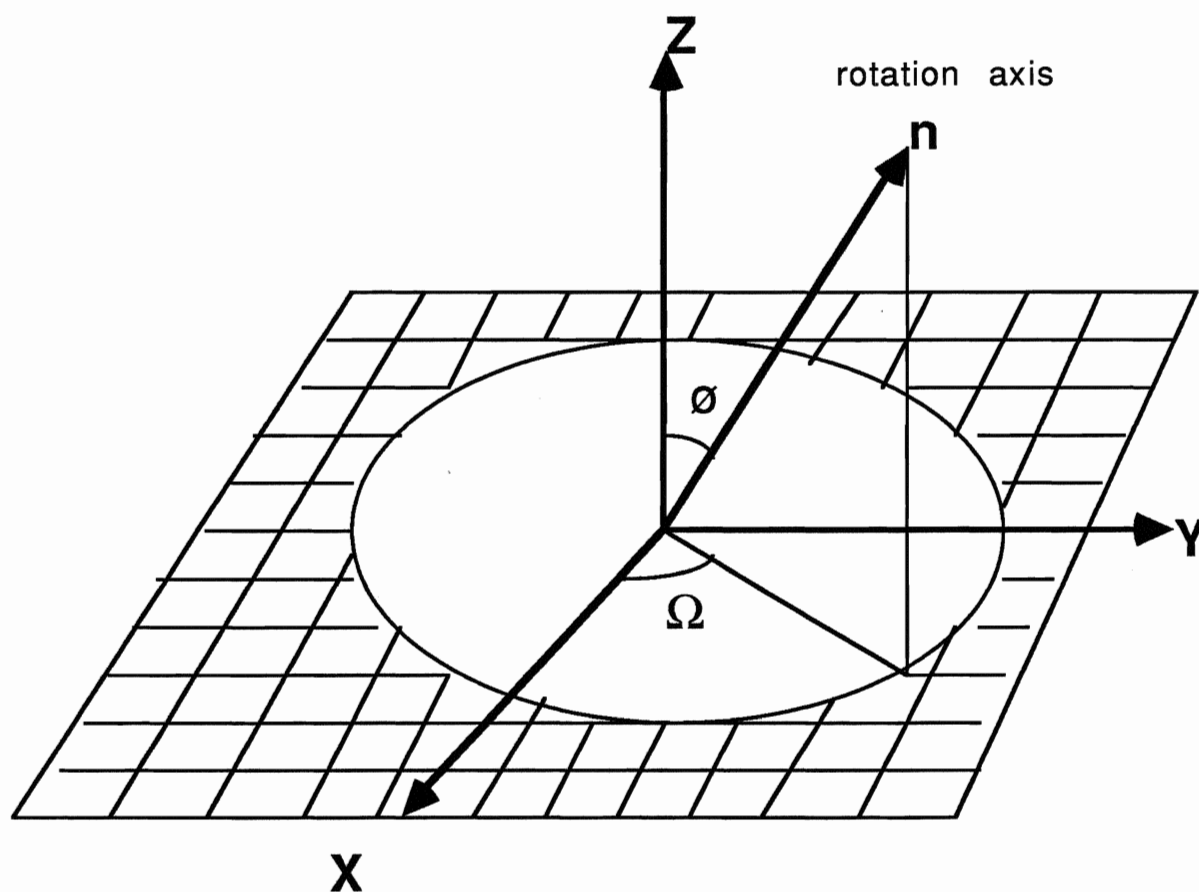


Figure 22 Orientation of the rotation axis and the plane of measurement with respect to the crystal axes x , y , z

For a given line in the nmr spectra, data traced through various orientations are least squares fitted to the equations 4.4 to 4.6, and twelve shielding elements are obtained; among them only six are distinct. To get the final six components, we must calculate the average of the same two elements for all data. A two dimensional nmr technique has been proposed to overcome the ambiguity of line assignments.⁷⁴

At this stage the shielding tensor elements are in the laboratory or bulk crystal frame. Diagonalizing the tensor produces principal elements and the

orientation of principal axes in the sample frame. X-ray data is used to relate the crystallographical axes to sample frame. Finally, the crystal and molecular symmetry is required to transform the data to the molecular frame.

IV.A.2 Advances in ^{13}C and ^{29}Si single crystal nmr

With the rapid development of high-resolution NMR in solids, the chemical shielding tensor of the carbon nucleus has been studied extensively in various chemical environments.⁷⁵⁻⁸¹ The experimental studies of carbon chemical shielding tensors are greatly complemented by theoretical calculations⁸²⁻⁸⁴ which are believed to be important in the analysis of the mechanism that determines the shielding interactions.

On the other hand, little ^{29}Si shielding tensor information is available, since most high-resolution solid-state ^{29}Si nmr was done on silicates using magic-angle spinning technique.⁸⁵⁻⁸⁷ The principal values of the ^{29}Si shielding tensor in solid silicates have been correlated with Si-O bond lengths.⁸⁸ The solid state ^{29}Si chemical shift of dodecasil-1H and dodecasil-3C have been reported and the shift found to be linearly related to the mean Si-Si distance between sites.⁸⁹ Most recently, ^{29}Si MAS NMR chemical shifts of silicate mineral structures have been calculated, and a simple correlation between MAS NMR chemical shift and molecular geometry has been found to be applicable to all silicate minerals.⁹⁰ Yet, as far as we know, ^{29}Si and ^{13}C single crystal nmr of SiC polytypes have only been reported in Winsborrow's M. Sc. thesis.²³

In brief, chemical shielding tensors provide "three-dimensional" information on solid state structures and the associated electronic features. These tensorial shifts are easily obtained by the single crystal approach. Unfortunately, the single crystal method is not applicable when the samples are liquids or gases at

room temperature and a low temperature is required for crystallization, or the crystals are very difficult to grow. Therefore, liquid or powdered samples have to be used. As we mentioned earlier, molecules reorientate so rapidly in non-viscous liquids that only isotropic shift given by one-third of the tensor's trace is obtainable and the chemical shift anisotropy is lost. On the other hand, more chemical shielding information is obtainable in powder samples, but it suffers two limitations: 1) Only the principal elements of tensors are available;^{91,92} the orientations of principal axes can not be determined unambiguously even with symmetry arguments. 2) If more than one line is present, overlapping of peaks may make the analysis of the static powder patterns either cumbersome or impossible. Despite these defects, the assignments of lines may be disentangled considerably by computational techniques.^{93,94}

However, in the case that single crystals are available (e.g. SiC single crystals can be grown at very high temperature), the studies of chemical shift anisotropy by single crystal nmr have advantages over those by MAS nmr, since the former method would provide much more information about chemical shift anisotropy, and it is easily accessible with a goniometer head. Moreover, a single crystal gives sharp nmr lines even when the sample is not spinning. The line positions vary with the crystal orientations. On the other hand, powders give broad peaks due to each crystal having signals in different places. This work uses SiC single crystal to study the nature of the magnetic environment about silicon and carbon nuclei.

The other but more significant purpose of this chapter is to develop a preliminary method to refine a crystal structure by using chemical shielding tensor information. It is an imperative task as we have shown that the number of unknowns in MAS nmr refinement of crystal structures exceeds the number of knowns in equation 3.1. For example, in 6H-SiC, seven unknowns require to be

extracted from six knowns, provided a common bond magnetic anisotropy ($\Delta\chi$) of 15R and 6H, and an electrical centre of gravity (ECG) value have already been decided. Moreover, different bulk magnetic susceptibilities for different samples would result in errors in $\Delta\chi$, thus in the calculated chemical shifts and the layer spacing shifts. The refinement from MAS nmr information done before was possible, since the calculation was performed in two steps. It seems reasonable, however, as a whole, the solutions to the unknowns would not be restrained, if the unknowns were determined by one step according to equation 3.1.

IV.B. Experimental

IV.B.1 Samples

The samples used in this research are commercially grown in General Abrasive Operations, Dresser Canada Incorporation, 3807 Stanley Avenue, Niagara Falls, Ontario, Canada.

IV.B.2 Identification of polytypic structures by precession method

The big crystals were broken to approximately $1 \times 1 \times 0.5 \text{ mm}^3$ sizes for X-ray studies. The identification of a crystal is determined by examining the precession photograph according to the rule described in I.B.2. Unfortunately, all of the twenty eight samples studied were 6H polytype. Thus the intention to find a 15R SiC single crystal was given up.

IV.B.3 ^{29}Si and ^{13}C single crystal nmr

Single crystal nmr studies of ^{29}Si and ^{13}C were carried out on a Bruker AC-200 spectrometer with a standard Bruker broad band probe (non-spinning). Crystals were carefully selected in order to avoid any non-single crystal character (e.g. two pieces of crystals stuck together). We also found that a thicker crystal would give sharper lines in the nmr spectra. Among the three crystals we have tried, the one sized approximately $5 \times 5 \times 5 \text{ mm}^3$ gave the best result. A comparison between the ^{29}Si spectrum (acquired under the crystal c-axis being parallel to the applied magnetic field) with the result from Winsborrow²³ reveals that its identity is 6H. A series of spectra were acquired at different orientations of the crystal c-axis with respect to the external magnetic field by using the angle glass wedges with certain angles which are inserted into a 10 mm nmr tube (figure 23).

In setting nmr experimental parameters, a line broadening (LB) of 25 Hz was selected for both ^{29}Si and ^{13}C spectra. For ^{29}Si , relaxation delays (RD) of 30 seconds as used by Winsborrow²³ were adopted, and 1800 transients were acquired for satisfactory signal to noise ratios. For ^{13}C , it was found that a pulse interval of 20 seconds would give a better result than 5 seconds as used by Winsborrow²³ within the same time limit. 2700 transients were acquired for ^{13}C spectra. In the cases of spectra with severely overlapped peaks, simulations were done to resolve these lines by employing LINESIM computer program.

IV.C.1 Results and rotation plots

Figure 24 shows a collection of ^{29}Si spectra acquired at various orientations of crystal c-axis ($0^\circ \sim 90^\circ$) with respect to applied magnetic field. The same procedure was performed on ^{13}C nmr (figure 25). The corresponding chemical shifts in figures 24 and 25 are reported in table 21 in which simulated chemical

shifts are also given in brackets. As routine, plots of chemical shifts versus orientation angles are carried out and demonstrated in figures 26 and 27. The lines are sinusoidal curves that best fit the data.

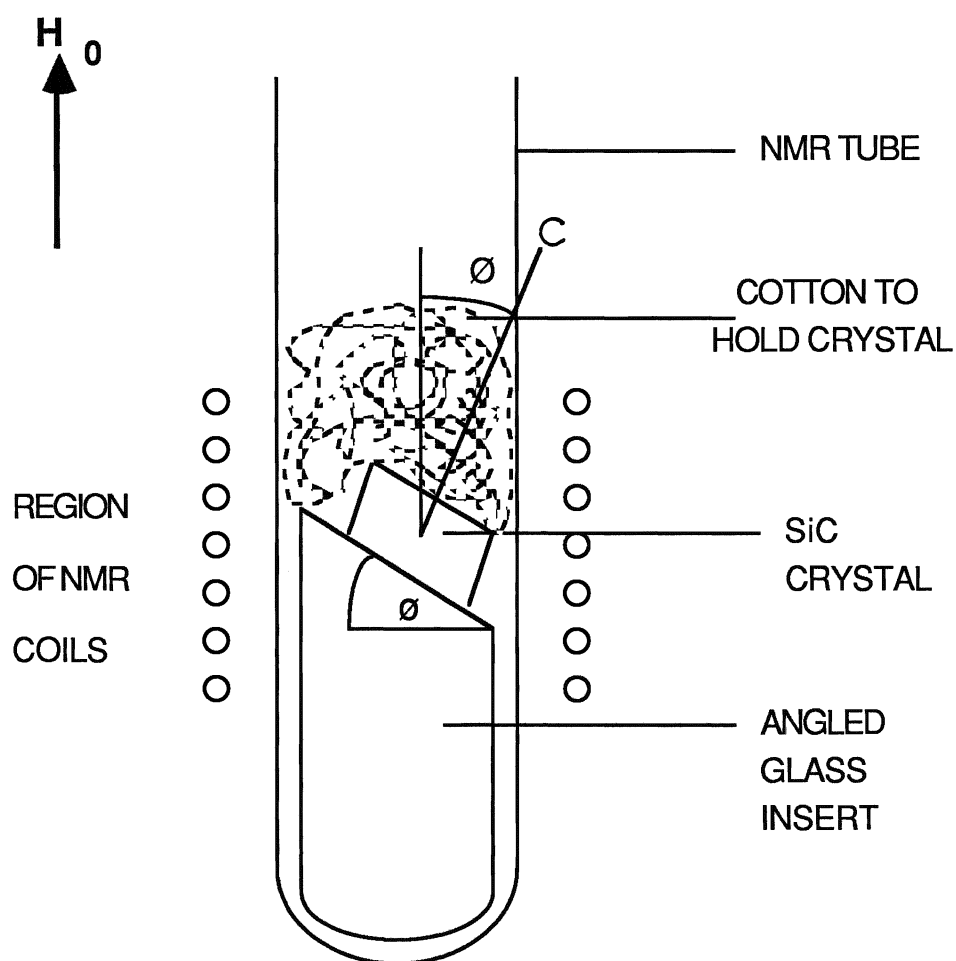


Figure 23 Diagram of an apparatus used in the single crystal nmr experiment to set the orientation angle, θ

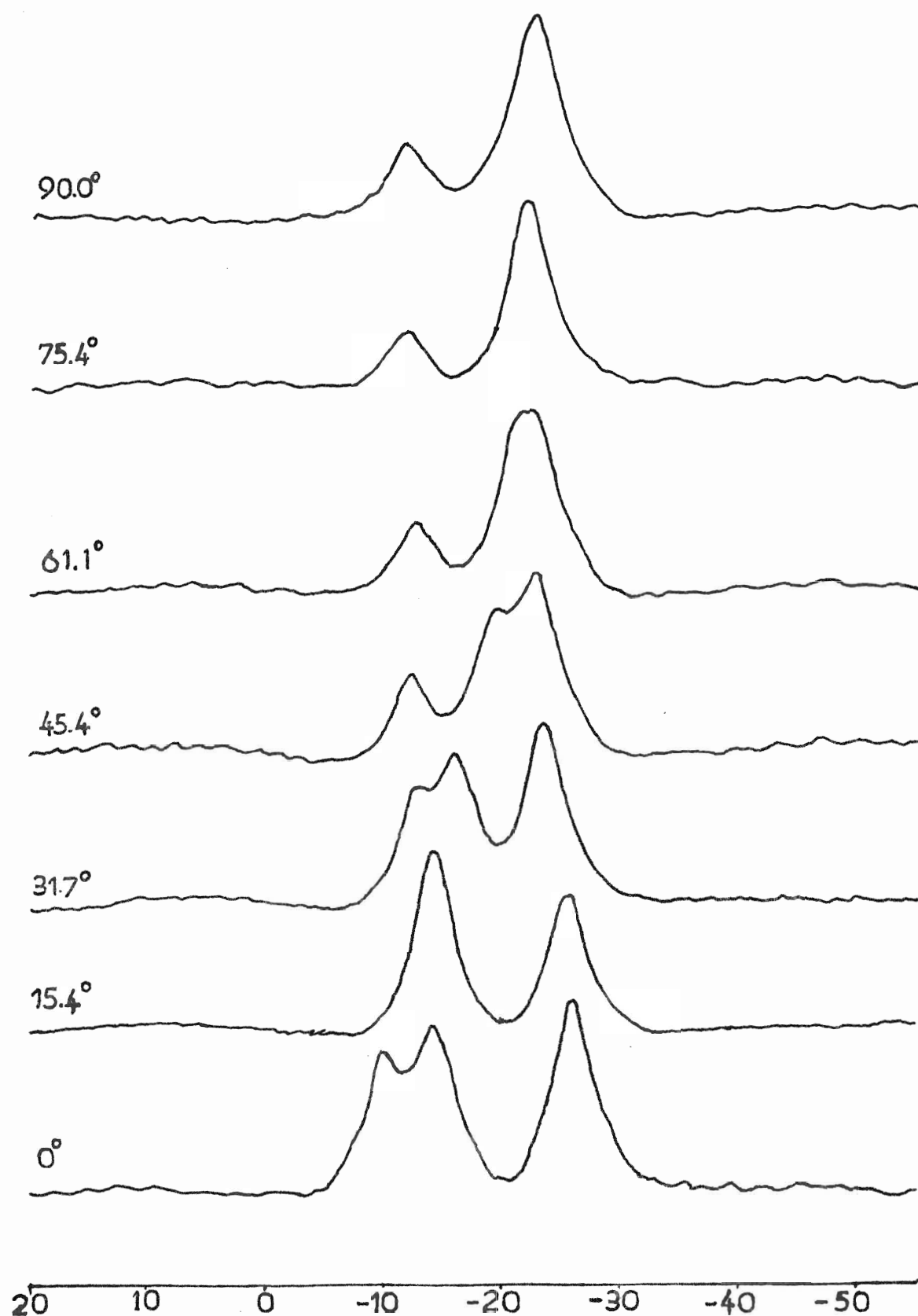


Figure 24 ^{29}Si single crystal nmr spectra of 6H SiC, oriented at series angles to the applied magnetic field H_0 ; relaxation delay was thirty sec.

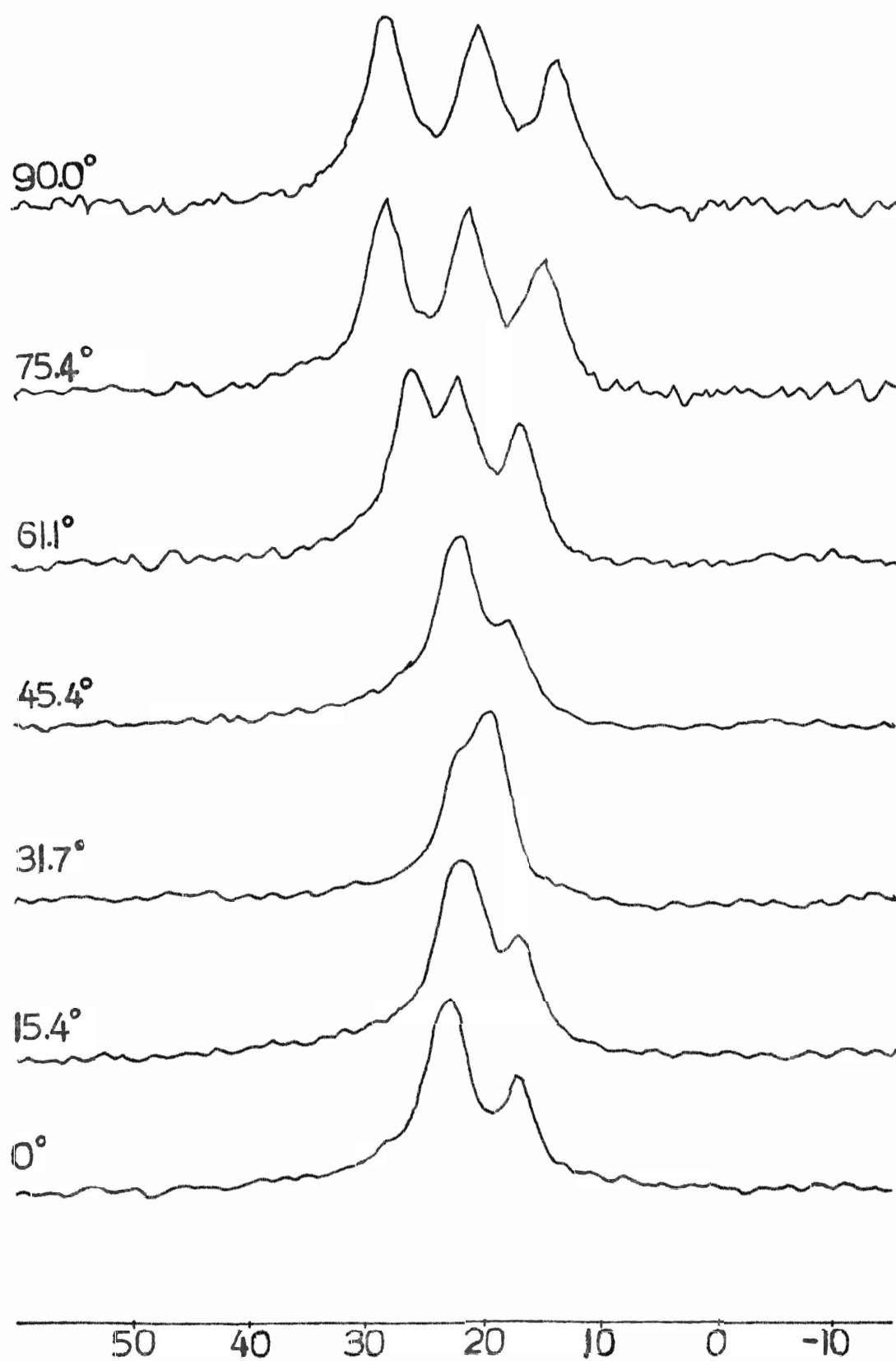


Figure 25 ^{13}C single crystal nmr spectra of 6H SiC, oriented at series angles to the applied magnetic field H_0 ; relaxation delay was twenty sec.

Table 21 Summary of Single Crystal NMR Chemical Shifts†

Orientation angle(degr.)	²⁹ Si				¹³ C			
	ppm		Int.*		ppm		Int.*	
0.0	-10.2	-14.3	-26.0	1:1:1	16.7	22.5		1:2
					(16.7	23.1	22.6)	
15.4	-12.0	-15.1	-26.8	1:1:1	17.0	21.4		1:2
					(17.0	22.6	21.1)	
31.7	-14.2	-25.5		2:1	19.5	22.4		2:1
45.4	-16.3	-13.3	-23.7	1:1:1	21.7	18.0		2:1
					(23.3	22.1	18.0)	
61.1	-19.4	-12.5	-22.8	1:1:1	26.3	22.4	17.1	1:1:1
65.8	-21.4	-12.2	-22.2	1:1:1				
75.4	-21.8	-11.4		2:1	28.7	21.7	15.3	1:1:1
					(-22.4	-11.4	-21.1)	
90.0	-22.6	-11.8		2:1	28.6	21.7	15.3	1:1:1
					(-22.6	-11.8	-21.4)	

†—the values in the brackets are obtained via simulations.

*—intensity ratios are approximate.

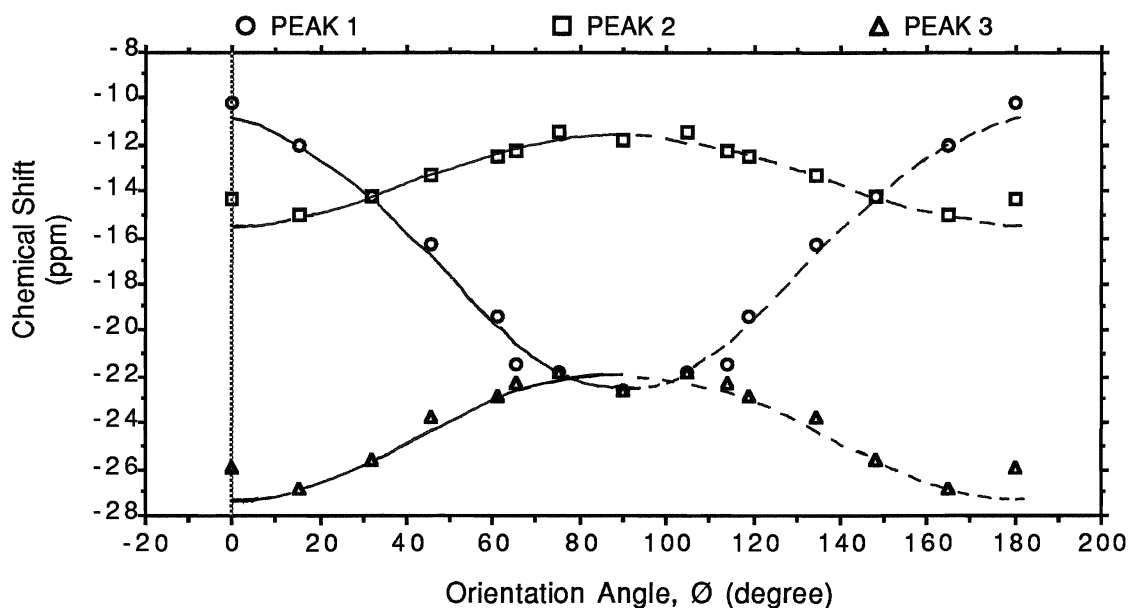


Figure 26 Plots of silicon-29 chemical shift versus orientation angle, \varnothing , for single crystal nmr experiment; slashed lines are symmetry based extrapolations.

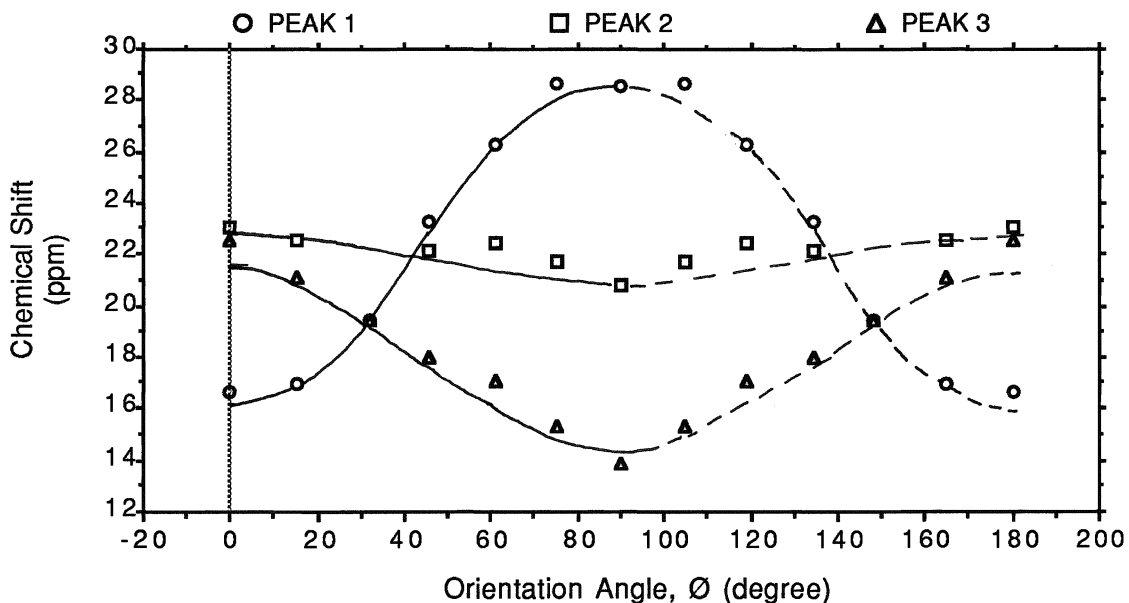


Figure 27 Plots of carbon-13 chemical shift versus orientation angle, \varnothing for single crystal nmr experiment; slashed lines are symmetry based extrapolations.

As one can see, some points do not correlate with sinusoidal curves. These errors may arise from several sources under the experimental conditions: first, angular errors introduced through glass wedge; second, uncertainties of chemical shift measurements; third, impurities in the crystal. The first error can be overcome by using a goniometer probe that is not available at Brock University at the present, while the third error can be eliminated by using pure materials to grow crystals. In spite of these uncertainties, the trends of variations are clear. According to the crystal symmetry (2-fold axes perpendicular to the crystal c-axis) and the experimental fact,²³ the curves are symmetrical about 90°, and consequently, the parts over 90° are given by extrapolations.

IV.C.2 Extraction of magnetic shielding tensor components via least squares fits

The chemical shift δ is related to the zz component of the shielding tensor in the laboratory frame, where z is the direction of magnetic field. For rotations about three perpendicular axes, chemical shifts are related to rotation angles as in equations 4.4-4.6. According to symmetry arguments in $6H$ SiC, the chemical shifts remain unchanged upon rotating the crystal about c-axis. The situations are exactly the same for the rotations about a and b axes. Thus, the general expression 4.3 is reduced to one distinct equation only:

$$\delta_{yz}(\Omega_x) = \sigma_{zx}(\Omega_y) = \sigma_{xx}\sin^2\Omega + \sigma_{zz}\cos^2\Omega \quad (4.7)$$

The coefficients containing the elements of σ tensor are determined by fitting the rotation data to equation 4.7 for each rotation; such a process is accomplished by means of least squares fits (see appendix 7). The crystal symmetry makes the determination of principal components and of orientations of principal axes trivial, because of the fact that the laboratory frame coincides with crystallographic frame. Tables 22 and 23 summarize ^{29}Si and ^{13}C chemical

shielding tensor components extracted from least-squares-fitting of the rotation plots, meanwhile, MAS nmr chemical shifts are given for references.

Table 22 ^{29}Si single crystal and MAS nmr result

single crystal				MAS*
σ_{xx} (ppm)	σ_{yy} (ppm)	σ_{zz} (ppm)	1/3(trace)	σ_M (ppm)
-22.7	-22.7	-10.7	-18.7	-20.6
-11.6	-11.6	-14.9	-12.7	-14.5
-21.7	-21.7	-26.5	-23.3	-25.1

Table 23 ^{13}C single crystal and MAS nmr results

single crystal				MAS*
σ_{xx} (ppm)	σ_{yy} (ppm)	σ_{zz} (ppm)	1/3(trace)	σ_M (ppm)
29.3	29.3	16.3	24.6	23.7
21.5	21.5	22.9	22.0	20.4
14.7	14.7	22.0	17.1	15.1

* — MAS NMR data are from reference 22

IV.D Theoretical approach

IV.D.1 Tensor rotations

Following McConnell,⁴³ the long-range contribution from Gth group of electrons to shielding of particular nucleus is given by

$$\sigma_N^G = 1/L_0 \{ X_G/R_G^3 - X_G \cdot R_G R_G/R_G^5 \} \quad (1.4)$$

By the rules of vector and tensor algebra,⁹⁵ the equation is expanded to (see appendix 1)

$$\sigma_N^G = 1/(3L_0 R^3) \begin{pmatrix} x_{xx}(1-3\cos^2\phi_x) & 0 & 0 \\ 0 & x_{yy}(1-3\cos^2\phi_y) & 0 \\ 0 & 0 & x_{zz}(1-3\cos^2\phi_z) \end{pmatrix} \quad (4.8)$$

Where ϕ_x, ϕ_y, ϕ_z are the angles between radial vector \mathbf{R} and the principal axes xx, yy, zz of the bond magnetic susceptibility tensor.

To sum up tensors with different orientations by components of corresponding positions (e.g. $\sigma_{12}^x + \sigma_{12}^y + \sigma_{12}^z = \sigma_{12}^{\text{total}}$), we must rotate all contributing tensors to the same direction with respect to the bulk crystal frame. A contribution tensor is defined as a bond magnetic susceptibility tensor that contributes to the shielding of nuclei in the applied magnetic field. Thus for a vertical bond W, no rotation of its tensor is required. For all lateral bonds (labeled X,Y,Z, see figure 28), one or two rotations in turn would bring all tensors into z-direction. Details of tensor rotation are discussed elsewhere.⁵⁶ In selection of angles ϕ_x and ϕ_y , because the principal axes xx and yy of magnetic susceptibility tensors are arbitrarily chosen, average angles $(\phi_x)_{\text{ave}}$ and $(\phi_y)_{\text{ave}}$ are used, as a result, $(\phi_x)_{\text{ave}} = (\phi_y)_{\text{ave}}$, that is, $\phi_x = \phi_y$ in equation 4.8. An average angle is defined as the average of the variable angles between the radius vector \mathbf{R} and the magnetic susceptibility principal axis xx (or yy) that is rotating about the bond axis.

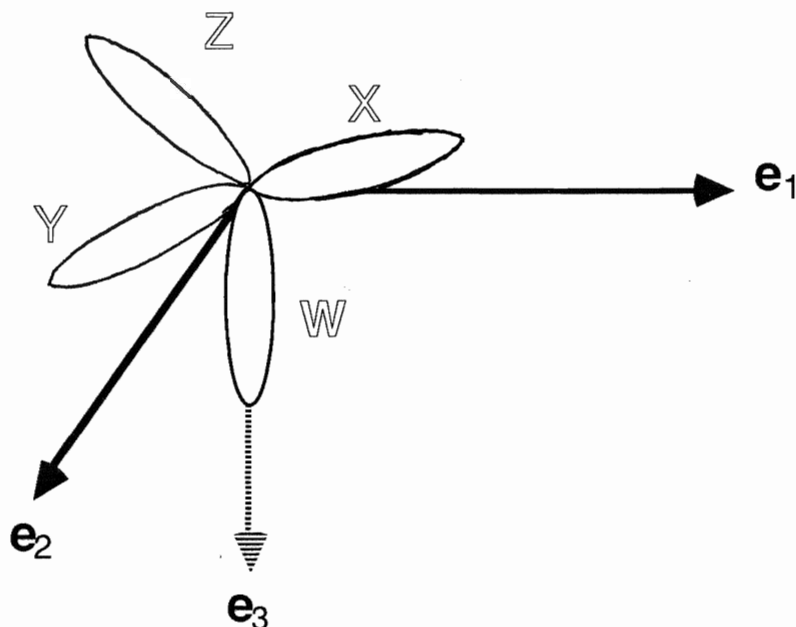


Figure 28 Schematic representation of bond magnetic susceptibility tensor of silicon carbide polytype

For X-bond, $\sigma_N^X = 1/(3L_0R^3) \cdot$

$$\begin{pmatrix} .333296x_{xx}(1-3\cos^2\phi_x) & -.384922x_{xx}(1-3\cos^2\phi_x) & .272112x_{xx}(1-3\cos^2\phi_x) \\ +.666704x_{zz}(1-3\cos^2\phi_z) & +.384922x_{zz}(1-3\cos^2\phi_z) & -.272112x_{zz}(1-3\cos^2\phi_z) \\ -.384922x_{xx}(1-3\cos^2\phi_x) & .777765x_{xx}(1-3\cos^2\phi_x) & .157104x_{xx}(1-3\cos^2\phi_x) \\ +.384922x_{zz}(1-3\cos^2\phi_z) & +.222235x_{zz}(1-3\cos^2\phi_z) & -.157104x_{zz}(1-3\cos^2\phi_z) \\ .272112x_{xx}(1-3\cos^2\phi_x) & .157104x_{xx}(1-3\cos^2\phi_x) & .888939x_{xx}(1-3\cos^2\phi_x) \\ -.272112x_{zz}(1-3\cos^2\phi_z) & -.157104x_{zz}(1-3\cos^2\phi_z) & +.111061x_{zz}(1-3\cos^2\phi_z) \end{pmatrix}$$

(4.9)

For Y-bonds, $\sigma_N^Y = 1/(3L_0R^3) \cdot$

$$\left[\begin{array}{l}
 .333296x_{xx}(1-3\cos^2\phi_x) \\
 +.666704x_{zz}(1-3\cos^2\phi_z) \\
 \\
 .384922x_{xx}(1-3\cos^2\phi_x) \quad .777765x_{xx}(1-3\cos^2\phi_x) \\
 -.384922x_{zz}(1-3\cos^2\phi_z) \quad +.222235x_{zz}(1-3\cos^2\phi_z) \\
 \\
 .272112x_{xx}(1-3\cos^2\phi_x) \quad -.157104x_{xx}(1-3\cos^2\phi_x) \quad .888939x_{xx}(1-3\cos^2\phi_x) \\
 -.272112x_{zz}(1-3\cos^2\phi_z) \quad +.157104x_{zz}(1-3\cos^2\phi_z) \quad +.111061x_{xx}(1-3\cos^2\phi_z)
 \end{array} \right]$$

(4.10)

For Z-bonds, $\sigma_N^Z = 1/(3L_0R^3) \cdot$

$$\left[\begin{array}{l}
 x_{xx}(1-3\cos^2\phi_x) \\
 \\
 0 \quad .111061x_{xx}(1-3\cos^2\phi_x) \\
 \quad +.888939x_{zz}(1-3\cos^2\phi_z) \\
 \\
 0 \quad .314208x_{xx}(1-3\cos^2\phi_x) \quad .888939x_{xx}(1-3\cos^2\phi_x) \\
 \quad -.314208x_{zz}(1-3\cos^2\phi_z) \quad +.111061x_{zz}(1-3\cos^2\phi_z)
 \end{array} \right]$$

(4.11)

The original bond magnetic susceptibility tensor is symmetrical, so are the transformed bond contribution tensors. The equations 4.8–4.11 are formulae that

calculate nuclear shieldings of layers 1 to 3 in 6H. For layers 4 to 6, the principal components are equal to those of corresponding bonds from layers 1 to 3, but the off components are opposite in sign. It can be proven that the sum of the corresponding components of these four bonds in layers 4 to 6 are exactly the same as in layers 1 to 3. Now, summations of all tensors by corresponding components are carried out to any desired limit, and these summations are performed with the computer program in appendix 7.

IV.D.2 Theoretical calculation of tensor components and determination of layer spacings

Analogous to equation 3.1, for silicons and carbons in each site, nine equations which relate the chemical shielding tensor components to the z coordinates of the layers can be set up. Due to the crystal symmetry, however, only the principal components are non zero, moreover, the principal components σ_{xx} and σ_{yy} are the same. Consequently, only two equations are independent. The equations are given by

$$(\sigma_{xx})_{N(j)} = (\sigma_{xx}^i)_N + (\sigma_{xx})_{N(j)} x_{\perp} + (\sigma_{zz})_{N(j)} x_{\parallel} + \sum_k a_k [(\sigma_{xx}^k)_{N(j)} x_{\perp} + (\sigma_{zz}^k)_{N(j)} x_{\parallel}] \quad (4.12)$$

$$(\sigma_{zz})_{N(j)} = (\sigma_{zz}^i)_N + (\sigma_{xx})_{N(j)} x_{\perp} + (\sigma_{zz})_{N(j)} x_{\parallel} + \sum_k a_k [(\sigma_{xx}^k)_{N(j)} x_{\perp} + (\sigma_{zz}^k)_{N(j)} x_{\parallel}] \quad (4.13)$$

where $(\sigma_{xx})_{N(j)}$ and $(\sigma_{zz})_{N(j)}$ are the magnetic shielding components along the X and Z axes of nucleus N(j); $(\sigma_{xx}^i)_N$ and $(\sigma_{zz}^i)_N$ are intrinsic magnetic shielding tensor components along the X and Z axes of nuclei type N; x_{\perp} , x_{\parallel} are bond magnetic susceptibilities perpendicular and parallel to the bond direction; $(\sigma_{xx})_{N(j)}$ and $(\sigma_{zz})_{N(j)}$ are geometric factors in the X and Z directions of nucleus

$N(j)$; $(\sigma_{xx}^k)_{N(j)}$, $(\sigma_{zz}^k)_{N(j)}$ are the changes in $(\sigma_{xx})_{N(j)}$ and $(\sigma_{zz})_{N(j)}$ caused by moving the k th layer of atom by a fixed amount of Δd , and a_k 's are coefficients whose values are to be determined. Then the change in layer spacing is $(a_k)(\Delta d)$.

In the case of 6H SiC, eleven unknowns have to be extracted from twelve magnetic shielding data given. As in MAS nmr, the entire procedure consists of three parts (see III.C.2), but is more complicated. The program in appendix 8 is designed to solve the problem.

IV.E Results and Discussions

The peak assignments in single crystal are basically according to the try and comparison method, that is, try different assignments and compare their results. For a single bond, x_{\parallel} is positive and x_{\perp} is negative.⁶¹ Thus one would expect a larger chemical shift corresponding with a larger g_{\parallel} and a smaller g_{\perp} , for the chemical shift σ is expressed as $(g_{\parallel}x_{\parallel} + g_{\perp}x_{\perp} + \dots)$. The assignments of the observed ^{13}C chemical shift tensor components to the geometric factors are simple, since the correspondences between the former and the latter are clearly seen. On the other hand, the assignments in ^{29}Si single crystal nmr case is not obvious. In sum, six ways of assignments are possible, thus all of them have to be tried. Table 24 shows the comparisons between the observed chemical shifts and the calculated for each of the six assignments. The intrinsic shifts, bond anisotropies are summarized in table 25.

From table 24 and 25, it is clear that the assignments 1 and 5 are more reasonable, since the calculated chemical shifts are more consistent with the experimental shielding tensor components; moreover, the bond magnetic anisotropies are comparable to the value determined from MAS nmr chemical

Table 24 The observed chemical shielding tensor components
Versus calculated for various ways of assignments in single
crystal chemical shift calculation (ECG=0.490)*

	Assign. 1		Assign. 2		Assign. 3		Assign. 4		Assign. 5		Assign. 6	
	Obsd.	Calcd.	Obsd.	Calcd.	Obsd.	Calcd.	Obsd.	Calcd.	Obsd.	Calcd.	Obsd.	Calcd.
$(\sigma_{xx})_{Si(1)}$	-21.7	-19.8	-22.7	-18.6	-11.6	-19.5	-11.6	-19.0	-22.7	-20.4	-21.7	-19.1
$(\sigma_{zz})_{Si(1)}$	-26.5	-17.8	-10.6	-16.7	-14.9	-18.2	-14.9	-16.7	-10.6	-18.6	-26.5	-17.7
$(\sigma_{xx})_{Si(2)}$	-11.6	-11.8	-21.7	-17.7	-22.7	-15.7	-21.7	-15.5	-11.6	-11.5	-22.7	-16.8
$(\sigma_{zz})_{Si(2)}$	-14.9	-19.4	-26.5	-22.7	-10.6	-14.6	-26.5	-23.7	-14.9	-15.5	-10.6	-16.8
$(\sigma_{xx})_{Si(3)}$	-22.7	-24.3	-11.6	-19.7	-21.7	-20.8	-22.7	-21.5	-21.7	-24.1	-11.6	-20.1
$(\sigma_{zz})_{Si(3)}$	-10.6	-14.8	-14.9	-12.8	-26.5	-19.2	-10.6	-11.5	-26.5	-17.9	-14.9	-17.5
$(\sigma_{xx})_{C(1)}$	21.5	21.3	21.5	21.4	21.5	22.2	21.5	21.4	21.5	22.2	21.5	21.9
$(\sigma_{zz})_{C(1)}$	22.9	21.6	22.9	20.8	22.9	20.8	22.9	21.2	22.9	21.5	22.9	20.7
$(\sigma_{xx})_{C(2)}$	14.7	14.4	14.7	21.0	14.7	19.4	14.7	19.2	14.7	15.9	14.7	20.3
$(\sigma_{zz})_{C(2)}$	22.0	21.7	22.0	24.8	22.0	18.2	22.0	25.7	22.0	19.0	22.0	20.0
$(\sigma_{xx})_{C(3)}$	29.3	29.8	29.3	23.0	29.3	23.9	29.3	24.9	29.3	27.3	29.3	23.3
$(\sigma_{zz})_{C(3)}$	16.3	17.8	16.3	15.5	16.3	22.2	16.3	14.2	16.3	20.7	16.3	20.5

* Before layer shifts

Table 25 Summary of the bond magnetic anisotropies,
intrinsic shielding tensor components
for each of the six assignments
(before layer shifts)

Assign. #	1	2	3	4	5	6
$x_{\parallel}(10^{-33}\text{m}^3/\text{bond})$	75.80	22.37	18.78	44.54	57.96	15.27
$x_{\perp}(10^{-33}\text{m}^3/\text{bond})$	-13.77	43.49	-34.03	44.92	-41.11	-11.44
$\Delta x(10^{-33}\text{m}^3/\text{bond})$	89.57	-21.12	52.81	-0.38	99.07	26.71
$(\sigma_{xx})^i_{\text{Si}}(\text{ppm})$	-38.89	-11.69	-38.57	-19.99	-56.76	-28.9
$(\sigma_{zz})^i_{\text{Si}}(\text{ppm})$	-33.48	-7.48	-37.14	-14.30	-53.03	-27.00
$(\sigma_{xx})^i_{\text{C}}(\text{ppm})$	1.60	22.40	18.57	20.75	15.15	20.03
$(\sigma_{zz})^i_{\text{C}}(\text{ppm})$	4.25	23.15	17.22	22.63	15.57	19.08

shifts. However, assignment 1 is more possible, since assignment 5 results in too large layer spacing shifts (see table 26).

Table 26 The layer spacing shifts of silicons and carbons
for each of the six assignments (Å)

Layer site	Assgn.1	Assgn.2	Assgn.3	Assgn.4	Assgn.5	Assgn.6
Si(1)	0.0000	0.0000	0.0000	0.0000	0.0000	0.0000
C(1)	-0.0016	-0.0158	0.0346	0.0006	0.0115	-0.0092
Si(2)	-0.0004	-0.0086	0.0057	-0.0027	0.0000	-0.0097
C(2)	-0.0048	-0.0052	0.0388	0.0067	0.0146	-0.0369
Si(3)	-0.0039	0.0025	0.0060	0.0063	0.0027	-0.0311
C(3)	-0.0003	-0.0077	0.0245	-0.0023	0.0110	-0.0015

Table 27 gives the assignments from MAS and single crystal nmr spectra. The comparisons between the MAS nmr chemical shifts and the chemical shifts calculated from 1/3 of the trace of the magnetic shielding tensors reveal that the two assignments are consistent. Both assignments show that Si(1) has the most negative chemical shifts (-25.1 ppm for the former and -23.3 ppm for the latter, and Si(2) has the least negative chemical shifts (-14.5 and -12.7 ppm). Similarly, the assignments are consistent for carbons.

Table 27 Comparisons between the assignments from
MAS and single crystal nmr Spectra

	$\sigma(1/3 \text{ trace})(\text{ppm})$	$\sigma(\text{MAS})(\text{ppm})$	Type
Si(1)	-23.3	-25.1	B
Si(2)	-12.7	-14.5	C
Si(3)	-18.7	-20.6	A
C(1)	22.0	20.4	B
C(2)	17.1	15.1	A
C(3)	24.6	23.4	C

In the calculation, eleven unknowns are extracted from twelve known chemical shift tensor components. The number of unknowns would exactly match the number of knowns if the electrical centre of gravity were included. Thus several ECG's have been tested, and the results indicate that the calculated chemical shifts and layer spacing shifts do not change so considerably as those in

MAS nmr calculations do. For comparisons with the results from the last chapter, an ECG of 0.490 has been selected.

From table 25, the bond magnetic anisotropy ($93.70 \times 10^{-33} \text{m}^3/\text{bond}$ in SI unit) is different from the value of the MAS nmr calculation ($88.81 \times 10^{-33} \text{m}^3/\text{bond}$). One of the reasons could be the different bulk magnetic susceptibility effects for powder and single crystal sample, as indicated in tables 22 and 23 where the $1/3(\text{trace})$'s are about 0.9 to 2.0 ppm different from the MAS nmr chemical shifts.

Another interesting fact is that the calculated chemical shifts of carbons fit much better to the known chemical shift tensor components than those of silicon do. This can be explained in the following : carbon is a second period element, while Si is a third one; the energy difference between 3p and 3d orbitals is smaller than that between 2p and 3s, thus, the electron in the silicon highest occupied orbital is more easily excited to higher energy levels, consequently, the nuclear paramagnetic shielding can be very large. An opposite example of this is that the hydrogen paramagnetic shielding is always neglected in the magnetic shielding calculation, since the large energy difference between 1s and 2s orbitals makes the probability of electron excitation very low. A conclusion from above is that the non-local paramagnetic shielding of silicon nucleus should be included in the single crystal chemical shift calculation.

Compared the layer spacing shifts determined from MAS nmr chemical shifts, the layer spacing shifts calculated via single crystal method are quite far apart, and are outside the X-ray standard deviations. This may also arise from the negligence of non-local paramagnetic shielding of silicon nucleus in the single crystal chemical shift calculation.

CHAPTER V CONCLUSION

Our purely geometric and empirical approach to relating structures and chemical shifts is promising and has the virtue of simplicity. It leads to a method for using chemical shifts to determine and refine crystal structures. From this work, we have the following conclusions :

1) Long-range dipolar shielding is most responsible for the MAS nmr chemical shift differences among the chemically equivalent but crystallographically independent silicons and carbons in SiC polytypes. The convergence of long-range shielding is so slow that contributions from bonds up to 100 Å must be considered in the calculation.

2) The chemical shifts calculated depend on the layer stacking sequence, the electrical centre of gravity, and the spacings between silicon and carbon layers.

3) The geometric factors for all silicons and carbons are linearly dependent on layer spacing changes and are almost additive for simultaneous shifts in positions of several atoms.

4) Relationships between MAS nmr chemical shifts and layer spacing changes have been suggested. The layer spacings of 6H calculated by using a computer program are within X-ray standard deviations. From this the layer spacings of 15R have also been predicted.

5) The silicon and carbon intrinsic shifts of 6H are about 1 ppm different from those of 15R. The discrepancies may arise from the different bulk magnetic susceptibility effects on different samples and different amount of impurities in samples.

6) Preliminary studies on single crystal chemical shift calculations show that the paramagnetic shielding in silicon should be accounted in the single crystal chemical shift calculation.

REFERENCES

- 1 A. H. Boerdijk, Philips Res. Rept., 7 (1952), 303.
- 2 H. Baumhauer, Z. Krist., 50 (1912), 33-39.
- 3 H. Baumhauer, Z. Krist., 55 (1915), 249-259.
- 4 M. L. Frankenheim, J. Prakt. Chem., 16 (1839), 1-14
- 5 A. R. Verma and P. Krishna, Polymorphism and Polytypism in Crystals, Wiley, New York (1966).
- 6 L. S. Ramsdell, Am. Mineralogist, 32 (1947), 64-82.
- 7 H. Ott., Z. Krist. 61(1925), 515-531.
- 8 Gunna Hagg, Arkiv. For Kemi, Mineralogi Och Geologi, 16B (1943), 1-6.
- 9 G. S. Zhdanov, Compt. Rend. Acad. Sci. USSR, 48(1945), 43.
- 10 E. G. Acheson, Chem. News, 68 (1893), 179; J. Franklin Inst. 136(1893), 194-203, 279-287.
- 11 L. Pauling, Nature of the Chemical Bond, Cornell Univ. Press, Ithaca (1950).
- 12 M. J. Buerger, The Precession Method, Wiley, New York (1964).
- 13 E. Lippmaa, M. Magi, A. Samoson, G. Engelhardt, and A. R. Grimmer, J. Am. Chem. Soc., 102 (1980), 4889.
- 14 X. Liu, J. Kliniowski, J. M. Thomas, Chem. Phys. Lett., 127 (1986), 563.
- 15 K. A. Smith, R. J. Kirkpatrick, E. Oldfield, D. M. Henderson, Mineral., 68 (1983), 1206.
- 16 R. Dupree, D. Holland, D. S. Williams, J. Non-Cryst. Solids, 81 (1986), 185.
- 17 G. L. Turner, R. J. Kirkpatrick, S. H. Risbud, E. Oldfield, Am. Ceram. Soc. Bull., 66 (1987), 656.
- 18 S. Hayashi, K. Hayamizu, S. Yamasaki, A. Matsuda, K. Tanaka, J. Appl. Phys.,

- 60 (1986), 1839.
- 19 F. C. Schilling, F. A. Bovey, A. J. Lovinger, J. M. Zeigler, *Macromolecules*, 19 (1986), 2660.
 - 20 G. R. Finlay, J. S. Hartman, M. F. Richardson, B. L. Williams, *J. Chem. Soc. Chem. Commun.*, 1985, 159
 - 21 J. R. Guth, W. T. Petuskey, *J. Phys. Chem.*, 91 (1987), 5361.
 - 22 J. S. Hartman, M. F. Richardson, B. L. Sheriff, B. G. Winsborrow, *J. Am. Chem. Soc.*, 109 (1987), 6059
 - 22(a) E. Fukushima, S. B. W. Roeder, Experimental Pulse NMR, A Nuts and Bolts Approach, Addison-Wesley, Reading, Mass. (1981).
 - 23 B. G. Winsborrow, Polytypism and Silicon Carbide—A Solid State Nuclear Magnetic Resonance Study (1987), M.Sc. thesis, Brock University, St. Catharines, Ontario, Canada.
 - 24 M. J. Duijvestijn, C. Van Derlugt, J. Smidt, R. A. Wind, K. W. Zilm, D. C. Staplin, *Chem. Phys. Lett.*, 102 (1983), 25
 - 25 H. Ott, *Z. Krist.*, 62 (1925), 201-217.
 - 26 A. W. Hull, *Phys. Rev.*, 13 (1919), 292-295.
 - 27 A. W. Hull, *Phys. Rev.* 15 (1920), 545-546.
 - 28 A. H. Gomes de Mesquita, *Acta Cryst.*, 23 (1967), 610.
 - 29 J. Guth, W. T. Petuskey, *J. Phys. Chem. Solids*, 48 (1987), 541-549.
 - 30 Y. M. Tairov, V. F. Tsvetkov, *Prog. Crystal Growth Charact.*, 111 (1983), 7.
 - 31 A. Taylor, R. M. Jones, *Proc. Conf. Silicon Carbide*, Boston (1960), 147.
 - 32 R. F. Adamsky, K. M. Merz, *Z. Kristallogr.*, 111 (1959), 350.
 - 33 H. Schulz, K. H. Thiemann, *Solid St. Commun.*, 32 (1979), 783.
 - 34 J. D. H. Donnay, Crystal Data Determinative Tables, 2nd edn. (1963).
 - 35(a) M. O'keeffe, B. G. Hyde, Structure and Bonding in Crystals (1981), 227.
 - 35(b) E. D. Becker, High Resolution NMR, Academic Press, New York (1980).

- 36 I. Morishima, K. Yoshikawa, K. Okada, T. Yonezawa, and K. Goto, J. Am. Chem. Soc., 95 (1973), 165.
- 37 N. D. Sung, C.K.Park, M.K.Park, K.S.Kown, and T.R.Kim, Taehan Hwahakhoe Chi, 29(1985), 277.
- 38 M.Ul Hasan and S.A.Ali, Magn. Reson. Chem., 23(1985), 23.
- 39 Y. Takeuchi, H. Furuyama, S. Fukushi and S. Fujiwara, J. Chem. Soc., Perkin Trans, 2(1985), 175.
- 40 M. I. Qureshi, J. Chem. Educ., 62(1985), 861
- 41 H. Volger, Chem. Scr., 24(1984), 188.
- 42 (a) N. F. Ramsey, Nuclear Moments, John Wiley and Sons, Inc., New York (1953); (b) Molecular Beams, Clarendon Press, Oxford (1956).
- 43 H. M. McConnell, Ann. Rev. Phys. Chem., 8(1957), 105.
- 44 J. F. Hornig and J. O. Hirschfelder, J. Chem. Phys., 23 (1955), 474.
- 45 T. P. Das and R. Bersohn, Phys. Rev., 104(1956), 849.
- 46 B. R. McGarvey, J. Chem. Phys., 27 (1957), 68.
- 47 J. A. Pople, Proc. Roy. Soc. (London), A239 (1957), 541-550.
- 48 H. M. McConnell, J. Chem. Phys., 27 (1957), 226.
- 49 M. J. Stephen, Proc. Roy. Soc. (London), A243 (1957), 264.
- 50 N. F. Ramsey, Phys. Rev. 78 (1950), 699; 86 (1952), 243.
- 51 P. T. Narasimhan, M. T. Rogers, J. Phys. Chem., 63 (1959), 1388.
- 52 L. H. Piette, J. D. Ray, and R. A. Ogg, J. Mol. Spectroscopy, 2 (1958), 66.
- 53 W. D. Philips, J. Chem. Phys., 23 (1955), 1363.
- 54(a) H. S. Gutowsky, and C. H. Holm, *ibid.*, 25 (1956), 1228.
- 54(b) W.T. Paynes, Nuclear Magnetic Resonance, Vol.3, Chapter 1, R. K. Harris, Senior Reporter, Specialist Periodical Reports, The Chemical Society, London, 1974.
- 55 M. J. McGlinchey, R. C. Burns, R. Hofer, S. Top, G. Jaouen, Organometallics,

- 5 (1986), 104.
- 56 D. E. Sands, Vectors and Tensors in Crystallography, Addison-Wesley Publishings Company, Massachusetts (1982), 1-29.
- 57 S. Trinath, Phys. letts. A, 115,4 (1986), 173.
- 58 R. F. Adamsky, K. M. Merz, Z. Kristallogr. III (1959), 350.
- 59 J. Schlichting, G. Czack, E. Koch-Bienemann, P. Kuhn, and F. Schroder, Gmelin Handbook of Inorganic Chemistry, Si-Silicon ,Supp. Vol. B2,(1984), 63.
- 60 Y. M. Tairov, V. F. Tsvetkov, Prog. Crystal Growth Charact., 7 (1983), 111.
- 61 R. K. Harris, Nuclear Magnetic Resonance Spectroscopy, Pitman, London (1983), 195.
- 62 M. Schindler and W. Kutzelnigg, J. Am. Chem. Soc., 105 (1983), 1360.
- 63 G. H. Stout, L. H. Jensen, X-ray structure determination, Macmillan Publishing Co. Inc., New York (1968), 393.
- 64 M. E. Rose, Elementary Theory of Angular Momentum, Wiley, New York (1967).
- 65 A. Abragam, The Principles of Nuclear Magnetism, Oxford University Press, London (1961).
- 66 R. F. Schneider, J. Chem. Phys., 48 (1968), 4905.
- 67 R. M. Lynden-Bell, Mol. Phys., 29 (1975), 301.
- 68 U. Haeberlen, High Resolution NMR in Solids—Selective Averaging, Supplement to Advances in Magnetic Resonance, Academic Press, New York (1976), 34.
- 69 J. C. Facelli, A. M. Orendt, D. M. Grant, J. Michl, Chem. Phys. Lett., 112 (1984),147.
- 70 A. D. Buckingham, S. M. Malm, Mol. Phys., 22 (1971), 1127.
- 71 J. B. Robert, L. Wiesenfeld, Phys. Rep., 86(1982), 363.
- 72 J. A. Weil, T. Buck, and J. E. Clapp, Adv. Magn. Reson. 6 (1973), 183.

- 73 W. S. Veeman, Phil. Trans. R. Soc. Lond., A299(1981), 629-641.
- 74 C. M. Carter, D. W. Alderman, D. M. Grant, J. Magn. Reson., 65(1985), 183.
- 75 C. A. Fyfe, Solid State NMR for Chemists; C. F. C. Press, Guelph (1983).
- 76 M. Mehring, High Resolution NMR in Solids, 2nd ed.; Springer, Berlin (1983).
- 77 W. S. Veeman, Prog. NMR Spectrosc., 16 (1984), 193.
- 78 J. C. Facelli, A. M. Orendt, A. C. Beeler, M. S. Solum, D. Depke, K. D. Malsch, J. W. Downing, P. S. Murthy, D. M. Grant, and J. Michl, J. Am. Chem. Soc., 107(1985), 6749.
- 79 K. Takegoshi, C. A. McDowell, Chem. Phys. Letts, No.1 123, No.3 159(1985).
- 80 C. M. Carter, D. W. Alderman, J. C. Facelli, D. M. Grant, J. Am. Chem. Soc. 109 (1987), 2639.
- 81 J. C. Facelli, D. M. Grant, J. Michl, Acc. Chem. Res., 20 (1987), 152.
- 82 J. B. Lambert, F. G. Riddell, NATO ASI Ser., Ser. C.,103 (Multinucl. Approach NMR Spectrosc.,1983), 29.
- 83 M. J. Forster, Nucl. Magn. Reson., 16 (1987), 38-83.
- 84 J. C. Facelli, D. M. Grant, J. Michl, Inter. J. Quantum Chem., 31(1),1987, 45-55.
- 85 J. Klinowski, Progr. NMR Spectry., 16 (1984),237.
- 86 R. A. Kinsey, R. J. Kirkpatrick, J. Hawer, K. A. Smith, and E. Oldfield, Am. Miner., 70 (1985), 537-548.
- 87 B. L. Sherriff, H. D. Grundy, and J. S. Hartman, Can. Miner., 25 (1987), 717.
- 88 A. R. Grimmer, Chem. Phys. Lett., 119 (1983), 416.
- 89 E. J. J. Groenen, N. C. M. Alma, J. Dorrepaal, G. R. Hays and A. G. T. G. Kortbeek, Zeolites, 5 (1985), 361.
- 90 B. L. Sherriff, H. D. Grundy, Nature 332(1988), 819.
- 91 U. Haeblerlen, High Resolution NMR in Solids, Selective Averaging Advances in Magnetic Resonance; Academic: New York (1976); Suppl.1.

- 92 M. Mehring, NMR: Basic Princ. Prog. ,11(1976),1.
- 93 D. W. Alderman, M. S. Solum, D. M. Grant, J. Chem. Phys., 84(1986), 3717.
- 94 N. K. Sethi, D. M. Grant, R. J. Pugmire, J. Magn. Reson., 71(1987), 476-479.
- 95 J. W. Gibbs, E. B. Wilson, Vector Analysis, Dover Publications, Inc., New York (1960), Chapter V.

APPENDIX 1

Derivation of the Shielding Constant σ_N^G
from the shielding tensor σ_N^G

Magnetic shielding tensor related to the bond magnetic susceptibility tensor is given by (from reference 28)

$$\sigma_N^G = 1/L_0 [X^G/R^3 - 3X^G \cdot RR/R^5]$$

Where

$$\begin{aligned} X^G \cdot RR &= \begin{pmatrix} X_X^G \cdot X_X^G & 0 & 0 \\ 0 & X_Y^G \cdot X_Y^G & 0 \\ 0 & 0 & X_Z^G \cdot X_Z^G \end{pmatrix} \cdot RR \\ &= \begin{pmatrix} X_X^G \cdot X_X^G \cdot RR & 0 & 0 \\ 0 & X_Y^G \cdot X_Y^G \cdot RR & 0 \\ 0 & 0 & X_Z^G \cdot X_Z^G \cdot RR \end{pmatrix} \\ &= \begin{pmatrix} (X_X^G \cdot R)(X_X^G \cdot R) & 0 & 0 \\ 0 & (X_Y^G \cdot R)(X_Y^G \cdot R) & 0 \\ 0 & 0 & (X_Z^G \cdot R)(X_Z^G \cdot R) \end{pmatrix} \\ &= \begin{pmatrix} x_{xx}R^2\cos^2\theta_{Rx} & 0 & 0 \\ 0 & x_{yy}R^2\cos^2\theta_{Ry} & 0 \\ 0 & 0 & x_{zz}R^2\cos^2\theta_{Rz} \end{pmatrix} \\ &= \begin{pmatrix} x_{xx}\cos^2\theta_{Rx} & 0 & 0 \\ 0 & x_{yy}\cos^2\theta_{Ry} & 0 \\ 0 & 0 & x_{zz}\cos^2\theta_{Rz} \end{pmatrix} R^2 \end{aligned}$$

Then

$$\sigma_N^G = 1/L_0 \left[X^G/R^3 - 3 \cdot \begin{pmatrix} x_{xx}\cos^2\theta_{Rx} & 0 & 0 \\ 0 & x_{yy}\cos^2\theta_{Ry} & 0 \\ 0 & 0 & x_{zz}\cos^2\theta_{Rz} \end{pmatrix} R^2/R^5 \right]$$

$$=1/L_0R^3 \begin{pmatrix} x_{xx}(1-3\cos^2\theta_{Rx}) & 0 & 0 \\ 0 & x_{yy}(1-3\cos^2\theta_{Ry}) & 0 \\ 0 & 0 & x_{zz}(1-3\cos^2\theta_{Rz}) \end{pmatrix}$$

$$\sigma_N^G = 1/3 \text{ Tr. } \langle \sigma_N^G \rangle_{\text{ave.}}$$

$$=1/(3L_0R^3)[x_{xx}(1-3\cos^2\theta_{Rx})+x_{yy}(1-3\cos^2\theta_{Ry})+x_{zz}(1-3\cos^2\theta_{Rz})]$$

$$\text{because } \cos^2\theta_{Rx} + \cos^2\theta_{Ry} + \cos^2\theta_{Rz} = 1$$

$$\text{and } x_{xx}=x_{yy} \text{ for SiC polytypes}$$

$$\sigma_N^G = \Delta\chi / (3L_0R^3)(1-3\cos^2\theta_{Rz})$$

APPENDIX 2

PROGRAM FOR THE CALCULATION OF GEOMETRIC
FACTORS OF SILICONS (SIC 6H POWDERED SAMPLE)

```

COMMON/CELL/G(3,3)
DIMENSION W(15,3),X(15,3),Y(15,3),Z(15,3)
DIMENSION WM(15,3),XM(15,3),YM(15,3),ZM(15,3)
DIMENSION GEOM(15),WMAG(15),XMAG(15),YMAG(15),ZMAG(15)
DIMENSION SIREF(3), R(15,3), S(15,3), T(15,3), U(15,3)
DIMENSION SI(6,3), C(5,3)
DIMENSION RA(15,3),SA(15,3),TA(15,3),UA(15,3)

C
C THIS PROGRAM CALCULATES THE DIAMAGNETIC ANISOTROPIC
C CONTRIBUTION TO THE CHEMICAL SHIFT FOR SIC. SEE MIKE
C MCGLINCHEY, ORGANOMETALLICS, VOL. 5, 104, 1986. THE
C COORDINATES AND CELL DIMENSIONS ARE FROM GOMES DE
C MESQUITE.

C
C SIREF(1) = 0.0
C SIREF(2) = 0.0
C SIREF(3) = 0.0
C KOUNT = 0

C SET DMAX
C DMAX =100.0

C ECG IS FACTOR OF ELECTRICAL CENTER OF GRAVITY FOR SI'S;
C (1- ECG) IS FACTOR OF ELECTRICAL CENTER OF GRAVITY FOR C'S;
C ECG*BOND LENGTH EQUALS TO CARBON COVALENT RADIUS.

C SET ECG
C ECG=.490
C GTOT = 0.0
C NTOT = 0

C
C LOAD METRIC TENSOR FOR SIC 6H FORM THE GEOMETRIC FACTOR IS
C EXCEEDNGLY SENSITIVE TO THE MAGNITUDE OF THE CELL
C DIMENSIONS. THE DIMENSIONS ARE FROM GOMES DE MESQUITE.

C
C G(1,1) = 3.08065**2
C G(1,2) = -0.5*G(1,1)
C G(1,3) = 0.0
C G(2,1) = G(1,2)
C G(2,2) = G(1,1)

```

```

G(2,3) = 0.0
G(3,1) = G(1,3)
G(3,2) = G(2,3)
G(3,3) = 15.1174**2
CH = SQRT(G(3,3))
C PUT IN COORDINATES OF SI AND C ATOMS
SI(1,1) = 0.0
SI(1,2) = 0.0
SI(1,3) = 0.0
C(1,1) = 0.0
C(1,2) = 0
C(1,3) = 0.12527
SI(2,1) = 1./3.
SI(2,2) = 2./3.
SI(2,3) = 0.16678
C(2,1) = SI(2,1)
C(2,2) = SI(2,2)
C(2,3) = 0.29188
SI(3,1) = 2./3.
SI(3,2) = 4./3.
SI(3,3) = 0.33323
C(3,1) = SI(3,1)
C(3,2) = SI(3,2)
C(3,3) = 0.45850
SI(4,1) = 1.0
SI(4,2) = 2.0
SI(4,3) = 0.5
W(1,1) = 0.0
W(1,2) = 0.0
W(1,3) = C(1,3) - SI(1,3)
X(1,1) = SI(2,1) - C(1,1)
X(1,2) = SI(2,2) - C(1,2)
X(1,3) = SI(2,3) - C(1,3)
Y(1,1) = X(1,1)
Y(1,2) = X(1,2) - 1.
Y(1,3) = X(1,3)
Z(1,1) = X(1,1) - 1.
Z(1,2) = X(1,2) - 1.
Z(1,3) = X(1,3)
W(2,1) = 0.0
W(2,2) = 0.0
W(2,3) = C(2,3) - SI(2,3)
X(2,1) = SI(3,1) - C(2,1)

```

```

X(2,2) = SI(3,2) - C(2,2)
X(2,3) = SI(3,3) - C(2,3)
Y(2,1) = X(2,1)
Y(2,2) = X(2,2) - 1.
Y(2,3) = X(2,3)
Z(2,1) = X(2,1) - 1.
Z(2,2) = X(2,2) - 1.
Z(2,3) = X(2,3)
W(3,1) = 0
W(3,2) = 0
W(3,3) = C(3,3) - SI(3,3)
X(3,1) = SI(4,1) - C(3,1)
X(3,2) = SI(4,2) - C(3,2)
X(3,3) = SI(4,3) - C(3,3)
Y(3,1) = X(3,1)
Y(3,2) = X(3,2) - 1.
Y(3,3) = X(3,3)
Z(3,1) = X(3,1) - 1.
Z(3,2) = X(3,2) - 1.
Z(3,3) = X(3,3)
DO 2 I = 4,6
DO 2 J = 1,2
C  NOW FIX BOND VECTORS FOR THE 4TH, 5TH, AND 6TH LAYERS.
W(I,J) = W(3,J)
X(I,J) = -X(3,J)
Y(I,J) = -Y(3,J)
Z(I,J) = -Z(3,J)
2  CONTINUE
DO 3 I = 1,3
J = I + 3
W(J,3) = W(I,3)
X(J,3) = X(I,3)
Y(J,3) = Y(I,3)
3  Z(J,3) = Z(I,3)
DO 4 I = 1,3
DO 4 J = 1,3
WM(I,J) = ECG*SI(I,J) +(1.-ECG)*C(I,J)
K = I + 1
4  XM(I,J) = ECG*SI(K,J) +(1.-ECG)*C(I,J)
DO 5 I = 1,3
YM(I,1) = XM(I,1)
YM(I,2) = XM(I,2) - ECG
YM(I,3) = XM(I,3)

```

```

ZM(I,1) = XM(I,1) -ECG
ZM(I,2) = XM(I,2) -ECG
5  ZM(I,3) = XM(I,3)
   DO 6 I = 1,3
     J = 7 - I
     X1=2.*I-1.0
     XM(J,1) =X1/3.0- XM(I,1)
     X2=4.*I-2.0
     XM(J,2) =X2/3.0- XM(I,2)
     YM(J,1) = X1/3.0- YM(I,1)
     Y2=4.*I-5.
     YM(J,2) = Y2/3.0- YM(I,2)
     Z1=2.*I-4.
     ZM(J,1)= Z1/3.0-ZM(I,1)
6  ZM(J,2)= Y2/3.0-ZM(I,2)
     WM(4,1) = SI(1,1)
     WM(4,2) = SI(1,2)
     WM(5,1) = SI(3,1)
     WM(5,2) = SI(3,2)
     WM(6,1) = SI(2,1)
     WM(6,2) = SI(2,2)
     DO 7 I = 1,3
       J = I + 3
       WM(J,3) = WM(I,3) + 0.5
       XM(J,3) = XM(I,3) + 0.5
       YM(J,3) = YM(I,3) + 0.5
7  ZM(J,3) = ZM(I,3) + 0.5
C  NOW CALCULATE BON DISTANCES IN EACH LAYER
   DO 10 L = 1,6
     CALL DOTP(W,W,L,DOT)
     WMAG(L) = SQRT(DOT)
     CALL DOTP(X,X,L,DOT)
     XMAG(L) = SQRT(DOT)
     CALL DOTP(Y,Y,L,DOT)
     YMAG(L) = SQRT(DOT)
     CALL DOTP(Z,Z,L,DOT)
     ZMAG(L) = SQRT(DOT)
10  WRITE(6,1000)L, WMAG(L),XMAG(L),YMAG(L),ZMAG(L)
     WRITE(6,999)
999  FORMAT(1H1)
1000 FORMAT(1H , "BOND DISTANCES IN LAYER NUMBER ",I2,";",4F10.3)
4  DO 20 L = 1,6
    DO 15 N = 1,3

```



```

R(L,N) = WM(L,N) - SIREF(N)
S(L,N) = XM(L,N) - SIREF(N)
T(L,N) = YM(L,N) - SIREF(N)
15 U(L,N) = ZM(L,N) - SIREF(N)
C NOW CHECK THAT THE R(I) ETC. ARE IN THE STARTING UNIT CELL
DO 20 N = 1,3
IF(R(L,N).GT.1.0) R(L,N) = R(L,N) - 1.0
IF(S(L,N).GT.1.0) S(L,N) = S(L,N) - 1.0
IF(T(L,N).GT.1.0) T(L,N) = T(L,N) - 1.0
IF(U(L,N).GT.1.0) U(L,N) = U(L,N) - 1.0
IF(R(L,N).LT.0.0) R(L,N) = R(L,N) + 1.0
IF(S(L,N).LT.0.0) S(L,N) = S(L,N) + 1.0
IF(T(L,N).LT.0.0) T(L,N) = T(L,N) + 1.0
20 IF(U(L,N).LT.0.0) U(L,N) = U(L,N) + 1.0
C NOW MOVE DOWN 8 UNIT CELLS IN Z AND PREPARE TO LOOP
DO 25 L = 1,6
RA(L,3) = R(L,3) - 8.0
SA(L,3) = S(L,3) - 8.0
TA(L,3) = T(L,3) - 8.0
25 UA(L,3) = U(L,3) - 8.0
DO 42 NCEL = 1,17
C NCEL IS A DUMMY VARIABLE WHICH ALLOWS US TO MOVE OVER 17
UNIT CELLS IN THE Z DIRECTION
C DO 40 L = 1,6
GEOM(L) = 0.0
C PREPARE TO LOOP THROUGH 101 UNIT CELLS IN X AND Y DIRECTIONS
C THUS MOVE 50 CELLS NEGATIVE IN BOTH X AND Y
C THIS NUMBER IS NECESSARY TO BE SURE TO GET 100A AWAY FROM
THE ORIGIN. SEE NOTEBOOK VOL. 17.

DO 30 N = 1,2
RA(L,N) = R(L,N) - 50.0
SA(L,N) = S(L,N) - 50.0
TA(L,N) = T(L,N) - 50.0
30 UA(L,N) = U(L,N) - 50.0
DO 36 I = 1,101
DO 35 J = 1,101
CALL DOTP(RA,RA,L,DOT)
RAMAG = SQRT(DOT)
IF(RAMAG.LT.1.65) GO TO 31
IF(RAMAG.GT.DMAX) GO TO 31
NTOT = NTOT + 1
CALL DOTP(RA,W,L,DOT)

```

```

      CPHI = DOT/(RAMAG*WMAG(L))
      IF(ABS(CPHI).GT.1.0) WRITE (6,1020) CPHI
1020 FORMAT(1H , "ERROR IN COS PHI",F12.9)
      GEO = (1. - 3.*CPHI*CPHI)/(3.*RAMAG*RAMAG*RAMAG)
      GEOM(L) = GEOM(L) + GEO
C      WRITE(6,1030)(RA(L,N),W(L,N),N=1,3),RAMAG,GEO
1030 FORMAT(1H ,3(F8.4,1X),10X,3(F8.4,1X),10X,F10.3,2X,F8.4)
      31 CALL DOTP(SA,SA,L,DOT)
      SAMAG = SQRT(DOT)
C      ELIMINATE FIRST NEIGHBOR CONTRIBUTIONS
      IF(SAMAG.LT.1.65) GO TO 32
C      ELIMINATE FIRST NEIGHBOR CONTRIBUTIONS
      IF(SAMAG.GT.DMAX) GO TO 32
      NTOT = NTOT + 1
      CALL DOTP(SA,X,L,DOT)
      CPHI = DOT/(SAMAG*XMAG(L))
      IF(ABS(CPHI).GT.1.0) WRITE (6,1020) CPHI
      GEO = (1. - 3.*CPHI*CPHI)/(3.*SAMAG*SAMAG*SAMAG)
      GEOM(L) = GEOM(L) + GEO
C      WRITE(6,1030)(SA(L,N),X(L,N),N=1,3),SAMAG,GEO
      32 CALL DOTP(TA,TA,L,DOT)
      TAMAG = SQRT(DOT)
      IF(TAMAG.LT.1.65) GO TO 33
C      ELIMINATE FIRST NEIGHBOR CONTRIBUTIONS
      IF(TAMAG.GT.DMAX) GO TO 33
      NTOT = NTOT + 1
      CALL DOTP(TA,Y,L,DOT)
      CPHI = DOT/(TAMAG*YMAG(L))
      IF(ABS(CPHI).GT.1.0) WRITE (6,1020) CPHI
      GEO = (1. - 3.*CPHI*CPHI)/(3.*TAMAG*TAMAG*TAMAG)
      GEOM(L) = GEOM(L) + GEO
C      WRITE(6,1030)(TA(L,N),Y(L,N),N=1,3),TAMAG,GEO
      33 CALL DOTP(UA,UA,L,DOT)
      UAMAG = SQRT(DOT)
      IF(UAMAG.LT.1.65) GO TO 34
C      ELIMINATE FIRST NEIGHBOR CONTRIBUTIONS
      IF(UAMAG.GT.DMAX) GO TO 34
      NTOT = NTOT + 1
      CALL DOTP(UA,Z,L,DOT)
      CPHI = DOT/(UAMAG*ZMAG(L))
      IF(ABS(CPHI).GT.1.0) WRITE (6,1020) CPHI
      GEO = (1. - 3.*CPHI*CPHI)/(3.*UAMAG*UAMAG*UAMAG)
      GEOM(L) = GEOM(L) + GEO

```

```

C   WRITE(6,1030)(UA(L,N),Z(L,N),N=1,3),UAMAG,GEO
34  RA(L,1) = RA(L,1) + 1.0
    SA(L,1) = SA(L,1) + 1.0
    TA(L,1) = TA(L,1) + 1.0
    UA(L,1) = UA(L,1) + 1.0
35  CONTINUE
C   RESET X COORDINATE OF RA AFTER PASS THROUH 101 CELLS IN X
    DIRECTION
    RA(L,1) = RA(L,1) - 101.0
    SA(L,1) = SA(L,1) - 101.0
    TA(L,1) = TA(L,1) - 101.0
    UA(L,1) = UA(L,1) - 101.0
    RA(L,2) = RA(L,2) + 1.0
    SA(L,2) = SA(L,2) + 1.0
    TA(L,2) = TA(L,2) + 1.0
    UA(L,2) = UA(L,2) + 1.0
36  CONTINUE
    RA(L,2) = RA(L,2) - 101.0
    SA(L,2) = SA(L,2) - 101.0
    TA(L,2) = TA(L,2) - 101.0
    UA(L,2) = UA(L,2) - 101.0
    GTOT = GEOM(L) + GTOT
40  CONTINUE
    DO 41 L = 1,6
    RA(L,3) = RA(L,3) + 1.0
    SA(L,3) = SA(L,3) + 1.0
    TA(L,3) = TA(L,3) + 1.0
    UA(L,3) = UA(L,3) + 1.0
41  CONTINUE
    KOUNT = KOUNT + 1
    WRITE(6,1050) GTOT, NTOT, KOUNT
1050 FORMAT(1H0,"TOTAL GEOM FACTOR IS ",F12.9," AND TOTAL NO. OF
      1 INTERACTIONS IS ",I10," FOR SI ",I2)
    GTOT = 0.0
    NTOT = 0
    GO TO (43,44,45,48),KOUNT
C   NOW CALCULATE FOR OTHER INDEPENDENT SI'S
43  SIREF(1) = SI(2,1)
    SIREF(2) = SI(2,2)
    SIREF(3) = SI(2,3)
    GO TO 14
44  SIREF(1) = SI(3,1)
    SIREF(2) = SI(3,2)

```

```
SIREF(3) = SI(3,3)
GO TO 14
45  SIREF(1) = SI(4,1)
    SIREF(2) = SI(4,2)
    SIREF(3) = SI(4,3)
    GO TO 14
48  STOP
    END
    SUBROUTINE DOTP(A,B,L,DOT)
    COMMON/CELL/ G(3,3)
    DIMENSION A(15,3), B(15,3)
    DOT = 0.0
    DO 10 I = 1,3
    DO 10 J = 1,3
10   DOT = A(L,I)*B(L,J)*G(I,J) + DOT
    RETURN
    END
```

APPENDIX 3

PROGRAM FOR THE CALCULATION OF GEOMETRIC FACTORS
OF SILICONS (SIC15R POWDERED SAMPLE)

```

?BEGIN JOB EX15RGIANT;
QUEUE=30;MAXPROCTIME=7200;
COMPILE CMFRPDF/SHIFT FORTRAN GO;
COMPILER DATA CARD
COMMON/CELL/G(3,3)
DIMENSION W(15,3),X(15,3),Y(15,3),Z(15,3)
DIMENSION WM(15,3),XM(15,3),YM(15,3),ZM(15,3)
DIMENSION WMAG(15),XMAG(15),YMAG(15),ZMAG(15)
DIMENSION CREF(3), R(15,3), S(15,3), T(15,3), U(15,3)
DIMENSION SI(6,3), C(5,3)
DIMENSION RA(15,3),SA(15,3),TA(15,3),UA(15,3)
C THIS PROGRAM CACULATES THE DIAMAGNETIC ANISOTROPIC
CONTRIBUTION TO THE CHEMICAL SHIFT FOR SIC. SEE MIKE
MCGLINCHEY, ORGANOMETALLICS, VOL. 5, 104, 1986. THIS VERSION
IS FOR A HYPOTHETICAL 15R STRUCTUR
THE LAYER SPACINGS OF SI AND C ARE TAKEN FROM GOMES DE
MESQUITE, WHO GIVES THE SPACINGS OF ADJACENT H-C AND C-C
LAYERS PLUS THE COORDINATES OF THE CARBONS WHICH ALLOWS
CONVERSION OVER TO 15R. THE 15R FORM HAS AN HCHCC
STRUCTURE. THE EXACT STRUCTURE IS UNKNOWN; GIVEN THE
SENSITIVITY OF THE DIAMAGNETIC ANISOTROPIC SHIFT TO THE
BOND DISTANCES IT SEEMED BEST TO PREDICT AN EXACT
STRUCTURE AND WORK FROM THERE. RES. NOTEBOOK V. 16.
KOUNT = 1
C SET DMAX
DMAX=100
C SET ECG
ECG=.490
C
C LOAD METRIC TENSOR FOR SIC 15R FORM
C THE GEOMETRIC FACTOR IS EXCEEDNGLY SENSITIVE TO THE
MAGNITUDE OF THE CELL DIMENSIONS. THE C DIMENSION IS
PREDICTED FROM GOMES DE MESQUITE'S LAYER SPACINGS. A IS
OBTAINED FROM THE C/A RATIO OF THE 15R FORM, P. 63 GMELIN SI
SUPP VOL. B2.
C
G(1,1) = 3.08058**2

```

$$G(1,2) = -0.5 * G(1,1)$$

$$G(1,3) = 0.0$$

$$G(2,1) = G(1,2)$$

$$G(2,2) = G(1,1)$$

$$G(2,3) = 0.0$$

$$G(3,1) = G(1,3)$$

$$G(3,2) = G(2,3)$$

$$G(3,3) = 37.8033 ** 2$$

$$CH = \text{SQRT}(G(3,3))$$

C PUT IN COORDINATES OF SI AND C ATOMS

$$SI(1,1) = 0.0$$

$$SI(1,2) = 0.0$$

$$SI(1,3) = 0.0$$

$$C(1,1) = 0.0$$

$$C(1,2) = 0$$

$$C(1,3) = (0.12527 * 15.11738) / CH$$

$$SI(2,1) = 1./3.$$

$$SI(2,2) = 2./3.$$

$$SI(2,3) = 2.5212 / CH$$

$$C(2,1) = SI(2,1)$$

$$C(2,2) = SI(2,2)$$

$$C(2,3) = 2.5212 / CH + 0.12527 * 15.11738 / CH$$

$$SI(3,1) = 2./3.$$

$$SI(3,2) = 4./3.$$

$$SI(3,3) = 2. * 2.5212 / CH$$

$$C(3,1) = SI(3,1)$$

$$C(3,2) = SI(3,2)$$

$$C(3,3) = 2 * 2.5212 / CH + 0.12527 * 15.11738 / CH$$

$$SI(4,1) = 1./3.$$

$$SI(4,2) = 2./3.$$

$$SI(4,3) = 3. * 2.5212 / CH$$

$$C(4,1) = SI(4,1)$$

$$C(4,2) = SI(4,2)$$

$$C(4,3) = 3. * 2.5212 / CH + 0.12510 * 15.11738 / CH$$

$$SI(5,1) = 0$$

$$SI(5,2) = 0$$

$$SI(5,3) = (3. * 2.5212 + 2.5163) / CH$$

$$SI(6,1) = -1./3.$$

$$SI(6,2) = -2./3.$$

$$SI(6,3) = 1./3.$$

$$C(5,1) = 0$$

$$C(5,2) = 0$$

$$C(5,3) = 10.0799 / CH + 0.12527 * 15.11738 / CH + .001 / CH$$

```

W(1,1) = 0.0
W(1,2) = 0.0
W(1,3) = C(1,3) - SI(1,3)
X(1,1) = SI(2,1) - C(1,1)
X(1,2) = SI(2,2) - C(1,2)
X(1,3) = SI(2,3) - C(1,3)
Y(1,1) = X(1,1)
Y(1,2) = X(1,2) - 1.
Y(1,3) = X(1,3)
Z(1,1) = X(1,1) - 1.
Z(1,2) = X(1,2) - 1.
Z(1,3) = X(1,3)
W(2,1) = 0.0
W(2,2) = 0.0
W(2,3) = C(2,3) - SI(2,3)
X(2,1) = SI(3,1) - C(2,1)
X(2,2) = SI(3,2) - C(2,2)
X(2,3) = SI(3,3) - C(2,3)
Y(2,1) = X(2,1)
Y(2,2) = X(2,2) - 1.
Y(2,3) = X(2,3)
Z(2,1) = X(2,1) - 1.
Z(2,2) = X(2,2) - 1.
Z(2,3) = X(2,3)
W(3,1) = 0
W(3,2) = 0
W(3,3) = C(3,3) - SI(3,3)
X(3,1) = SI(4,1) - C(3,1)
X(3,2) = SI(4,2) - C(3,2)
X(3,3) = SI(4,3) - C(3,3)
Y(3,1) = X(3,1)
Y(3,2) = X(3,2) + 1.
Y(3,3) = X(3,3)
Z(3,1) = X(3,1) + 1.
Z(3,2) = X(3,2) + 1.
Z(3,3) = X(3,3)
DO 2 I = 4,5
DO 2 J = 1,2

```

C THE X AND Y COMPONENTS OF THE BOND VECTORS IN THE 4TH AND 5TH LAYERS ARE THE SAME AS IN THE THIRD. Z IS NOT NECESSARILY, HOWEVER

```

W(I,J) = W(3,J)
X(I,J) = X(3,J)

```

```

    Y(I,J) = Y(3,J)
    Z(I,J) = Z(3,J)
2 CONTINUE
    W(4,3) = C(4,3) - SI(4,3)
    W(5,3) = C(5,3) - SI(5,3)
    X(4,3) = SI(5,3) - C(4,3)
    X(5,3) = SI(1,3) - C(5,3) + 1./3.
    Y(4,3) = X(4,3)
    Z(4,3) = X(4,3)
    Y(5,3) = X(5,3)
    Z(5,3) = X(5,3)
    DO 3 I = 1,10
    DO 3 J = 1,3
    K = I + 5
    W(K,J) = W(I,J)
    X(K,J) = X(I,J)
    Y(K,J) = Y(I,J)
3    Z(K,J) = Z(I,J)
    DO 4 I = 1,5
    DO 4 J = 1,3
    WM(I,J) = ECG*SI(I,J) +(1.-ECG)*C(I,J)
    K = I + 1
4    XM(I,J) = ECG*SI(K,J) +(1.-ECG)*C(I,J)
    DO 5 I = 1,2
    YM(I,1) = XM(I,1)
    YM(I,2) = XM(I,2) - ECG
    YM(I,3) = XM(I,3)
    ZM(I,1) = XM(I,1) -ECG
    ZM(I,2) = XM(I,2) - ECG
5    ZM(I,3) = XM(I,3)
    DO 6 I = 3,5
    YM(I,1) = XM(I,1)
    YM(I,2) = XM(I,2) + ECG
    YM(I,3) = XM(I,3)
    ZM(I,1) = XM(I,1) + ECG
    ZM(I,2) = XM(I,2) + ECG
6    ZM(I,3) = XM(I,3)
    DO 7 I = 1,5
    J = I + 5
    WM(J,1) = WM(I,1) + 2./3.
    WM(J,2) = WM(I,2) + 1./3.
    WM(J,3) = WM(I,3) + 1./3.
    XM(J,1) = XM(I,1) + 2./3.

```



```

XM(J,2) = XM(I,2) + 1./3.
XM(J,3) = XM(I,3) + 1./3.
YM(J,1) = YM(I,1) + 2./3.
YM(J,2) = YM(I,2) + 1./3.
YM(J,3) = YM(I,3) + 1./3.
ZM(J,1) = ZM(I,1) + 2./3.
ZM(J,2) = ZM(I,2) + 1./3.
ZM(J,3) = ZM(I,3) + 1./3.
7  CONTINUE
   DO 8 I = 1,5
     J = I + 10
     WM(J,1) = WM(I,1) + 1./3.
     WM(J,2) = WM(I,2) + 2./3.
     WM(J,3) = WM(I,3) + 2./3.
     XM(J,1) = XM(I,1) + 1./3.
     XM(J,2) = XM(I,2) + 2./3.
     XM(J,3) = XM(I,3) + 2./3.
     YM(J,1) = YM(I,1) + 1./3.
     YM(J,2) = YM(I,2) + 2./3.
     YM(J,3) = YM(I,3) + 2./3.
     ZM(J,1) = ZM(I,1) + 1./3.
     ZM(J,2) = ZM(I,2) + 2./3.
     ZM(J,3) = ZM(I,3) + 2./3.
8  CONTINUE
C  NOW CALCULATE BON DISTANCES IN EACH LAYER
   DO 10 L = 1,15
     CALL DOTP(W,W,L,DOT)
     WMAG(L) = SQRT(DOT)
     CALL DOTP(X,X,L,DOT)
     XMAG(L) = SQRT(DOT)
     CALL DOTP(Y,Y,L,DOT)
     YMAG(L) = SQRT(DOT)
     CALL DOTP(Z,Z,L,DOT)
     ZMAG(L) = SQRT(DOT)
10  WRITE(6,1000)L, WMAG(L),XMAG(L),YMAG(L),ZMAG(L)
     WRITE(6,999)
999  FORMAT(1H1)
1000 FORMAT(1H , "BOND DISTANCES IN LAYER NUMBER ",I2,":",4F10.3)
     WRITE(6,1050)
1050 FORMAT(1H0,"C ",10X,"GEOM100A",13X,"NO.OF BONDS")
     GO TO (59,43,44,45,46,47),KOUNT
14  NS100=0
     NL100=0

```

```

GS100=0.0
GL100=0.0
N100=0
G100=0.0
DO 20 L = 1,15
DO 15 N = 1,3
R(L,N) = WM(L,N) - CREF(N)
S(L,N) = XM(L,N) - CREF(N)
T(L,N) = YM(L,N) - CREF(N)
15 U(L,N) = ZM(L,N) - CREF(N)
C  NOW CHECK THAT THE R(I) ETC. ARE IN THE STARTING UNIT CELL
DO 20 N = 1,3
IF(R(L,N).GT.1.0) R(L,N) = R(L,N) - 1.0
IF(S(L,N).GT.1.0) S(L,N) = S(L,N) - 1.0
IF(T(L,N).GT.1.0) T(L,N) = T(L,N) - 1.0
IF(U(L,N).GT.1.0) U(L,N) = U(L,N) - 1.0
IF(R(L,N).LT.0.0) R(L,N) = R(L,N) + 1.0
IF(S(L,N).LT.0.0) S(L,N) = S(L,N) + 1.0
IF(T(L,N).LT.0.0) T(L,N) = T(L,N) + 1.0
20 IF(U(L,N).LT.0.0) U(L,N) = U(L,N) + 1.0
C  NOW MOVE DOWN 4 UNIT CELLS IN Z AND PREPARE TO LOOP
DO 25 L = 1,15
RA(L,3) = R(L,3) - 4.0
SA(L,3) = S(L,3) - 4.0
TA(L,3) = T(L,3) - 4.0
25 UA(L,3) = U(L,3) - 4.0
DO 42 NCEL = 1,9
C  NCEL IS A DUMMY VARIABLE WHICH ALLOWS US TO MOVE OVER 9
UNIT CELLS IN THE Z DIRECTION
DO 40 L = 1,15
C  PREPARE TO LOOP THROUGH 101 UNIT CELLS IN X AND Y DIRECTIONS
C  THUS MOVE 50 CELLS NEGATIVE IN BOTH X AND Y
DO 30 N = 1,2
RA(L,N) = R(L,N) - 50.0
SA(L,N) = S(L,N) - 50.0
TA(L,N) = T(L,N) - 50.0
30 UA(L,N) = U(L,N) - 50.0
DO 36 I = 1,101
DO 35 J = 1,101
CALL DOTP(RA,RA,L,DOT)
RAMAG = SQRT(DOT)
IF(RAMAG.GT.DMAX) GO TO 31
IF(RAMAG.LT.1.25) GO TO 31

```

```

C   ELIMINATE FIRST NEIGHBORS
    CALL DOTP(RA,W,L,DOT)
    CPHI = DOT/(RAMAG*WMAG(L))
C   IF(ABS(CPHI).GT.1.0) WRITE (6,1020) CPHI
1020 FORMAT(1H , "ERROR IN COS PHI",F12.9)
    GEO = (1. - 3.*CPHI*CPHI)/(3.*RAMAG*RAMAG*RAMAG)
    NL100 = NL100 + 1
    GL100 = GL100 + GEO
31  CALL DOTP(SA,SA,L,DOT)
    SAMAG = SQRT(DOT)
    IF(SAMAG.GT.DMAX) GO TO 32
    IF(SAMAG.LT.1.25) GO TO 32
C   ELIMINATE FIRST NEIGHBORS
    CALL DOTP(SA,X,L,DOT)
    CPHI = DOT/(SAMAG*XMAG(L))
C   IF(ABS(CPHI).GT.1.0) WRITE (6,1020) CPHI
    GEO = (1. - 3.*CPHI*CPHI)/(3.*SAMAG*SAMAG*SAMAG)
    NS100 = NS100 + 1
    GS100 = GS100 + GEO
32  CALL DOTP(TA,TA,L,DOT)
    TAMAG = SQRT(DOT)
    IF(TAMAG.GT.DMAX) GO TO 33
    IF(TAMAG.LT.1.25) GO TO 33
    ELIMINATE FIRST NEIGHBORS
    CALL DOTP(TA,Y,L,DOT)
    CPHI = DOT/(TAMAG*YMAG(L))
C   IF(ABS(CPHI).GT.1.0) WRITE (6,1020) CPHI
    GEO = (1. - 3.*CPHI*CPHI)/(3.*TAMAG*TAMAG*TAMAG)
    NS100 = NS100 + 1
    GS100 = GS100 + GEO
33  CALL DOTP(UA,UA,L,DOT)
    UAMAG = SQRT(DOT)
    IF(UAMAG.GT.DMAX) GO TO 34
    IF(UAMAG.LT.1.25) GO TO 34
C   ELIMINATE FIRST NEIGHBORS
    CALL DOTP(UA,Z,L,DOT)
    CPHI = DOT/(UAMAG*ZMAG(L))
C   IF(ABS(CPHI).GT.1.0) WRITE (6,1020) CPHI
    GEO = (1. - 3.*CPHI*CPHI)/(3.*UAMAG*UAMAG*UAMAG)
    NS100 = NS100 + 1
    GS100 = GS100 + GEO
34  RA(L,1) = RA(L,1) + 1.0
    SA(L,1) = SA(L,1) + 1.0

```

```

    TA(L,1) = TA(L,1) + 1.0
    UA(L,1) = UA(L,1) + 1.0
35  CONTINUE
C    RESET X COORDINATE AFTER PASS THROUH 101 CELLS IN X DIRECTI
    RA(L,1) = RA(L,1) - 101.0
    SA(L,1) = SA(L,1) - 101.0
    TA(L,1) = TA(L,1) - 101.0
    UA(L,1) = UA(L,1) - 101.0
    RA(L,2) = RA(L,2) + 1.0
    SA(L,2) = SA(L,2) + 1.0
    TA(L,2) = TA(L,2) + 1.0
    UA(L,2) = UA(L,2) + 1.0
36  CONTINUE
    RA(L,2) = RA(L,2) - 101.0
    SA(L,2) = SA(L,2) - 101.0
    TA(L,2) = TA(L,2) - 101.0
    UA(L,2) = UA(L,2) - 101.0
40  CONTINUE
    DO 41 L = 1,15
    RA(L,3) = RA(L,3) + 1.0
    SA(L,3) = SA(L,3) + 1.0
    TA(L,3) = TA(L,3) + 1.0
41  UA(L,3) = UA(L,3) + 1.0
42  CONTINUE
    N100=NS100+NL100
    G100=GS100+GL100
    WRITE(6,1051) KOUNT,G100,N100
1051 FORMAT(1H0,I2,10X,F12.10,10X,I8)
    KOUNT=KOUNT+1
    GO TO (59,43,44,45,46,47) KOUNT
C
59  CREF(1) = C(1,1)
    CREF(2) = C(1,2)
    CREF(3) = C(1,3)
    GO TO 14
43  CREF(1) = C(2,1)
    CREF(2) = C(2,2)
    CREF(3) = C(2,3)
    GO TO 14
44  CREF(1) = C(3,1)
    CREF(2) = C(3,2)
    CREF(3) = C(3,3)
    GO TO 14

```

```
45 CREF(1) = C(4,1)
   CREF(2) = C(4,2)
   CREF(3) = C(4,3)
   GO TO 14
46 CREF(1) = C(5,1)
   CREF(2) = C(5,2)
   CREF(3) = C(5,3)
   GO TO 14
47 STOP
   END
   SUBROUTINE DOTP(A,B,L,DOT)
   COMMON/CELL/ G(3,3)
   DIMENSION A(15,3), B(15,3)
   DOT = 0.0
   DO 10 I = 1,3
   DO 10 J = 1,3
10 DOT = A(L,I)*B(L,J)*G(I,J) + DOT
   RETURN
   END
   END JOB;
```

APPENDIX 4

PROGRAM FOR LEAST SQUARES FITS AND LAYER SPACING SHIFTS
IN MAS NMR CHEMICAL SHIFT CALCULATION

```

$RESET FREE
FILE 3(KIND=DISK,TITLE="ECG/GEOM/IN/6H/488",DEPENDENTSPECS=TRUE,
      CPROTECTION=SAVE)
FILE 6(KIND=PACK,TITLE="GEOM/OUT",MAXRECSIZE=15,BLOCKSIZE=420,
      CPROTECTION=SAVE)
REAL OBSSI(10),OBSC(10),GSI(10),GC(10),CACSI(10),CACC(10)
REAL SIC(20,20),CSI(20,20),DELTA G(0:20,0:20),X(20,20)
REAL Y(0:20),DD,T,SI,CA,SSI(20),SC(20)
REAL ISSI,ISC,DELTAX,A,B,C,D,E,F,G,H
DIMENSION IS(20)
SET THE MAG. TO MOVE SI'S & C'S
CA=.001
SI=-.001
C   JUDGE=0, CALC. FINAL RESULT; OTHERWISE, JUDGE=1.
    READ(3,1,END=5) JUDGE
      1  FORMAT(I1)
      5  CONTINUE
C   N IS THE NUMBER OF SI OR C (N=3 FOR 6H; N=5 FOR 15R)
    READ(3,2,END=10) N
      2  FORMAT(I1)
     10  CONTINUE
        WRITE(6,12) N
     12  FORMAT(1H,"# OF SI OR C IS ",I2)
C   NOW PUT IN OBS. CHEM. SHIFT FOR SI'S
    WRITE(6,48)
    DO 211 I=1,N
      READ(3,201) OBSSI(I)
     201  FORMAT(F5.2)
        WRITE(6,210) OBSSI(I),I
     210  FORMAT(1H,"OBS. CHEM. SHIFT IS ",F8.3,2X,"FOR SI",I2)
     211  CONTINUE
C   NOW PUT IN OBS. CHEM. SHIFT FOR C'S
    WRITE(6,48)
    DO 231 I=1,N
      READ(3,221) OBSC(I)
     221  FORMAT(F5.2)
        WRITE(6,230) OBSC(I),I

```

```

230 FORMAT(1H,"OBS. CHEM. SHIFT IS ",F5.2,2X,"FOR C",I2)
231 CONTINUE
C   NOW PUT IN GEOM. FOR SI'S
    WRITE(6,48)
    DO 251 I=1,N
    READ(3,241) GSI(I)
241  FORMAT(F12.9)
    WRITE(6,250) GSI(I),I
250  FORMAT(1H,"GEOM. FACTOR IS ",F12.9,2X,"FOR SI",I2)
251  CONTINUE
C   NOW PUT IN GEOM. FOR C'S
    WRITE(6,48)
    DO 271 I=1,N
    READ(3,261) GC(I)
261  FORMAT(F12.9)
    WRITE(6,260)GC(I),I
260  FORMAT(1H,"GEOM. FACTOR IS ",F12.9,2X,"FOR C",I2)
271  CONTINUE
    IF (JUDGE.EQ.0) GOTO 35
C   PUT IN SHIFTED GEOM. FOR SI'S (E.G, 5 FOR SI(1) IN 6H, ETC.)
    DO 15 I=1,N
    DO 15 J=1,2*N-1
    READ(3,61) SIC(I,J)
61  FORMAT(F12.9)
15  CONTINUE
C   PUT IN SHIFTED GEOM. FOR C'S (E.G. 9 FOR C(1) IN 15R, ETC.)
    DO 25 I=1,N
    DO 25 J=1,2*N-1
    READ(3,62) CSI(I,J)
62  FORMAT(F12.9)
25  CONTINUE
C   CALC. INTRINSIC SHIFT FOR SI & C, DELTAX
35  A=0.
    B=0.
    C=0.
    D=0.
    E=0.
    F=0.
    G=0.
    H=0.
    DO 9 I=1,N
    A=A + OBSSI(I)
    B=B + GSI(I)

```

```

C=C + OBSC(I)
D=D + GC(I)
E=E + OBSSI(I)*GSI(I)
F=F + GSI(I)*GSI(I)
G=G + OBSC(I)*GC(I)
H=H + GC(I)*GC(I)
9  CONTINUE
DELTA $X$ =(A*B+C*D-N*E-N*G)/(B*B+D*D-N*F-N*H)
DELTA $X$ =6981.92
ISSI=(A-B*DELTA $X$ )/N
ISC=(C-D*DELTA $X$ )/N
DO 19 I=1,N
CACSI(I)=ISSI+GSI(I)*DELTA $X$ 
CACC(I)=ISC+GC(I)*DELTA $X$ 
19 CONTINUE
WRITE(6,48)
WRITE(6,31) ISSI,ISC,DELTA $X$ 
31 FORMAT("ISSI = ",F10.4,4X,"ISC = ",F10.4,4X,"DELTA $X$  = ",F10.4)
WRITE(6,48)
DO 29 I=1,N
WRITE(6,41) CACSI(I),I
41 FORMAT(1H,"CALC. CHEMICAL SHIFT IS",F9.4," FOR SI",I2)
29 CONTINUE
WRITE(6,48)
DO 30 I=1,N
WRITE(6,51) CACC(I),I
51 FORMAT(1H,"CALC. CHEMICAL SHIFT IS",F9.4," FOR C",I2)
30 CONTINUE
C  NOW DO DATA TRANSFORMATION AND LEAST-SQUARE-REFINEMENT
IF (JUDGE.EQ.0) GOTO 155
DO 39 I=1,N
DELTA $G$ (I,0)=.0
DO 39 J=1,2*N-1
DELTA $G$ (I,J)=SIC(I,J)-GSI(I)
39 CONTINUE
DO 49 I=N+1,2*N
DELTA $G$ (I,0)=.0
DO 49 J=1,2*N-1
K=I-N
DELTA $G$ (I,J)=CSI(K,J)-GC(K)
49 CONTINUE
DO 54 I=1,N
WRITE(6,48)

```



```

48  FORMAT(1H )
    DO 54 J=0,2*N-2,2
      I=J + 1
      M=J/2 + 1
      WRITE(6,50) I,M,DELTA(I,J)
50  FORMAT(1H ,"SI",I2,2X,"SI",I2,2X,"DELTA IS",F12.9)
      WRITE(6,52) I,M,DELTA(I,K)
52  FORMAT(1H ,"SI",I2,2X," C",I2,2X,"DELTA IS",F12.9)
54  CONTINUE
      DO 58 I=N+1,2*N
        L=I-N
        WRITE(6,53)
53  FORMAT(1H )
        DO 58 J=0,2*N-2,2
          K=J+1
          M=J/2+1
          WRITE(6,55) L,M,DELTA(I,J)
55  FORMAT(1H ," C",I2,2X,"SI",I2,2X,"DELTA IS",F12.9)
          WRITE(6,56) L,M,DELTA(I,K)
56  FORMAT(1H ," C",I2,2X," C",I2,2X,"DELTA IS",F12.9)
58  CONTINUE
          DO 59 I=1,N
            M=2*N
            DELTA(I,M)=(OBSSI(I)-CACSI(I))/DELTA
59  CONTINUE
            DO 69 I=N+1,2*N
              M=2*N
              K=I-N
              DELTA(I,M)=(OBSC(K)-CACCC(K))/DELTA
69  CONTINUE
            DO 79 I=1,2*N-1
              DO 79 J=1,2*N
                X(I,J)=0.
79  CONTINUE
            DO 89 K=1,2*N-1
              DO 89 L=1,2*N
                DO 89 I=1,2*N
                  X(K,L)=X(K,L)+DELTA(I,K)*DELTA(I,L)
89  CONTINUE
            WRITE(6,48)
            WRITE(6,90)
90  FORMAT(1H ,"X(1,J) ARE THE COEF.OF THE 1ST LINEA EQUATION")
            WRITE(6,48)

```

```

DO 98 J=1,2*N
WRITE(6,95)J, X(1,J)
95  FORMAT(1H,"X(1,",I2,") IS ",F15.12)
98  CONTINUE
C   NOW SOLVE LINEAR EQUATIONS BY GAUSSIAN ELIMINATION
WRITE(6,48)
WRITE(6,99)
99  FORMAT(1H,"FOR ODD I, Y(I)*.001A IS THE SHIFT REQUIRED FOR C'S")
WRITE(6,100)
100 FORMAT(1H,"FOR EVEN I,Y(I)*(-.001A) IS THE SHIFT REQ. FOR S'S")
NN =2*N-1
MM=2*N-1
JJ=0
DO 150 K=1,NN
DD=X(K,K)
DO 121 I=K+1,MM
IF (ABS(X(I,K)).LT.ABS(DD)) GO TO 121
L=I
DD=X(L,K)
121 CONTINUE
IF (ABS(DD).GT.1.0E-18) GOTO 135
PRINT 101,K
101 FORMAT (" SINGULAR, K=", I1)
JJ=JJ +1
IS(JJ)=K
GOTO 150
135 IF (DD.EQ.X(K,K)) GO TO 151
DO 141 J=K,NN+1
T=X(L,J)
X(L,J)=X(K,J)
X(K,J)=T
141 CONTINUE
151 DO 150 J=K+1,NN+1
X(K,J)=X(K,J)/X(K,K)
DO 150 I=K+1,MM
X(I,J)=X(I,J)-X(I,K)*X(K,J)
150 CONTINUE
DO 133 I=NN+1,MM
IF (ABS(X(I,NN+1)).GT.(1.0E-8)) GOTO 144
133 CONTINUE
DO 180 K=0,NN-1
140 Y(NN-K)=0
Y(NN+1)=0

```

```

      IF (JJ.EQ.0) GOTO 177
      DO 122 I=1,JJ
      Y(IS(I))=1
      IF ((NN-K).EQ.IS(I)) GOTO 180
122 CONTINUE
177 DO 190 J=NN-K+1, NN
      Y(NN-K)=Y(NN-K)+X((NN-K),J)*Y(J)
190 CONTINUE
      Y(NN-K)=-Y(NN-K)+X(NN-K,NN+1)
      WRITE (6,102) NN-K, Y(NN-K)
102 FORMAT (1H ," Y(",I2," )=",F12.8)
180 CONTINUE
      WRITE(6,48)
      Y(0)=.0
      DO 175 I=1,2*N-1,2
      K=I-1
      J=(I+1)/2
      SSI(J)=Y(K)*SI
      SC(J)=Y(I)*CA
      WRITE(6,160)J,SSI(J)
160 FORMAT(1H ,"SHIFT OF SI (" ,I2," ) = ",F12.8)
      WRITE(6,170)J,SC(J)
170 FORMAT(1H ,"SHIFT OF C (" ,I2," ) = ",F12.8)
175 CONTINUE
      IF (JJ.EQ.0) GOTO 155
      DO 123 K=1,JJ
123 WRITE (6,103) IS(K)
103 FORMAT (1H ,"Y(",I1,")=1")
      GOTO 155
144 PRINT 104
104 FORMAT (" NO SOLUTION")
155 STOP
      END

```

APPENDIX 5

PROGRAM FOR THE DETERMINATION OF LAYER SPACING SHIFTS
OF 15R AND 6H BY USING COMMON INTRINSIC SHIFTS
AND BOND MAGNETIC ANISOTROPY

```
$RESET FREE
FILE 2(KIND=DISK,TITLE="ECG/GEOM/IN/6H/488",DEPENDENTSPECS=TRUE,
      CPROTECTION=SAVE)
FILE 3(KIND=DISK,TITLE="ECG/GEOM/IN/15R/488",DEPENDENTSPECS=
      CTRUE,PROTECTION=SAVE)
FILE 4(KIND=DISK,TITLE="ECG/GEOM/IN/3C/488",DEPENDENTSPECS=TRUE,
      CPROTECTION=SAVE)
FILE 6(KIND=PACK,TITLE="GEOM/OUT",MAXRECSIZE=15,BLOCKSIZE=420,
      CPROTECTION=SAVE)
REAL ISSI,ISC,DELTA X
REAL X(20,20),Y(20),G(20,20),IS(20)
REAL SI6H(3),C6H(3),SI15R(5),C15R(5)
SI=-.001
C=0.001
N=17
C  NOW PUT IN THE OBSERVED CHEMICAL SHIFTS OF 6H
DO 10 I=1,6
  READ(2,5) X(I,1)
  5  FORMAT(F5.2)
  10 CONTINUE
C  NOW PUT IN THE OBSERVED CHEMICAL SHIFTS OF 15R
DO 20 I=7,16
  READ(3,15) X(I,1)
  15  FORMAT(F5.2)
  20 CONTINUE
C  PUT IN THE OBSERVED CHEMICAL SHIFT OF 3C
  READ(4,22) X(17,1)
  22  FORMAT(F5.2)
C  PUT IN GEOMETRIC FACTORS OF 6H
DO 30 I=1,6
  READ(2,25) X(I,18)
  25  FORMAT(F12.9)
  30 CONTINUE
C  PUT IN GEOMETRIC FACTORS OF 15R
DO 40 I=7,16
  READ(3,35) X(I,18)
```

```
35  FORMAT(F12.9)
40  CONTINUE
C    PUT IN GEOMETRIC FACTOR OF 3C
    READ(4,45) X(17,18)
45  FORMAT(F12.9)
C    PUT IN THE COEFFICIENTS OF INTRINSIC SHIFT TERMS(-1 OR 0)
    DO 50 I=1,3
      J=I+3
      X(I,2)=-1
      X(J,3)=-1
50  CONTINUE
    DO 55 I=7,11
      J=I+5
      X(I,2)=-1
      X(J,3)=-1
55  CONTINUE
      X(17,2)=-1
C    NOW PUT IN THE CHANGED GEOMETRIC FACTORS IN 6H
    DO 60 I=1,6
      DO 60 J=4,8
        READ(2,58) G(I,J)
58  FORMAT(F12.9)
      X(I,J)=X(I,18)-G(I,J)
60  CONTINUE
C    PUT IN THE CHANGED GEOMETRIC FACTORS OF 15R
    DO 80 I=7,16
      DO 80 J=9,17
        READ(3,75) G(I,J)
75  FORMAT(F12.9)
      X(I,J)=X(I,18)-G(I,J)
80  CONTINUE
      NN=N
      MM=N
      JJ=0
      DO 150 K=1,NN
        DD=X(K,K)
        DO 121 I=K+1,MM
          IF (ABS(X(I,K)).LT.ABS(DD)) GO TO 121
          L=I
          DD=X(L,K)
121  CONTINUE
      IF (ABS(DD).GT.1.0E-18) GOTO 135
      PRINT 101,K
```

```

101 FORMAT (" SINGULAR, K=", I1)
    JJ=JJ +1
    IS(JJ)=K
    GOTO 150
135 IF (DD.EQ.X(K,K)) GO TO 151
    DO 141 J=K,NN+1
    T=X(L,J)
    X(L,J)=X(K,J)
    X(K,J)=T
141 CONTINUE
151 DO 150 J=K+1,NN+1
    X(K,J)=X(K,J)/X(K,K)
    DO 150 I=K+1,MM
    X(I,J)=X(I,J)-X(I,K)*X(K,J)
150 CONTINUE
    DO 133 I=NN+1,MM
    IF (ABS(X(I,NN+1)).GT.(1.0E-8)) GOTO 144
133 CONTINUE
    DO 180 K=0,NN-1
140 Y(NN-K)=0
    Y(NN+1)=0
    IF (JJ.EQ.0) GOTO 177
    DO 122 I=1,JJ
    Y(IS(I))=1
    IF ((NN-K).EQ.IS(I)) GOTO 180
122 CONTINUE
177 DO 190 J=NN-K+1, NN
    Y(NN-K)=Y(NN-K)+X((NN-K),J)*Y(J)
190 CONTINUE
    Y(NN-K)=-Y(NN-K)+X(NN-K,NN+1)
    WRITE (6,102) NN-K, Y(NN-K)
102 FORMAT (1H , " Y(",I2," )=",F12.8)
180 CONTINUE
    DELTAX=1/Y(1)
    ISSI=Y(2)*DELTAX
    ISC=Y(3)*DELTAX
    WRITE(6,499)
    WRITE(6,200) DELTAX
200 FORMAT(1H ,"DELTA CHI IS ",F10.3)
    WRITE(6,499)
    WRITE(6,210) ISSI
210 FORMAT(1H ,"INTRINSIC CHEMICAL SHIFT OF SILICON IS ",F8.4)
    WRITE(6,499)

```

```
      WRITE(6,220) ISC
220 FORMAT(1H,"INTRINSIC CHEMICAL SHIFT OF CARBON IS ",F8.4)
      Y(3)=0.
      DO 250 I=1,3
      J=I*2+1
      K=J+1
      C6H(I)=Y(K)*CA
      SI6H(I)=Y(J)*SI
      WRITE(6,229)
229 FORMAT(1H )
      WRITE(6,230)I,SI6H(I)
230 FORMAT(1H0,"SHIFT OF SI(",I2," ) IN 6H IS ",F10.8)
      WRITE(6,229)
      WRITE(6,240)I,C6H(I)
240 FORMAT(1H,"SHIFT OF C(",I2," ) IN 6H IS ",F10.8)
250 CONTINUE
      Y(8)=0.
      DO 300 I=1,5
      J=2*I+6
      K=J+1
      SI15R(I)=Y(J)*SI
      C15R(I)=Y(K)*CA
      WRITE(6,259)
259 FORMAT(1H )
      WRITE(6,260)I,SI15R(I)
260 FORMAT(1H0,"SHIFT OF SI(",I2," ) IN 15R IS ",F10.8)
      WRITE(6,259)
      WRITE(6,280)I,C15R(I)
280 FORMAT(1H,"SHIFT OF C(",I2," ) IN 15R IS ",F10.8)
300 CONTINUE
      GOTO 155
144 PRINT 104
104 FORMAT (" NO SOLUTION")
499 FORMAT(1H )
155 STOP
      END
```

APPENDIX 6

PROGRAM FOR THE CALCULATION OF GEOMETRIC FACTORS
OF SILICONS (SIC 6H SINGLE CRYSTAL)

```

COMMON/CELL/G(3,3)
DIMENSION W(15,3),X(15,3),Y(15,3),Z(15,3)
DIMENSION WM(15,3),XM(15,3),YM(15,3),ZM(15,3)
DIMENSION WMAG(15),XMAG(15),YMAG(15),ZMAG(15)
DIMENSION SIREF(3), R(15,3), S(15,3), T(15,3), U(15,3)
DIMENSION SI(6,3), C(5,3),GEOMX(10,10),GEOMZ(10,10)
DIMENSION RA(15,3),SA(15,3),TA(15,3),UA(15,3)
REAL COSXS,COSYS,CPhi
C THIS PROGRAM CALCULATES THE DIAMAGNETIC ANISOTROPIC
  CONTRIBUTION TO THE CHEMICAL SHIFT FOR SIC. SEE MIKE
  MCGLINCHEY, ORGANOMETALLICS, VOL. 5, 104, 1986.
C THE COORDINATES AND CELL DIMENSIONS ARE FROM
C GOMES DE MESQUITE.
C
  SIREF(1) = 0.0
  SIREF(2) = 0.0
  SIREF(3) = 0.0
  KOUNT = 0
C SET DMAX
  DMAX =100.0
  DO 1 I=1,3
  DO 1 J=1,3
  GEOMX(I,J)=0.0
  GEOMZ(I,J)=0.0
1 CONTINUE
C SET ECG
  ECG=.498
  NTOT = 0
C
C LOAD METRIC TENSOR FOR SIC 6H FORM
C THE GEOMETRIC FACTOR IS EXCEEDINGLY SENSITIVE TO THE
C MAGNITUDE OF THE CELL DIMENSIONS. THE DIMENSIONS
C ARE FROM GOMES DE MESQUITE.
C
  G(1,1) = 3.08065**2
  G(1,2) = -0.5*G(1,1)
  G(1,3) = 0.0

```



```

G(2,1) = G(1,2)
G(2,2) = G(1,1)
G(2,3) = 0.0
G(3,1) = G(1,3)
G(3,2) = G(2,3)
G(3,3) = 15.1174**2
CH = SQRT(G(3,3))
C PUT IN COORDINATES OF SI AND C ATOMS
SI(1,1) = 0.0
SI(1,2) = 0.0
SI(1,3) = 0.0
C(1,1) = 0.0
C(1,2) = 0
C(1,3) = 0.12527+.001095/CH
SI(2,1) = 1./3.
SI(2,2) = 2./3.
SI(2,3) = 0.16678 +.0000339/CH
C(2,1) = SI(2,1)
C(2,2) = SI(2,2)
C(2,3) = 0.29188 +.0032344/CH
SI(3,1) = 2./3.
SI(3,2) = 4./3.
SI(3,3) = 0.33323 +.00206938/CH
C(3,1) = SI(3,1)
C(3,2) = SI(3,2)
C(3,3) = 0.45850 +.0005011/CH
SI(4,1) = 1.0
SI(4,2) = 2.0
SI(4,3) = 0.5
W(1,1) = 0.0
W(1,2) = 0.0
W(1,3) = C(1,3) - SI(1,3)
X(1,1) = SI(2,1) - C(1,1)
X(1,2) = SI(2,2) - C(1,2)
X(1,3) = SI(2,3) - C(1,3)
Y(1,1) = X(1,1)
Y(1,2) = X(1,2) - 1.
Y(1,3) = X(1,3)
Z(1,1) = X(1,1) -1.
Z(1,2) = X(1,2) - 1.
Z(1,3) = X(1,3)
W(2,1) = 0.0
W(2,2) = 0.0

```

$$W(2,3) = C(2,3) - SI(2,3)$$

$$X(2,1) = SI(3,1) - C(2,1)$$

$$X(2,2) = SI(3,2) - C(2,2)$$

$$X(2,3) = SI(3,3) - C(2,3)$$

$$Y(2,1) = X(2,1)$$

$$Y(2,2) = X(2,2) - 1.$$

$$Y(2,3) = X(2,3)$$

$$Z(2,1) = X(2,1) - 1.$$

$$Z(2,2) = X(2,2) - 1.$$

$$Z(2,3) = X(2,3)$$

$$W(3,1) = 0$$

$$W(3,2) = 0$$

$$W(3,3) = C(3,3) - SI(3,3)$$

$$X(3,1) = SI(4,1) - C(3,1)$$

$$X(3,2) = SI(4,2) - C(3,2)$$

$$X(3,3) = SI(4,3) - C(3,3)$$

$$Y(3,1) = X(3,1)$$

$$Y(3,2) = X(3,2) - 1.$$

$$Y(3,3) = X(3,3)$$

$$Z(3,1) = X(3,1) - 1.$$

$$Z(3,2) = X(3,2) - 1.$$

$$Z(3,3) = X(3,3)$$

$$DO\ 2\ I = 4,6$$

$$DO\ 2\ J = 1,2$$

C NOW FIX BOND VECTORS FOR THE 4TH, 5TH, AND 6TH LAYERS.

$$W(I,J) = W(3,J)$$

$$X(I,J) = -X(3,J)$$

$$Y(I,J) = -Y(3,J)$$

$$Z(I,J) = -Z(3,J)$$

2 CONTINUE

$$DO\ 3\ I = 1,3$$

$$J = I + 3$$

$$W(J,3) = W(I,3)$$

$$X(J,3) = X(I,3)$$

$$Y(J,3) = Y(I,3)$$

3 Z(J,3) = Z(I,3)

$$DO\ 4\ I = 1,3$$

$$DO\ 4\ J = 1,3$$

$$WM(I,J) = ECG*SI(I,J) + (1.-ECG)*C(I,J)$$

$$K = I + 1$$

4 XM(I,J) = ECG*SI(K,J) + (1.-ECG)*C(I,J)

$$DO\ 5\ I = 1,3$$

$$YM(I,1) = XM(I,1)$$

```

YM(I,2) = XM(I,2) - ECG
YM(I,3) = XM(I,3)
ZM(I,1) = XM(I,1) - ECG
ZM(I,2) = XM(I,2) - ECG
5  ZM(I,3) = XM(I,3)
DO 6 I = 1,3
  J = 7 - I
  X1=2.*I-1.0
  XM(J,1) =X1/3.0- XM(I,1)
  X2=4.*I-2.0
  XM(J,2) =X2/3.0- XM(I,2)
  YM(J,1) =X1/3.0- YM(I,1)
  Y2=4.*I-5.
  YM(J,2) =Y2/3.0- YM(I,2)
  Z1=2.*I-4.
  ZM(J,1)= Z1/3.0- ZM(I,1)
6  ZM(J,2)= Y2/3.0- ZM(I,2)
  WM(4,1) = SI(1,1)
  WM(4,2) = SI(1,2)
  WM(5,1) = SI(3,1)
  WM(5,2) = SI(3,2)
  WM(6,1) = SI(2,1)
  WM(6,2) = SI(2,2)
  DO 7 I = 1,3
    J = I + 3
    WM(J,3) = WM(I,3) + 0.5
    XM(J,3) = XM(I,3) + 0.5
    YM(J,3) = YM(I,3) + 0.5
7  ZM(J,3) = ZM(I,3) + 0.5
C  NOW CALCULATE BON DISTANCES IN EACH LAYER
DO 10 L = 1,6
  CALL DOTP(W,W,L,DOT)
  WMAG(L) = SQRT(DOT)
  CALL DOTP(X,X,L,DOT)
  XMAG(L) = SQRT(DOT)
  CALL DOTP(Y,Y,L,DOT)
  YMAG(L) = SQRT(DOT)
  CALL DOTP(Z,Z,L,DOT)
  ZMAG(L) = SQRT(DOT)
10  WRITE(6,1000)L, WMAG(L),XMAG(L),YMAG(L),ZMAG(L)
    WRITE(6,999)
999  FORMAT(1H1)
1000 FORMAT(1H , "BOND DISTANCES IN LAYER NUMBER ",I2,":",",4F10.3)

```

```

14 DO 20 L = 1,6
    DO 15 N = 1,3
        R(L,N) = WM(L,N) - SIREF(N)
        S(L,N) = XM(L,N) - SIREF(N)
        T(L,N) = YM(L,N) - SIREF(N)
15 U(L,N) = ZM(L,N) - SIREF(N)
C   NOW CHECK THAT THE R(I) ETC. ARE IN THE STARTING UNIT CELL
    DO 20 N = 1,3
        IF(R(L,N).GT.1.0) R(L,N) = R(L,N) - 1.0
        IF(S(L,N).GT.1.0) S(L,N) = S(L,N) - 1.0
        IF(T(L,N).GT.1.0) T(L,N) = T(L,N) - 1.0
        IF(U(L,N).GT.1.0) U(L,N) = U(L,N) - 1.0
        IF(R(L,N).LT.0.0) R(L,N) = R(L,N) + 1.0
        IF(S(L,N).LT.0.0) S(L,N) = S(L,N) + 1.0
        IF(T(L,N).LT.0.0) T(L,N) = T(L,N) + 1.0
20 IF(U(L,N).LT.0.0) U(L,N) = U(L,N) + 1.0
C   NOW MOVE DOWN 8 UNIT CELLS IN Z AND PREPARE TO LOOP
    DO 25 L = 1,6
        RA(L,3) = R(L,3) - 8.0
        SA(L,3) = S(L,3) - 8.0
        TA(L,3) = T(L,3) - 8.0
25 UA(L,3) = U(L,3) - 8.0
    DO 42 NCEL = 1,17
C   NCEL IS A DUMMY VARIABLE WHICH ALLOWS US TO MOVE OVER
    17 UNIT CELLS IN THE Z DIRECTION

C   DO 40 L = 1,6
C   PREPARE TO LOOP THROUGH 101 UNIT CELLS IN X AND Y DIRECTIONS
C   THUS MOVE 50 CELLS NEGATIVE IN BOTH X AND Y
C   THIS NUMBER IS NECESSARY TO BE SURE TO GET 100A AWAY FROM
    THE ORIGIN. SEE NOTEBOOK VOL. 17.
C   DO 30 N = 1,2
        RA(L,N) = R(L,N) - 50.0
        SA(L,N) = S(L,N) - 50.0
        TA(L,N) = T(L,N) - 50.0
30 UA(L,N) = U(L,N) - 50.0
    DO 36 I = 1,101
    DO 35 J = 1,101
        CALL DOTP(RA,RA,L,DOT)
        RAMAG = SQRT(DOT)
        IF(RAMAG.LT.1.25) GO TO 31
        IF(RAMAG.GT.DMAX) GO TO 31
        NTOT = NTOT + 1

```

```

CALL DOTP(RA,W,L,DOT)
CPHI = DOT/(RAMAG*WMAG(L))
IF(ABS(CPHI).GT.1.0) WRITE (6,1020) CPHI
1020 FORMAT(1H , "ERROR IN COS PHI",F12.9)
COSXS=0.5*(1.-CPHI*CPHI)
COSYS=COSXS
GEOMX(1,1)=GEOMX(1,1)+(1.0-3.*COSXS)/(RAMAG*RAMAG*RAMAG)
GEOMX(2,2)=GEOMX(2,2)+(1.0-3.*COSYS)/(RAMAG*RAMAG*RAMAG)
GEOMZ(3,3)=GEOMZ(3,3)+(1.- 3.*CPHI*CPHI) /
C(RAMAG*RAMAG*RAMAG)
WRITE(6,1030)(RA(L,N),W(L,N),N=1,3),RAMAG,GEO
1030 FORMAT(1H ,3(F8.4,1X),10X,3(F8.4,1X),10X,F10.3,2X,F8.4)
31 CALL DOTP(SA,SA,L,DOT)
SAMAG = SQRT(DOT)
C ELIMINATE FIRST NEIGHBOR CONTRIBUTIONS
IF(SAMAG.LT.1.25) GO TO 32
C ELIMINATE FIRST NEIGHBOR CONTRIBUTIONS
IF(SAMAG.GT.DMAX) GO TO 32
NTOT = NTOT + 1
CALL DOTP(SA,X,L,DOT)
CPHI = DOT/(SAMAG*XMAG(L))
IF(ABS(CPHI).GT.1.0) WRITE (6,1020) CPHI
COSXS=0.5*(1.-CPHI*CPHI)
SAMAGC=SAMAG*SAMAG*SAMAG
GEOMX(1,1)=GEOMX(1,1)+.333296*(1.-3.*COSXS)/SAMAGC
GEOMZ(1,1)=GEOMZ(1,1)+.666704*(1.-3.*CPHI*CPHI)/SAMAGC
GEOMX(1,2)=GEOMX(1,2)-.384922*(1.-3.*COSXS)/SAMAGC
GEOMZ(1,2)=GEOMZ(1,2)+.384922*(1.-3.*CPHI*CPHI)/SAMAGC
GEOMX(1,3)=GEOMX(1,3)+.272112*(1.-3.*COSXS)/SAMAGC
GEOMZ(1,3)=GEOMZ(1,3)-.272112*(1.-3.*CPHI*CPHI)/SAMAGC
GEOMX(2,2)=GEOMX(2,2)+.777765*(1.-3.*COSXS)/SAMAGC
GEOMZ(2,2)=GEOMZ(2,2)+.222235*(1.-3.*CPHI*CPHI)/SAMAGC
GEOMX(2,3)=GEOMX(2,3)+.157104*(1.-3.*COSXS)/SAMAGC
GEOMZ(2,3)=GEOMZ(2,3)-.157104*(1.-3.*CPHI*CPHI)/SAMAGC
GEOMX(3,3)=GEOMX(3,3)+.888939*(1.-3.*COSXS)/SAMAGC
GEOMZ(3,3)=GEOMZ(3,3)+.111061*(1.-3.*CPHI*CPHI)/SAMAGC
C WRITE(6,1030)(SA(L,N),X(L,N),N=1,3),SAMAG,GEO
32 CALL DOTP(TA,TA,L,DOT)
TAMAG = SQRT(DOT)
IF(TAMAG.LT.1.25) GO TO 33
C ELIMINATE FIRST NEIGHBOR CONTRIBUTIONS
IF(TAMAG.GT.DMAX) GO TO 33
NTOT = NTOT + 1

```

```

CALL DOTP(TA,Y,L,DOT)
CPHI = DOT/(TAMAG*YMAG(L))
IF(ABS(CPHI).GT.1.0) WRITE (6,1020) CPHI
COSXS=0.5*(1.-CPHI*CPHI)
TAMAGC=TAMAG*TAMAG*TAMAG
GEOMX(1,1)=GEOMX(1,1)+.333296*(1.-3.*COSXS)/TAMAGC
GEOMZ(1,1)=GEOMZ(1,1)+.666704*(1.-3.*CPHI*CPHI)/TAMAGC
GEOMX(1,2)=GEOMX(1,2)+.384922*(1.-3.*COSXS)/TAMAGC
GEOMZ(1,2)=GEOMZ(1,2)-.384922*(1.-3.*CPHI*CPHI)/TAMAGC
GEOMX(1,3)=GEOMX(1,3)-.272112*(1.-3.*COSXS)/TAMAGC
GEOMZ(1,3)=GEOMZ(1,3)+.272112*(1.-3.*CPHI*CPHI)/TAMAGC
GEOMX(2,2)=GEOMX(2,2)+.777765*(1.-3.*COSXS)/TAMAGC
GEOMZ(2,2)=GEOMZ(2,2)+.222235*(1.-3.*CPHI*CPHI)/TAMAGC
GEOMX(2,3)=GEOMX(2,3)+.157104*(1.-3.*COSXS)/TAMAGC
GEOMZ(2,3)=GEOMZ(2,3)-.157104*(1.-3.*CPHI*CPHI)/TAMAGC
GEOMX(3,3)=GEOMX(3,3)+.888939*(1.-3.*COSXS)/TAMAGC
GEOMZ(3,3)=GEOMZ(3,3)+.111061*(1.-3.*CPHI*CPHI)/TAMAGC
C   WRITE(6,1030)(TA(L,N),Y(L,N),N=1,3),TAMAG,GEO
33 CALL DOTP(UA,UA,L,DOT)
    UAMAG = SQRT(DOT)
    IF(UAMAG.LT.1.25) GO TO 34
C   ELIMINATE FIRST NEIGHBOR CONTRIBUTIONS
    IF(UAMAG.GT.DMAX) GO TO 34
    NTOT = NTOT + 1
    CALL DOTP(UA,Z,L,DOT)
    CPHI = DOT/(UAMAG*ZMAG(L))
    IF(ABS(CPHI).GT.1.0) WRITE (6,1020) CPHI
    COSXS=0.5*(1.-CPHI*CPHI)
    UAMAGC=UAMAG*UAMAG*UAMAG
    GEOMX(1,1)=GEOMX(1,1)+(1.0-3.*COSXS)/UAMAGC
    GEOMX(2,2)=GEOMX(2,2)+.111061*(1.-3.*COSXS)/UAMAGC
    GEOMZ(2,2)=GEOMZ(2,2)+.888939*(1.-3.*CPHI*CPHI)/UAMAGC
    GEOMX(2,3)=GEOMX(2,3)-.314208*(1.-3.*COSXS)/UAMAGC
    GEOMZ(2,3)=GEOMZ(2,3)+.314208*(1.-3.*CPHI*CPHI)/UAMAGC
    GEOMX(3,3)=GEOMX(3,3)+.888939*(1.-3.*COSXS)/UAMAGC
    GEOMZ(3,3)=GEOMZ(3,3)+.111061*(1.-3.*CPHI*CPHI)/UAMAGC
C   WRITE(6,1030)(UA(L,N),Z(L,N),N=1,3),UAMAG,GEO
34 RA(L,1) = RA(L,1) + 1.0
    SA(L,1) = SA(L,1) + 1.0
    TA(L,1) = TA(L,1) + 1.0
    UA(L,1) = UA(L,1) + 1.0
35 CONTINUE

```

```

C   RESET X COORDINATE OF RA AFTER PASS THROUH 101 CELLS IN X
    DIRECT
    RA(L,1) = RA(L,1) - 101.0
    SA(L,1) = SA(L,1) - 101.0
    TA(L,1) = TA(L,1) - 101.0
    UA(L,1) = UA(L,1) - 101.0
    RA(L,2) = RA(L,2) + 1.0
    SA(L,2) = SA(L,2) + 1.0
    TA(L,2) = TA(L,2) + 1.0
    UA(L,2) = UA(L,2) + 1.0
36  CONTINUE
    RA(L,2) = RA(L,2) - 101.0
    SA(L,2) = SA(L,2) - 101.0
    TA(L,2) = TA(L,2) - 101.0
    UA(L,2) = UA(L,2) - 101.0
40  CONTINUE
    DO 41 L = 1,6
    RA(L,3) = RA(L,3) + 1.0
    SA(L,3) = SA(L,3) + 1.0
    TA(L,3) = TA(L,3) + 1.0
41  UA(L,3) = UA(L,3) + 1.0
42  CONTINUE
    KOUNT = KOUNT + 1
    DO 1919 I=1,3
    DO 1919 J=I,3
    WRITE(6,1050) I,J, GEOMX(I,J),KOUNT
1050 FORMAT(1H0," GEOMXX(",I2,"","I2," ) IS ",F12.9," FOR SI",I2)
    WRITE(6,1150) I,J, GEOMZ(I,J),KOUNT
1150 FORMAT(1H0," GEOMZZ(",I2,"","I2," ) IS ",F12.9," FOR SI",I2)
1919 CONTINUE
    DO 1929 I=1,3
    DO 1929 J=1,3
    GEOMX(I,J)= 0.0
    GEOMZ(I,J)= 0.0
1929 CONTINUE
    NTOT = 0
    GO TO (43,44,45,48),KOUNT
C   NOW CALCULATE FOR OTHER INDEPENDENT SI'S
43  SIREF(1) = SI(2,1)
    SIREF(2) = SI(2,2)
    SIREF(3) = SI(2,3)
    GO TO 14
44  SIREF(1) = SI(3,1)

```

```
SIREF(2) = SI(3,2)
SIREF(3) = SI(3,3)
GO TO 14
45 SIREF(1) = SI(4,1)
SIREF(2) = SI(4,2)
SIREF(3) = SI(4,3)
GO TO 14
48 STOP
END
SUBROUTINE DOTP(A,B,L,DOT)
COMMON/CELL/ G(3,3)
DIMENSION A(15,3), B(15,3)
DOT = 0.0
DO 10 I = 1,3
DO 10 J = 1,3
10 DOT = A(L,I)*B(L,J)*G(I,J) + DOT
RETURN
END
```


APPENDIX 7

PROGRAM FOR THE CALCULATION OF MAGNETIC SHIELDING
TENSOR COMPONENTS BY LEAST SQUARES FITS

```

$RESET FREE
FILE 3(KIND=DISK,TITLE="MAG/IN/SINGLE",DEPENDENTSPECS=TRUE,
      CPRQTECTION=SAVE)
FILE 6(KIND=PACK,TITLE="MAG/OUT",MAXRECSIZE=15,BLOCKSIZE=420,
      CPROTECTION=SAVE)
C   THIS PROGRAMM IS DESIGNED TO CALCULATE MAGNETIC SHIELDING
C   S11 AND S33 BY LEAST-SQUARE-FITTING
      REAL Q(20),Y(20),PHI(20),S11,S33,CY(20)
C   N IS THE NUMBER OF POINTS USED IN THE CALCULATION
      READ(3,5,END=10) N
      5  FORMAT(I2)
      10 CONTINUE
          DO 50 I=1,N
              READ(3,20) Q(I)
              20  FORMAT(F8.3)
                  PHI(I)=Q(I)*3.1415926/180.0
                  READ(3,30) Y(I)
                  30  FORMAT(F8.3)
                      WRITE(6,40) Q(I),Y(I)
                      40  FORMAT(1H," ANGLE<H0/Z> IS ",F8.3," CHEM. SHIFT IS",F8.3)
                      50  CONTINUE
                          A=0.
                          B=0.
                          C=0.
                          D=0.
                          E=0.
                          DO 60 I=1,N
                              A=A+(SIN(PHI(I)))**4
                              B=B+((SIN(PHI(I)))**2)*((COS(PHI(I)))**2)
                              C=C+Y(I)*(SIN(PHI(I)))**2
                              D=D+(COS(PHI(I)))**4
                              E=E+Y(I)*(COS(PHI(I)))**2
                          60  CONTINUE
                              S11=(C*D-E*B)/(A*D-B*B)
                              S33=(C*B-E*A)/(B*B-D*A)
                              DO 70 I=1,N

```

```
      CY(I)=S11*(SIN(PHI(I)))**2+S33*(COS(PHI(I)))**2
70  CONTINUE
      WRITE(6,90) S11
90  FORMAT(1H,"MAGNETIC SHIELDING 11 IS",F9.4)
      WRITE(6,100) S33
100 FORMAT(1H,"MAGNETIC SHIELDING 33 IS",F9.4)
      DO 110 I=1,N
      WRITE(6,105) Q(I),CY(I)
105  FORMAT(" ANGLE(H0/Z) IS ",F8.3," CALC.SHIFT IS ",F8.3)
110  CONTINUE
      END
```

APPENDIX 8

PROGRAM FOR LEAST SQUARES FITS AND LAYER SPACING SHIFTS
IN SINGLE CRYSTAL NMR CHEMICAL SHIFT CALCULATION

```

$RESET FREE
FILE 3(KIND=DISK,TITLE="LSF/IN/SINGLE/3",DEPENDENTSPECS=TRUE,
      CPROTECTION=SAVE)
FILE 6(KIND=PACK,TITLE="LSF/OUT/SINGLE",MAXRECSIZE=15,BLOCKSIZE=
      C420, PROTECTION=SAVE)
C   THIS PROGRAMM IS DESIGNED TO DO LEAST-SQUARE FITTING FOR
C   THE SIC SIGLE CRYSTAL CALCULATION
      REAL IS11SI,IS33SI,IS11C,IS33C,KIXX,KIZZ
      REAL S11SI(5),S33SI(5),S11C(5),S33C(5)
      REAL CS11SI(5),CS33SI(5),CS11C(5),CS33C(5)
      REAL G11XSI(5),G11ZSI(5),G33XSI(5),G33ZSI(5)
      REAL G11XC(5),G11ZC(5),G33XC(5),G33ZC(5)
      REAL SIG11X(5,10),SIG11Z(5,10),SIG33X(5,10),SIG33Z(5,10)
      REAL CG11X(5,10),CG11Z(5,10),CG33X(5,10),CG33Z(5,10)
      REAL DG1XSI(5,10),DG1ZSI(5,10),DG3XSI(5,10),DG3ZSI(5,10)
      REAL DG1XC(5,10),DG1ZC(5,10),DG3XC(5,10),DG3ZC(5,10)
      REAL CCA(20,10),XXA(10,10),YYA(0:20),DD,T,SI,CA,SSI(20),SC(20)
      DIMENSION IS(20)
C   SET THE MAG. TO MOVE SI'S & C'S
      CA=.001
      SI=-.001
C   JUDGE=0, ONLY CALC.FINAL RESULT; OTHERWISE,JUDGE=1
      READ(3,1,END=2)JUDGE
1    FORMAT(I1)
2    CONTINUE
      READ(3,4,END=5) N
4    FORMAT(I1)
5    CONTINUE
      DO 59 I=1,N
      READ(3,11) S11SI(I)
11   FORMAT(F5.2)
      READ(3,21) S33SI(I)
21   FORMAT(F5.2)
      WRITE(6,32) S11SI(I),I
32   FORMAT(1H," MAGNETIC SHIELDING 11 IS ",F8.3," FOR SI",I2)
      WRITE(6,42) S33SI(I),I
42   FORMAT(1H," MAGNETIC SHIELDING 33 IS ",F8.3," FOR SI",I2)

```

```
59  CONTINUE
    DO 109 I=1,N
      READ(3,61) S11C(I)
61  FORMAT(F5.2)
      READ(3,71) S33C(I)
71  FORMAT(F5.2)
      WRITE(6,82) S11C(I),I
82  FORMAT(1H," MAGNETIC SHIELDING 11 IS ",F6.3," FOR C",I2)
      WRITE(6,92) S33C(I),I
92  FORMAT(1H," MAGNETIC SHIELDING 33 IS ",F6.3," FOR C",I2)
109 CONTINUE
    DO 179 I=1,N
      READ(3,121) G11XSI(I)
      READ(3,121) G11ZSI(I)
      READ(3,121) G33XSI(I)
      READ(3,121) G33ZSI(I)
121 FORMAT(F12.9)
179 CONTINUE
    DO 249 I=1,N
      READ(3,191) G11XC(I)
      READ(3,191) G11ZC(I)
      READ(3,191) G33XC(I)
      READ(3,191) G33ZC(I)
191 FORMAT(F12.9)
249 CONTINUE
    A=0.
    B=0.
    C=0.
    D=0.
    E=0.
    F=0.
    U=0.
    V=0.
    W=0.
    X=0.
    Y=0.
    Z=0.
    AB=0.
    BB=0.
    CB=0.
    DE=0.
    EE=0.
    FE=0.
```

```

UV=0.
VV=0.
WV=0.
XY=0.
YY=0.
ZY=0.
AC=0.
BC=0.
CC=0.
DF=0.
EF=0.
FF=0.
UW=0.
VW=0.
WW=0.
XZ=0.
YZ=0.
ZZ=0.
DO 299 I=1,N
A=A+S11SI(I)
B=B+G11XSI(I)
C=C+G11ZSI(I)
D=D+S33SI(I)
E=E+G33XSI(I)
F=F+G33ZSI(I)
U=U+S11C(I)
V=V+G11XC(I)
W=W+G11ZC(I)
X=X+S33C(I)
Y=Y+G33XC(I)
Z=Z+G33ZC(I)
AB=AB+S11SI(I)*G11XSI(I)
BB=BB+G11XSI(I)**2
CB=CB+G11ZSI(I)*G11XSI(I)
DE=DE+S33SI(I)*G33XSI(I)
EE=EE+G33XSI(I)**2
FE=FE+G33ZSI(I)*G33XSI(I)
UV=UV+S11C(I)*G11XC(I)
VV=VV+G11XC(I)**2
WV=WV+G11ZC(I)*G11XC(I)
XY=XY+S33C(I)*G33XC(I)
YY=YY+G33XC(I)**2
ZY=ZY+G33ZC(I)*G33XC(I)

```

```

AC=AC+S11SI(I)*G11ZSI(I)
BC=BC+G11XSI(I)*G11ZSI(I)
CC=CC+G11ZSI(I)**2
DF=DF+S33SI(I)*G33ZSI(I)
EF=EF+G33XSI(I)*G33ZSI(I)
FF=FF+G33ZSI(I)**2
UW=UW+S11C(I)*G11ZC(I)
VW=VW+G11XC(I)*G11ZC(I)
WW=WW+G11ZC(I)**2
XZ=XZ+S33C(I)*G33ZC(I)
YZ=YZ+G33XC(I)*G33ZC(I)
ZZ=ZZ+G33ZC(I)**2
299 CONTINUE
O=AB+DE+UV+XY
P=BB+EE+VV+YY
Q=CB+FE+WV+ZY
R=AC+DF+UW+XZ
S=BC+EF+VW+YZ
T=CC+FF+WW+ZZ
OO=O-(A*B+D*E+U*V+X*Y)/N
PP=(B*B+E*E+V*V+Y*Y)/N-P
QQ=(B*C+E*F+V*W+Y*Z)/N-Q
RR=R-(C*A+F*D+W*U+Z*X)/N
SS=(C*B+F*E+W*V+Z*Y)/N-S
TT=(C*C+F*F+W*W+Z*Z)/N-T
KIXX=(RR/TT-OO/QQ)/(PP/QQ-SS/TT)
KIZZ=(RR/SS-OO/PP)/(QQ/PP-TT/SS)
IS11SI=(A-B*KIXX-C*KIZZ)/N
IS33SI=(D-E*KIXX-F*KIZZ)/N
IS11C=(U-V*KIXX-W*KIZZ)/N
IS33C=(X-Y*KIXX-Z*KIZZ)/N
DO 399 I=1,N
CS11SI(I)=IS11SI+KIXX*G11XSI(I)+KIZZ*G11ZSI(I)
CS33SI(I)=IS33SI+KIXX*G33XSI(I)+KIZZ*G33ZSI(I)
CS11C(I)=IS11C+KIXX*G11XC(I)+KIZZ*G11ZC(I)
CS33C(I)=IS33C+KIXX*G33XC(I)+KIZZ*G33ZC(I)
399 CONTINUE
DELTAX=KIZZ-KIXX
WRITE(6,412) KIXX
412 FORMAT(1H," X PERPENDICULAR IS ",F10.3)
WRITE(6,422) KIZZ
422 FORMAT(1H," X PARALLEL IS ",F10.3)
WRITE (6,432) DELTAX

```

```

432 FORMAT(1H," DELTAX IS ",F10.3)
    WRITE(6,442) IS11SI
442 FORMAT(1H," INTRINSIC SHIFT 11 IS",F8.4," FOR SI")
    WRITE(6,452) IS33SI
452 FORMAT(1H," INTRINSIC SHIFT 33 IS",F8.4," FOR SI")
    WRITE(6,462) IS11C
462 FORMAT(1H," INTRINSIC SHIFT 11 IS",F8.4," FOR C ")
    WRITE(6,472) IS33C
472 FORMAT(1H," INTRINSIC SHIFT 33 IS",F8.4," FOR C ")
    DO 499 I=1,N
        WRITE(6,482) CS11SI(I),I
482 FORMAT(1H," CALC. SHIFT 11 IS ",F8.4," FOR SI",I2)
        WRITE(6,492) CS33SI(I),I
492 FORMAT(1H," CALC. SHIFT 33 IS",F8.4," FOR SI",I2)
499 CONTINUE
    DO 549 I=1,N
        WRITE(6,512) CS11C(I),I
512 FORMAT(1H," CALC. SHIFT 11 IS",F8.4," FOR C",I2)
        WRITE(6,522) CS33C(I),I
522 FORMAT(1H," CALC. SHIFT 33 IS",F8.4," FOR C",I2)
549 CONTINUE
    IF (JUDGE.EQ.0) GOTO 855
C    NOW PUT IN THE SHIFTED GEOM. FOR SI'S & C'S
    DO 559 I=1,N
        DO 559 J=1,2*N-1
            READ(3,551) SIG11X(I,J)
551 FORMAT(F12.9)
559 CONTINUE
        DO 569 I=1,N
            DO 569 J=1,2*N-1
                READ(3,561) SIG11Z(I,J)
561 FORMAT(F12.9)
569 CONTINUE
        DO 579 I=1,N
            DO 579 J=1,2*N-1
                READ(3,571) SIG33X(I,J)
571 FORMAT(F12.9)
579 CONTINUE
        DO 599 I=1,N
            DO 599 J=1,2*N-1
                READ(3,581) SIG33Z(I,J)
581 FORMAT(F12.9)
599 CONTINUE

```

```

        DO 629 I=1,N
        DO 629 J=1,2*N-1
        READ(3,611) CG11X(I,J)
611  FORMAT(F12.9)
629  CONTINUE
        DO 649 I=1,N
        DO 649 J=1,2*N-1
        READ(3,641) CG11Z(I,J)
641  FORMAT(F12.9)
649  CONTINUE
        DO 679 I=1,N
        DO 679 J=1,2*N-1
        READ(3,661) CG33X(I,J)
661  FORMAT(F12.9)
679  CONTINUE
        DO 699 I=1,N
        DO 699 J=1,2*N-1
        READ(3,691) CG33Z(I,J)
691  FORMAT(F12.9)
699  CONTINUE
        DO 711 I=1,N
        DO 711 J=1,2*N-1
        DG1XSI(I,J)=SIG11X(I,J)-G11XSI(I)
        DG1ZSI(I,J)=SIG11Z(I,J)-G11ZSI(I)
        DG3XSI(I,J)=SIG33X(I,J)-G33XSI(I)
        DG3ZSI(I,J)=SIG33Z(I,J)-G33ZSI(I)
        DG1XC(I,J) = CG11X(I,J)- G11XC(I)
        DG1ZC(I,J) = CG11Z(I,J)- G11ZC(I)
        DG3XC(I,J) = CG33X(I,J)- G33XC(I)
        DG3ZC(I,J) = CG33Z(I,J)- G33ZC(I)
711  CONTINUE
        DO 729 K=1,2*N-1,2
        I=(K+1)/2
        L=K+1
        DO 729 J=1,2*N-1
        CCA(K,J)=KIXX*DG1XSI(I,J) + KIZZ*DG1ZSI(I,J)
        CCA(L,J)=KIXX*DG3XSI(I,J) + KIZZ*DG3ZSI(I,J)
729  CONTINUE
        DO 739 K=2*N+1,4*N-1,2
        I=(K+1)/2-N
        L=K+1
        DO 739 J=1,2*N-1
        CCA(K,J)=KIXX*DG1XC(I,J)+KIZZ*DG1ZC(I,J)

```



```

      CCA(L,J)=KIXX*DG3XC(I,J)+KIZZ*DG3ZC(I,J)
739  CONTINUE
      DO 749 I=1,2*N-1,2
      K=I+1
      J=(I+1)/2
      M=2*N
      CCA(I,M)=S11SI(J)-CS11SI(J)
      CCA(K,M)=S33SI(J)-CS33SI(J)
749  CONTINUE
      DO 759 I=2*N+1,4*N-1,2
      K=I+1
      J=(I+1)/2-N
      M=2*N
      CCA(I,M)=S11C(J)-CS11C(J)
      CCA(K,M)=S33C(J)-CS33C(J)
759  CONTINUE
      DO 769 K=1,2*N-1
      DO 769 L=1,2*N
      XXA(K,L)=0.
769  CONTINUE
      DO 779 K=1,2*N-1
      DO 779 L=1,2*N
      DO 779 I=1,4*N
      XXA(K,L)=XXA(K,L)+CCA(I,K)*CCA(I,L)
779  CONTINUE
C    NOW SOLVE LINEAR EQUATIONS BY GAUSSIAN ELIMINATION
      WRITE(6,999)
      WRITE(6,799)
799  FORMAT(1H,"FOR ODD I, Y(I)*.001A IS THE SHIFT REQUIRED FOR C'S")
      WRITE(6,800)
800  FORMAT(1H,"FOR EVEN I,Y(I)*(-.001A) IS THE SHIFT REQ. FOR SI'S")
      NN=2*N-1
      MM=2*N-1
      JJ=0
      DO 850 K=1,NN
      DD=XXA(K,K)
      DO 821 I=K+1,MM
      IF (ABS(XXA(I,K)).LT.ABS(DD)) GO TO 821
      L=I
      DD=XXA(L,K)
821  CONTINUE
      IF (ABS(DD).GT.1.0E-18) GOTO 835
      PRINT 801,K

```

```

801 FORMAT (" SINGULAR, K=", I1)
      JJ=JJ +1
      IS(JJ)=K
      GOTO 850
835 IF (DD.EQ.XXA(K,K)) GO TO 851
      DO 841 J=K,NN+1
      T=XXA(L,J)
      XXA(L,J)=XXA(K,J)
      XXA(K,J)=T
841 CONTINUE
851 DO 850 J=K+1,NN+1
      XXA(K,J)=XXA(K,J)/XXA(K,K)
      DO 850 I=K+1,MM
      XXA(I,J)=XXA(I,J)-XXA(I,K)*XXA(K,J)
850 CONTINUE
      DO 833 I=NN+1,MM
      IF (ABS(XXA(I,NN+1)).GT.(1.0E-8)) GOTO 844
833 CONTINUE
      DO 880 K=0,NN-1
840 YYA(NN-K)=0
      YYA(NN+1)=0
      IF (JJ.EQ.0) GOTO 877
      DO 822 I=1,JJ
      YYA(IS(I))=1
      IF ((NN-K).EQ.IS(I)) GOTO 880
822 CONTINUE
877 DO 890 J=NN-K+1, NN
      YYA(NN-K)=YYA(NN-K)+XXA((NN-K),J)*YYA(J)
890 CONTINUE
      YYA(NN-K)=-YYA(NN-K)+XXA(NN-K,NN+1)
      WRITE (6,802) NN-K, YYA(NN-K)
802 FORMAT (1H , " Y(",I2," )=",F12.8)
880 CONTINUE
      WRITE(6,999)
      YYA(0)=.0
      DO 875 I=1,2*N-1,2
      K=I-1
      J=(I+1)/2
      SSI(J)=YYA(K)*SI
      SC(J)=YYA(I)*CA
      WRITE(6,860)J,SSI(J)
860 FORMAT(1H , "SHIFT OF SI (",I2," ) = ",F12.8)
      WRITE(6,870)J,SC(J)

```

```
870 FORMAT(1H,"SHIFT OF C(",I2," ) = ",F12.8)
875 CONTINUE
      IF (JJ.EQ.0) GOTO 855
      DO 823 K=1,JJ
823  WRITE (6,803) IS(K)
803  FORMAT (1H,"Y(",I1,")=1")
      GOTO 855
844  PRINT 804
804  FORMAT (" NO SOLUTION")
999  FORMAT(1H )
855  STOP
      END
```